

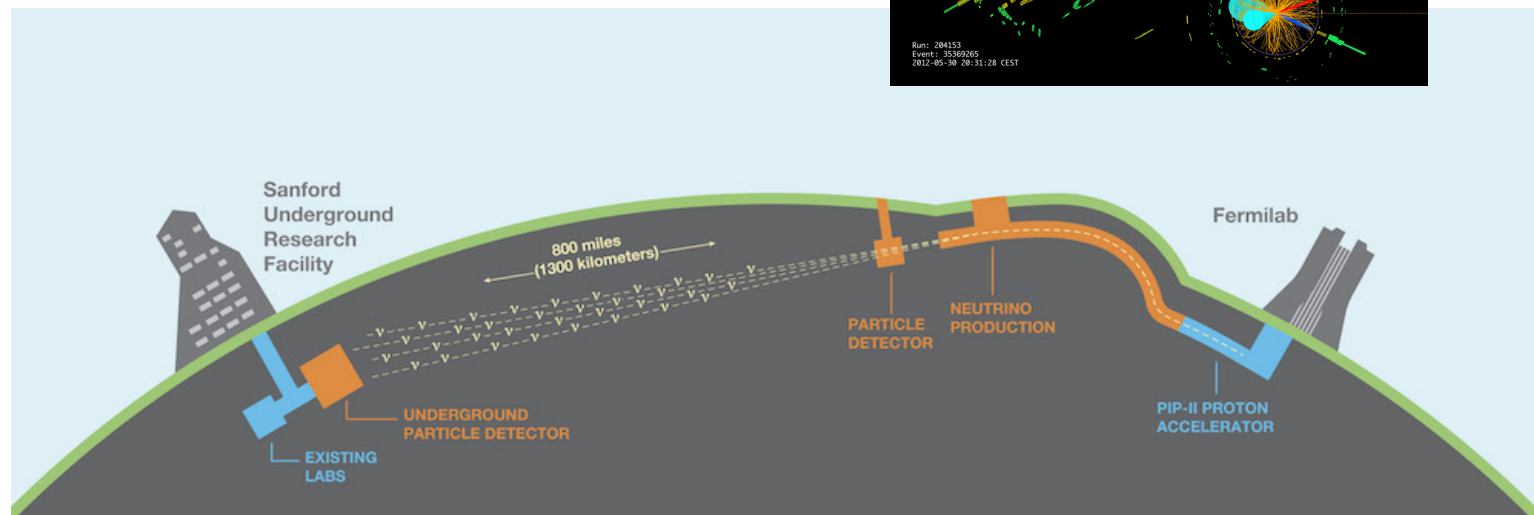
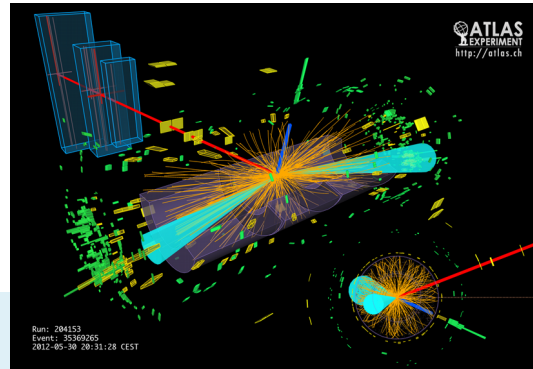
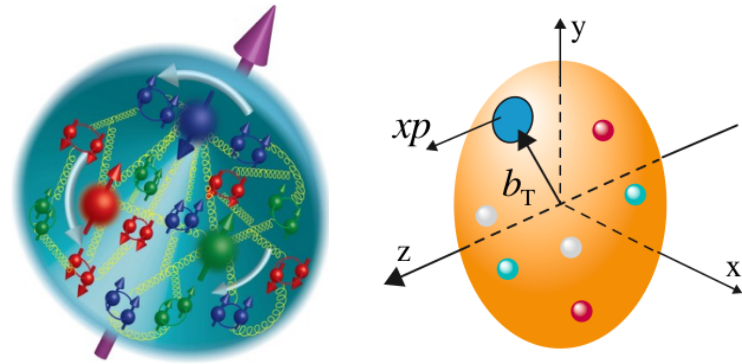
What the Electron-Ion Collider (EIC) can do for you

pushing back the energy and intensity frontiers with a lepton-nucleus collider

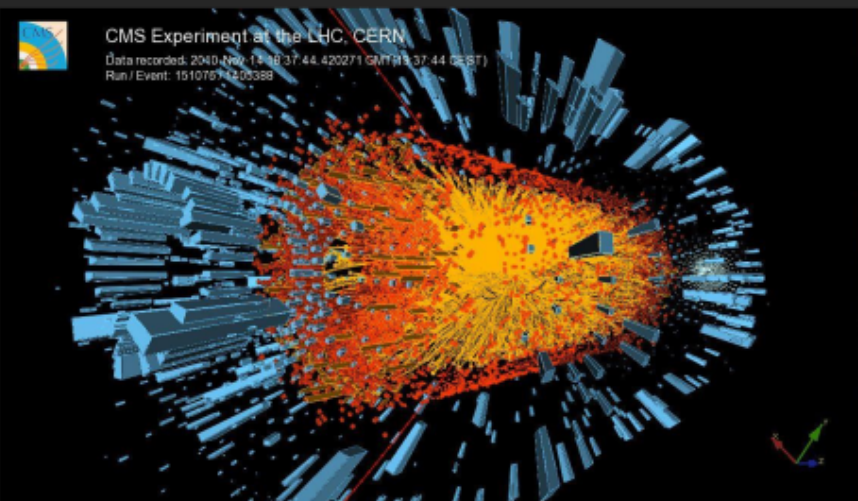
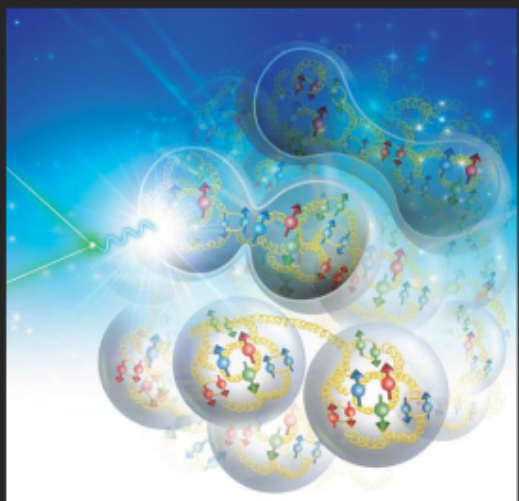
Tim Hobbs, JLab EIC Center & CTEQ@SMU

Nov 13th 2019

...and what you can do for EIC



first, a promotion: **join us upstairs!** LHC-EIC@LPC



Sunrise,
WH11NE

Nov 13-15

<https://indico.cern.ch/e/LHCEICPhysics>

LPC Workshop on

PHYSICS CONNECTIONS BETWEEN THE LHC AND EIC

Fermilab LHC Physics Center (LPC)
November 13-15, 2019

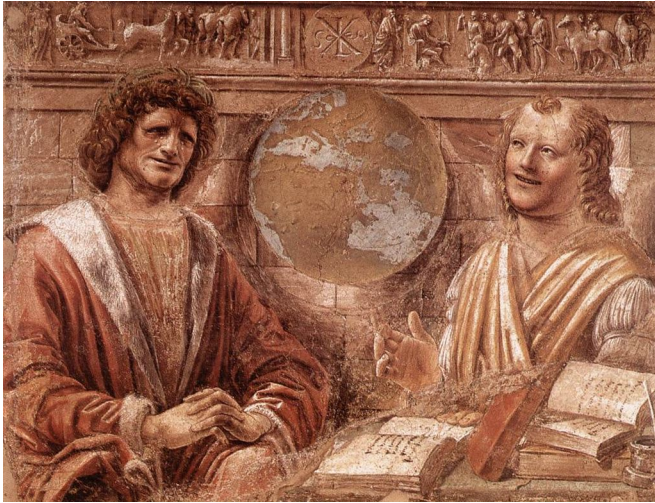
Exploring physics intersections between LHC
phenomenology and a future
Electron-Ion Collider (EIC) program via:



- Precision QCD
- Monte Carlo Event Generators
- Lattice QCD
- Electroweak/neutrino phenomenology
- BSM physics searches
- Machine learning & computation

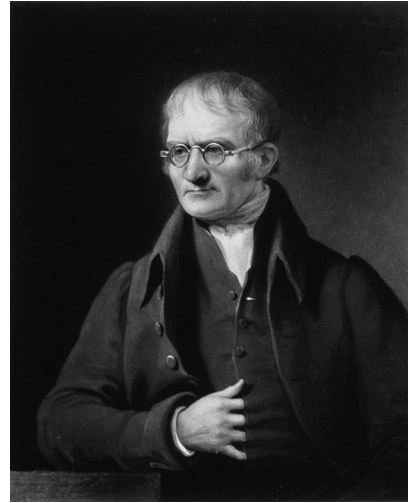
the quest to understand the structure of matter has been a series of lurches to successively smaller length scales

atomic hypothesis, $\lesssim 10^{-4}$ m



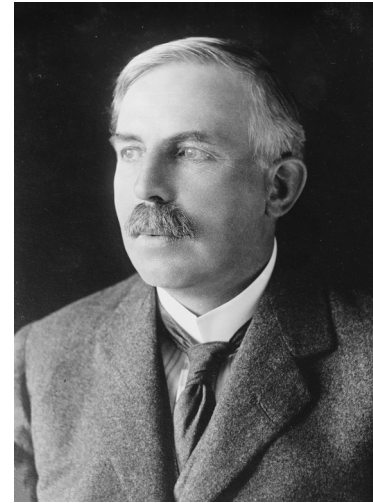
Heraclitus & Democritus

molecular theory, $\lesssim 10^{-9}$ m



Dalton

gold nucleus, $\sim 7.5 \times 10^{-15}$ m



Rutherford

neutron, $\sim 10^{-15}$ m

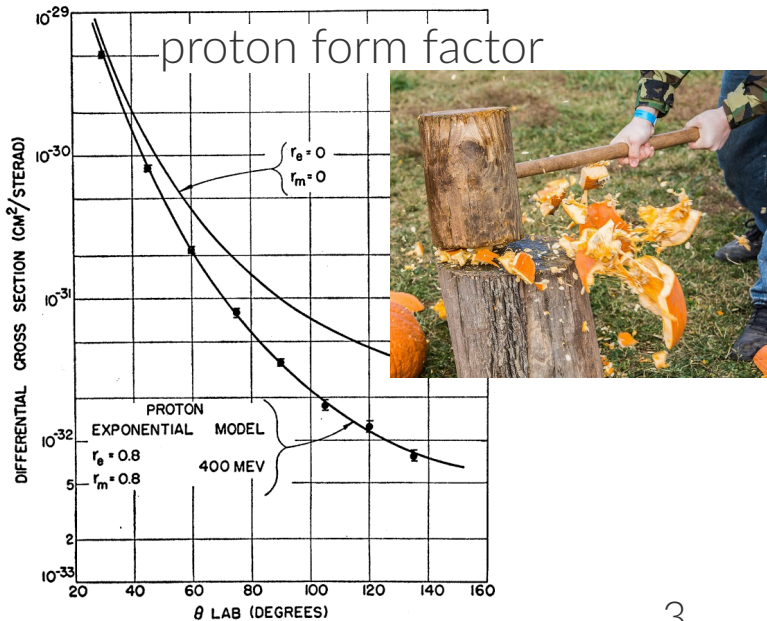


Chadwick

$< 10^{-15}$ m

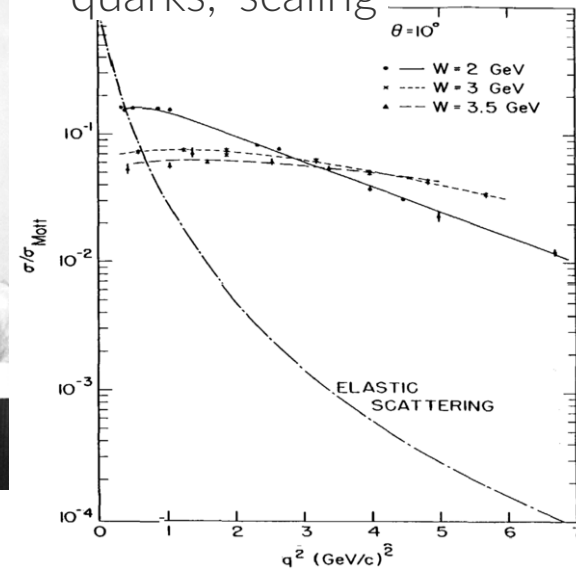


Hofstadter

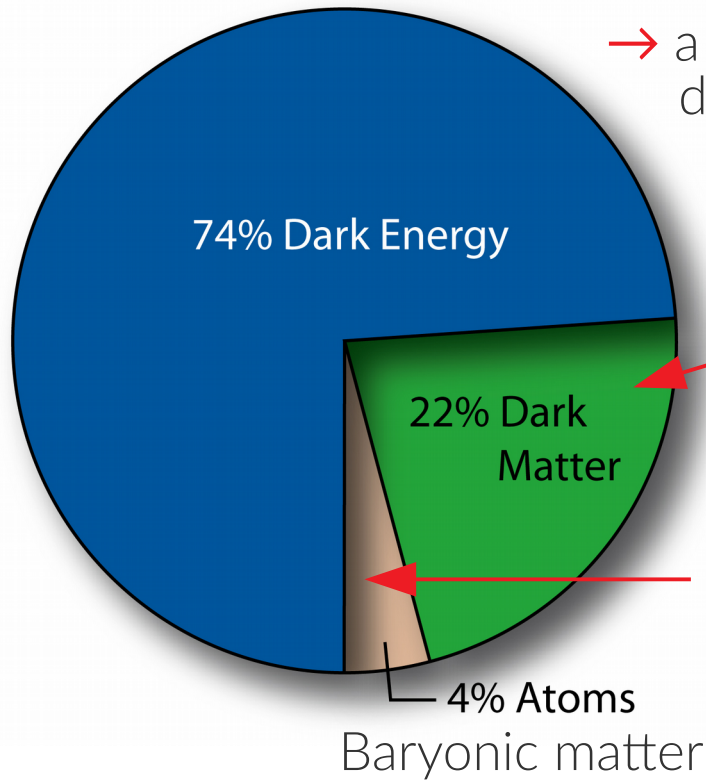


Feynman

evidence for quarks, 'scaling'



this history of advances has led to (an incomplete!) understanding of *visible* matter; many more “known unknowns” must exist.

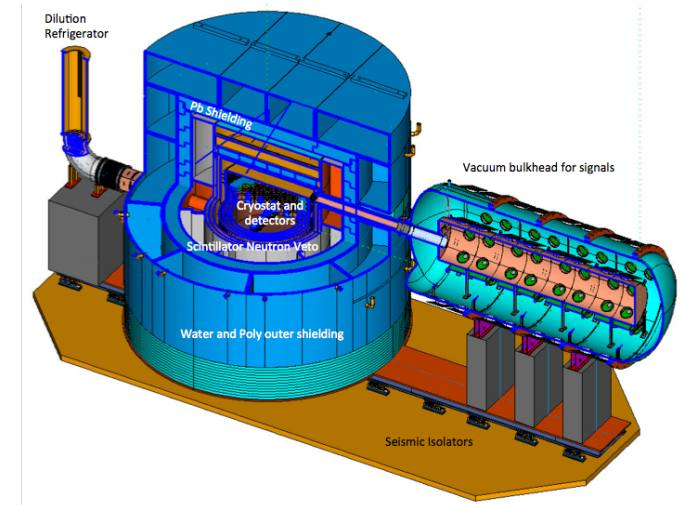


→ a vast enterprise now in motion to identify dark matter (or test the Standard Model [SM]):

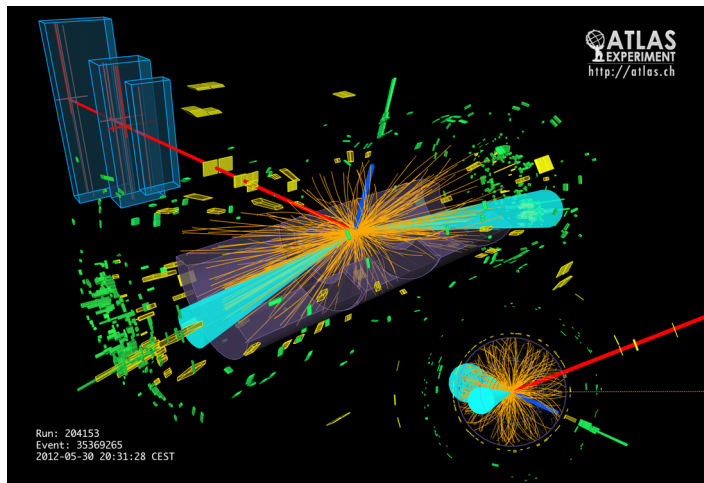
to find this

must understand this

“direct detection,” e.g., CDMS



collider detection

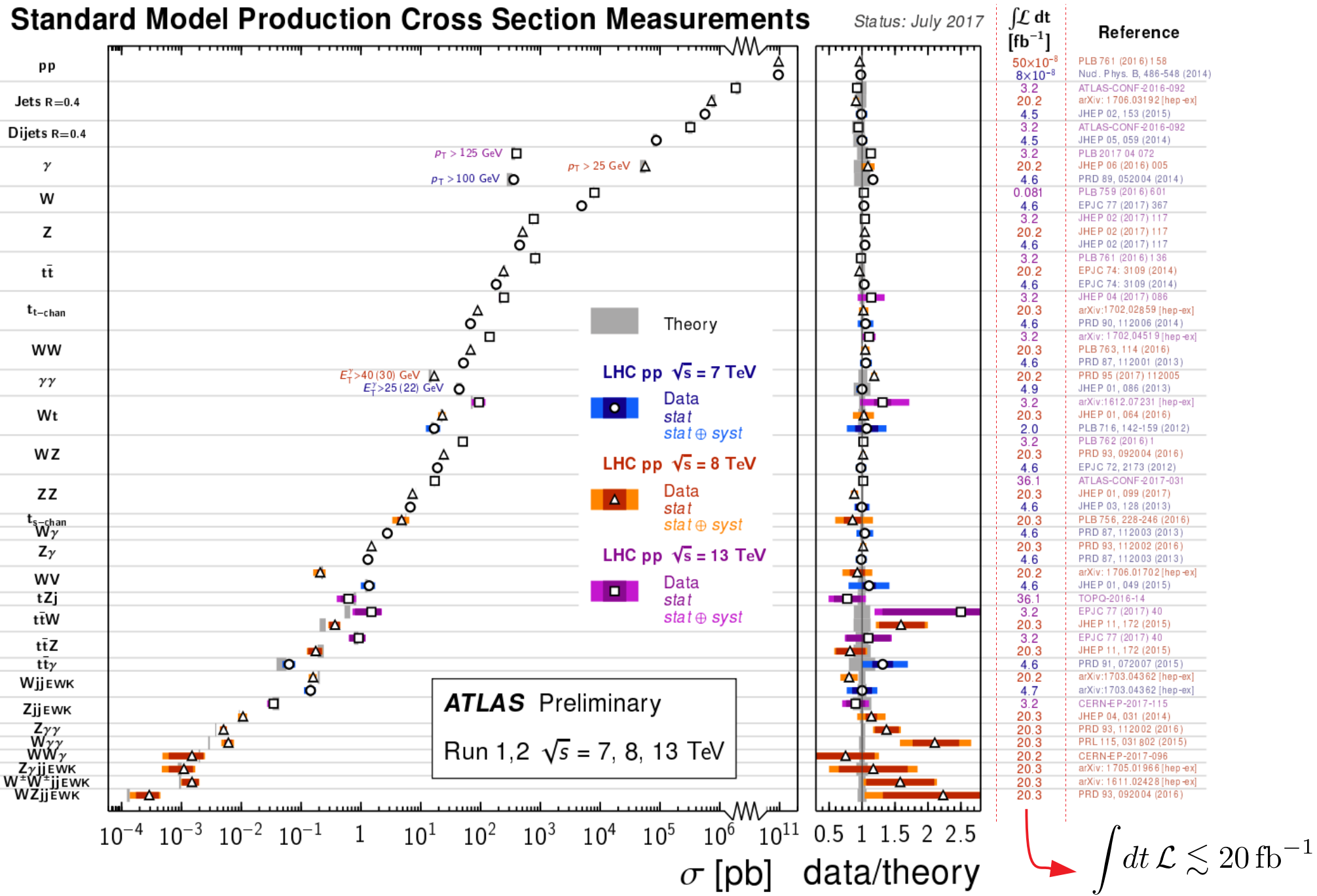


...look for the unexpected in SM processes

“indirect detection,” e.g., AMS



it's 2019, and the Standard Model has been phenomenally successful
 (frustratingly??)

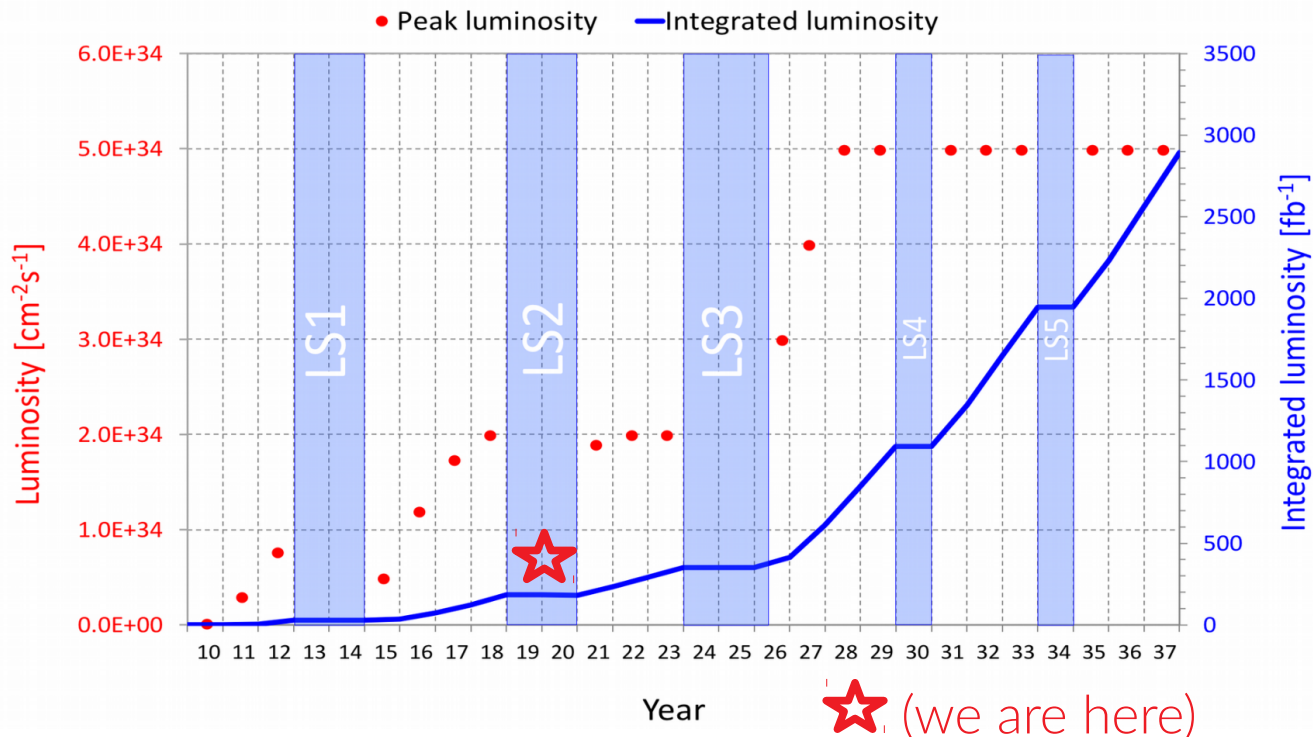


the view from particle physics: the big data era has arrived.

- with the completion of Run-2, LHC has accumulated copious data

MUCH more is coming!

(see talk, Jindariani – HL-LHC status.)



- this data is an opportunity, but also a challenge



WWW.PHDCOMICS.COM

...we now imbibe from the HEP data “firehose,” and all the more so soon...

drinking from a firehose is both an art and a science



“the bad way”



“a better way, but...”

- as accumulated HEP data sets approach $\mathcal{O}(1 \text{ ab}^{-1})$, more sophisticated inputs/approaches will be required to leverage **all** the data

- machine learning techniques, advanced statistics
- experimental benchmarks (e.g., EIC – [this talk](#))
- opportunities in quantum computing...

a holistic combination of approaches is preferred

...and having complementary approaches avoids pitfalls

→ Google Images identifies a small Maltese dog in two pictures:



Tulu Khatiwada-Hobbs

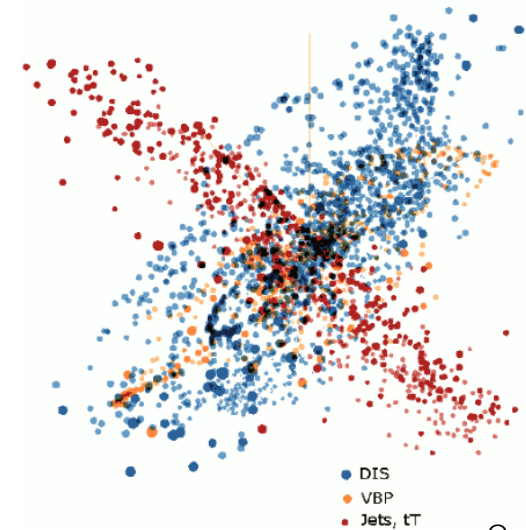


a washer-dryer from QCD@LHC'19



lesson: machine learning alone will not resolve all ambiguities in interpreting HEP data

→ similarly, more of the same data does not always help!



how do we make sense of high-energy data anyway?

→ a complex interplay of measurement, analysis, and **theoretical calculation**

computing a typical process at the LHC requires **perturbative matrix elements** and **nonperturbative parton distribution functions (PDFs)**

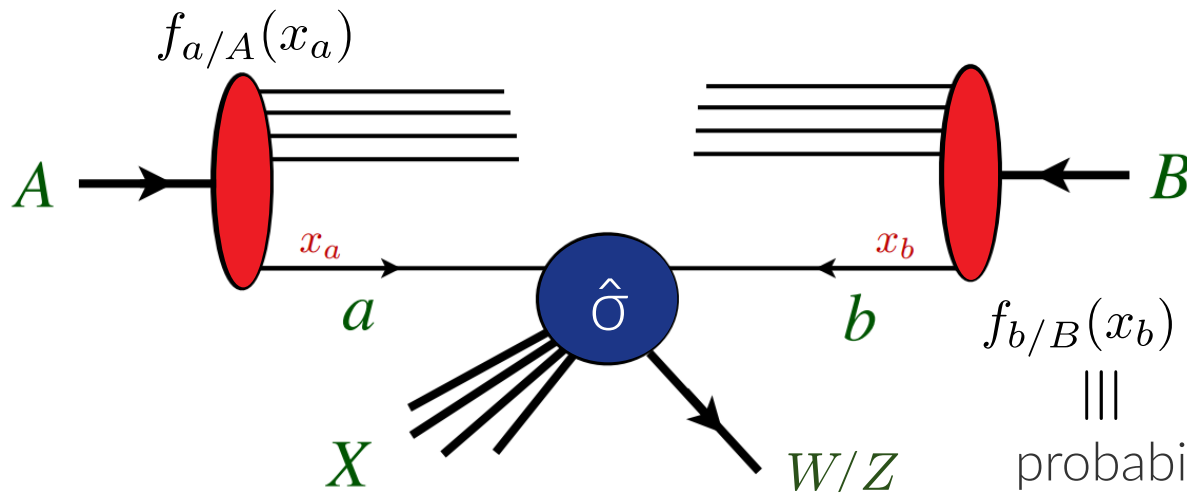
$$\sigma(AB \rightarrow W/Z + X) = \sum_n \alpha_s^n(\mu_R^2) \sum_{a,b} \int dx_a dx_b \quad \text{for EW boson pp production}$$

(see talk, Campbell.)

$$\times f_{a/A}(x_a, \mu^2) \hat{\sigma}_{ab \rightarrow W/Z+X}(\hat{s}, \mu^2, \mu_R^2) f_{b/B}(x_b, \mu^2)$$

pQCD matrix elements

unpolarized nucleon PDFs



NOTE! Any process involving identified hadrons depends on nonperturbative information – either PDFs or analogous functions

$$x_b \equiv \frac{p_b}{P_B}$$

probability to find parton (quark/gluon) b carrying long. momentum x_b of hadron B

why does this work? the remarkable properties of QCD!

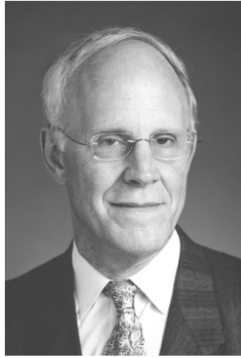


Photo from the Nobel Foundation archive.
David J. Gross
Prize share: 1/3



Photo from the Nobel Foundation archive.
H. David Politzer
Prize share: 1/3

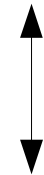


Photo from the Nobel Foundation archive.
Frank Wilczek
Prize share: 1/3

the β -function of QCD is negative-definite,

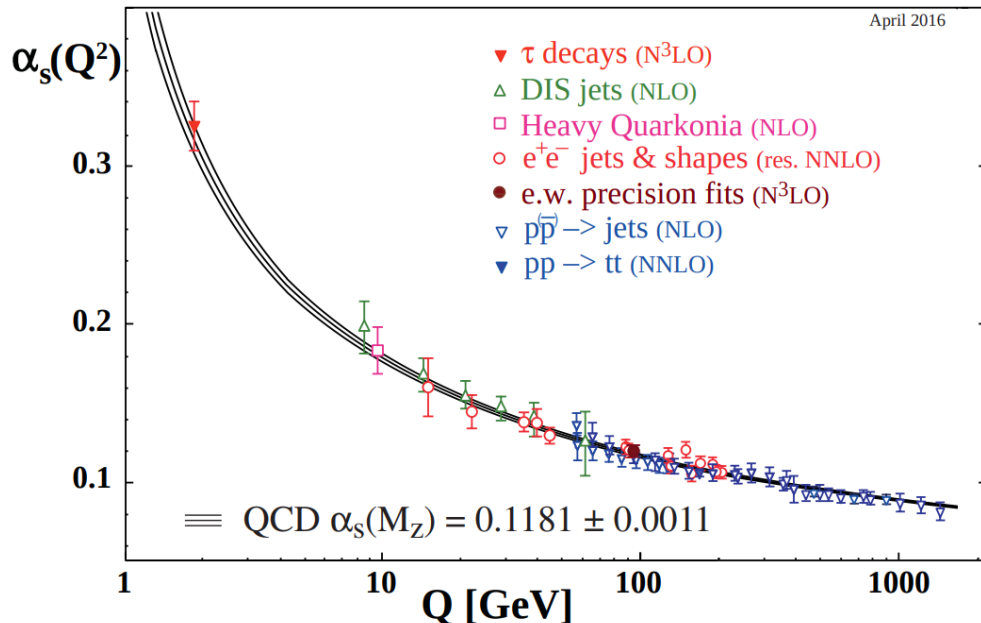
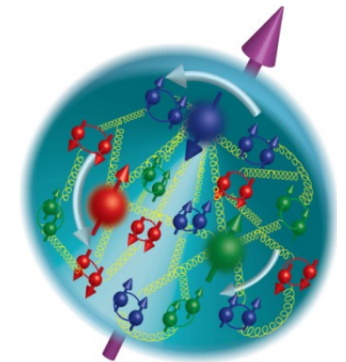
$$\beta(\alpha_s) = \mu_R^2 \frac{d\alpha_s}{d\mu_R^2} = -(b_0\alpha_s^2 + \dots) < 0$$

quark-gluon interactions become weak at high energies (asymptotic freedom), allowing a description based on perturbation theory



QCD factorization

at low energies, however, interactions are strong, and dynamics are inherently nonperturbative



fundamental question: how does QCD, which so successfully describes high-energy processes, give rise to the emergent properties of low-energy bound states?

→ the chief motivation for the Electron-Ion Collider (EIC)

QCD analyses operationalize this physics into global fits

- PDFs (& analogous distributions) are nonperturbative hadronic matrix elements,

$$f_{q/p}(x, \mu^2) = \int \frac{d\xi^-}{4\pi} e^{-i\xi^- k^+} \langle p | \bar{\psi}(\xi^-) \gamma^+ \mathcal{U}(\xi^-, 0) \psi(0) | p \rangle$$



challenging to compute from QCD!

there are lattice QCD developments
(see talks, Liu & Kronfeld.)



'The Big Bang Theory'

Amy: Maybe you could make your new field of study the calculation of nuclear matrix elements.

Sheldon: Oh, please!

philosophy: lacking a first-principles calculation, fit a flexible parametrization at a suitable boundary condition for QCD evolution:

$$f_{q/p}(x, \mu^2 = Q_0^2) = a_{q_0} x^{a_{q_1}} (1 - x)^{a_{q_2}} P[x, \{a_{qn-3}\}]$$

- perturbatively-calculable evolution then specifies dependence on $\mu^2 > Q_0^2$
- fit the world's data from a diverse range of scales and processes

BUT standard-candle measurements are limited by PDF uncertainties

→ this extends to, e.g., σ_H , $\sin^2 \theta_W$, m_W , ...

→ the PDF uncertainties are NOT another 'theory uncertainty'

ATLAS, 1701.07240

for example:

Channel	$m_{W^+} - m_{W^-}$ [MeV]	Stat. Unc.	Muon Unc.	Elec. Unc.	Recoil Unc.	Bckg. Unc.	QCD Unc.	EW Unc.	PDF Unc.	Total Unc.
$W \rightarrow e\nu$	-29.7	17.5	0.0	4.9	0.9	5.4	0.5	0.0	24.1	30.7
$W \rightarrow \mu\nu$	-28.6	16.3	11.7	0.0	1.1	5.0	0.4	0.0	26.0	33.2
Combined	-29.2	12.8	3.3	4.1	1.0	4.5	0.4	0.0	23.9	28.0

→ rather, they are fundamental gaps in empirical knowledge

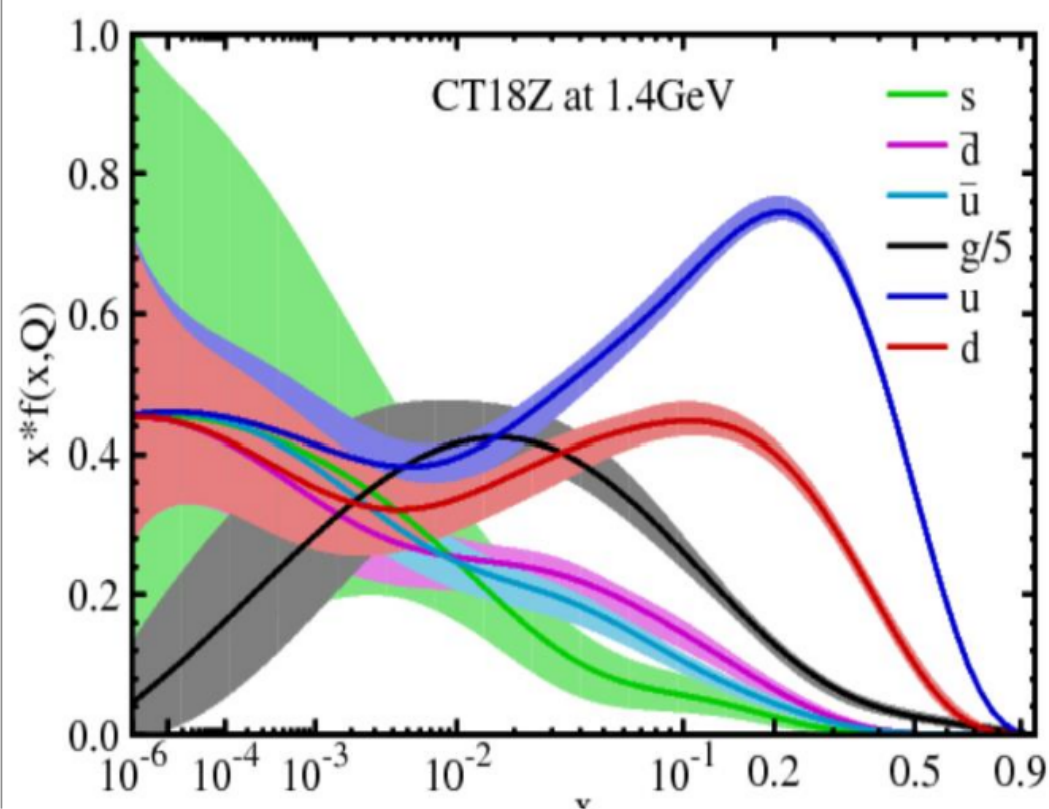
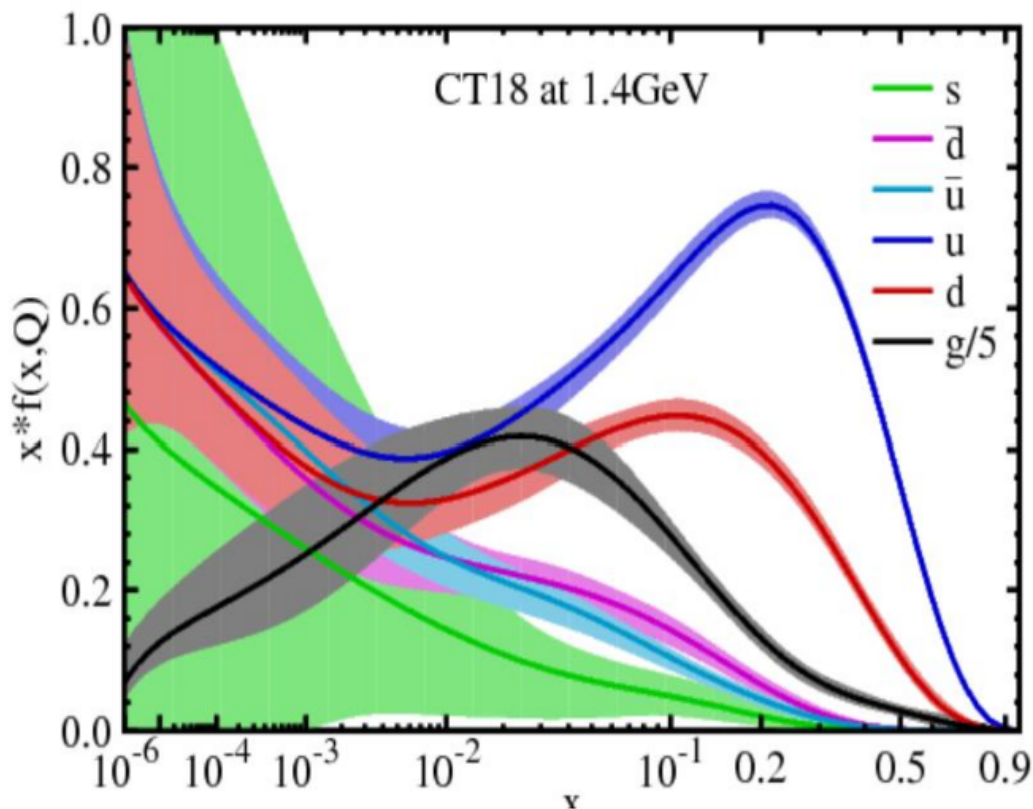
→ frontier efforts at the HL-LHC, LBNF aim for (sub)percent precision

→ this CANNOT be achieved without systematically dealing with these uncertainties.

→ **this must be a primary objective of US-HEP**

PDF analyses are challenging! (theoretically, computationally, statistically, ...)

Four PDF ensembles: CT18 (default), A, X, and Z



- a primary activity of the CTEQ collaborations (above, CT) is the determination of the proton and nuclear PDFs needed for HEP analyses
 - impacts on SM predictions are a central concern

- there remains considerable dependence (as large as $\sim 13\%$) upon PDF parametrization and running coupling

→ the situation is such that precision in Higgs phenom. is significantly **PDF-limited**

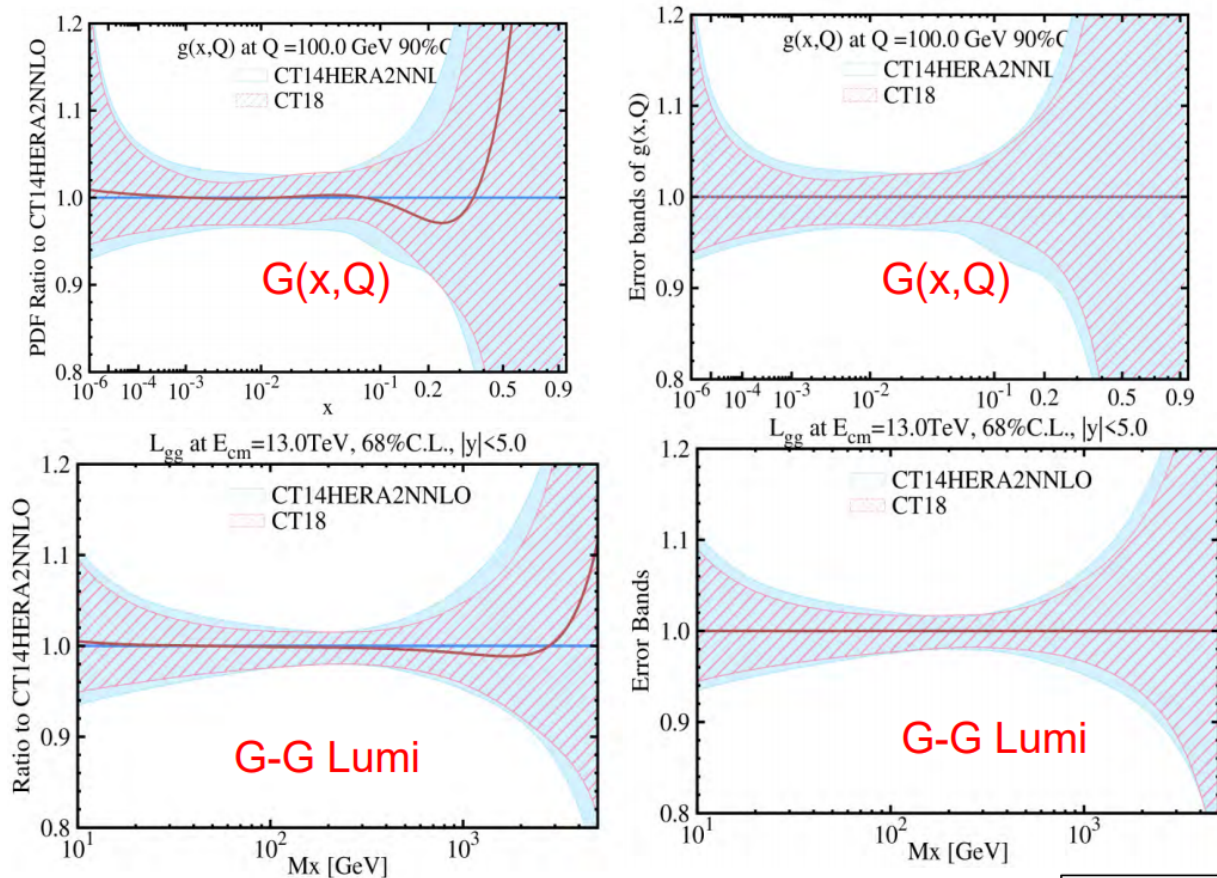
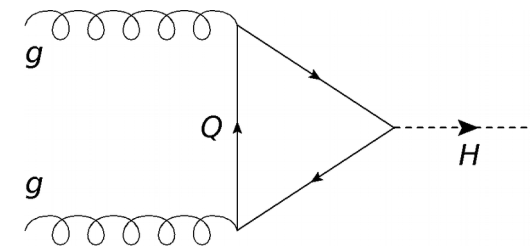
Accardi et al., EPJC76, 471 (2016).

PDF sets	$\sigma(H)^{\text{NNLO}}$ (pb) nominal $\alpha_s(M_Z)$	$\sigma(H)^{\text{NNLO}}$ (pb) $\alpha_s(M_Z) = 0.115$	$\sigma(H)^{\text{NNLO}}$ (pb) $\alpha_s(M_Z) = 0.118$
ABM12 [2]	39.80 ± 0.84	41.62 ± 0.46	44.70 ± 0.50
CJ15 [1] ^a	$42.45^{+0.43}_{-0.18}$	$39.48^{+0.40}_{-0.17}$	$42.45^{+0.43}_{-0.18}$
CT14 [3] ^b	$42.33^{+1.43}_{-1.68}$	$39.41^{+1.33}_{-1.56}$ (40.10)	$42.33^{+1.43}_{-1.68}$
HERAPDF2.0 [4] ^c	$42.62^{+0.35}_{-0.43}$	$39.68^{+0.32}_{-0.40}$ (40.88)	$42.62^{+0.35}_{-0.43}$
JR14 (dyn) [5]	38.01 ± 0.34	39.34 ± 0.22	42.25 ± 0.24
MMHT14 [6]	$42.36^{+0.56}_{-0.78}$	$39.43^{+0.53}_{-0.73}$ (40.48)	$42.36^{+0.56}_{-0.78}$
NNPDF3.0 [7]	42.59 ± 0.80	39.65 ± 0.74 (40.74 \pm 0.88)	42.59 ± 0.80
PDF4LHC15 [8]	42.42 ± 0.78	39.49 ± 0.73	42.42 ± 0.78

σ_H at NNLO and $\sqrt{s} = 13 \text{ TeV}$; $\mu_F = \mu_R = m_H$

→ enhancing the discovery potential in the Higgs sector will require improving these uncertainties!

CT14 \rightarrow CT18 modestly shifts Higgs cross sections and slightly reduces PDF uncertainties

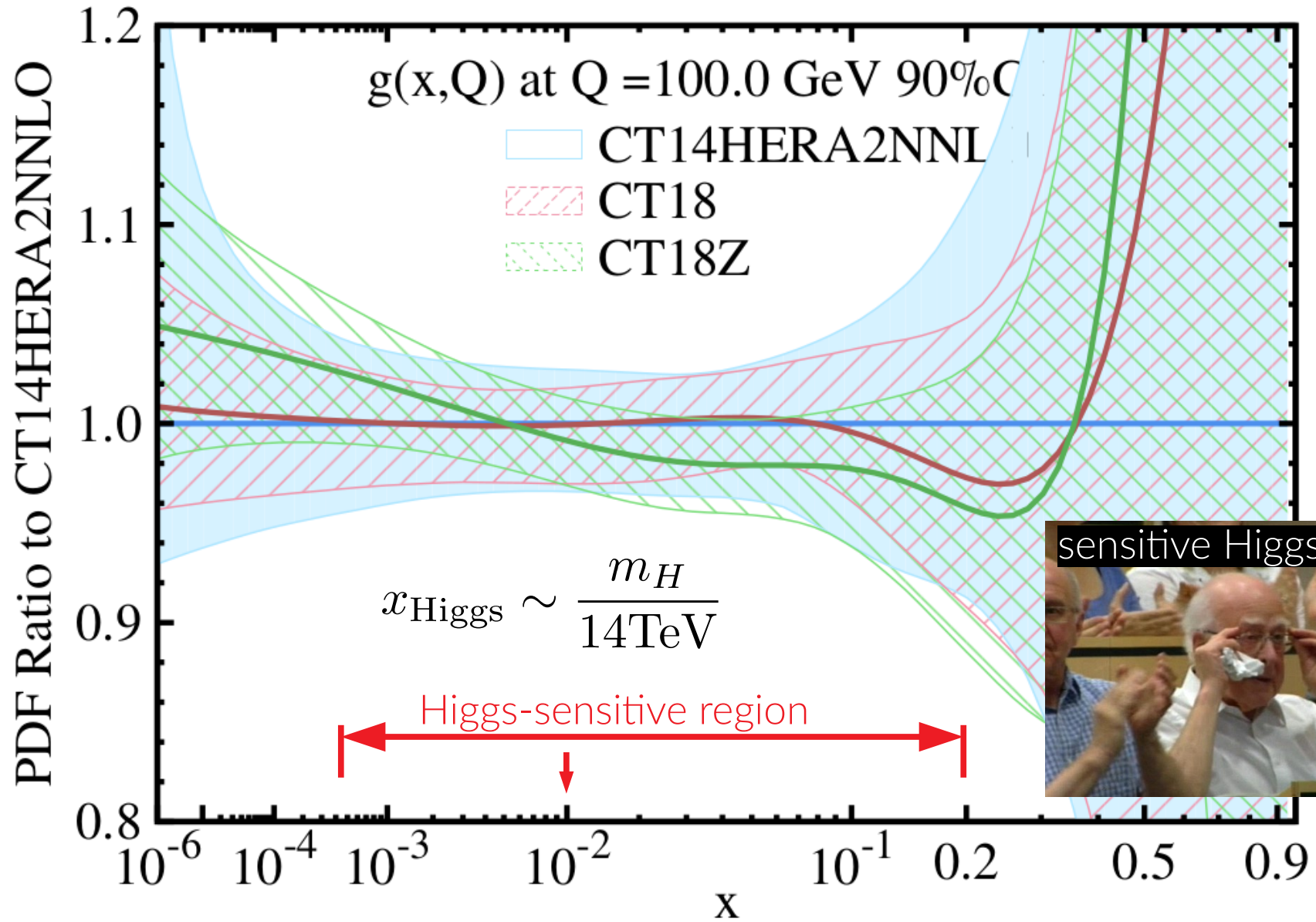


	7 TeV	
	$\sigma(\text{gg-h})$	$\delta\sigma \text{ sym}(90\% \text{C.L.})$
CT14NNLO	14.67	0.46
CT18	14.57	0.44
	8 TeV	
	$\sigma(\text{gg-h})$	$\delta\sigma \text{ sym}(90\% \text{C.L.})$
CT14NNLO	18.70	0.57
CT18	18.45	0.55
	13 TeV	
	$\sigma(\text{gg-h})$	$\delta\sigma \text{ sym}(90\% \text{C.L.})$
CT14NNLO	42.78	1.32
CT18	42.43	1.26
	14 TeV	
	$\sigma(\text{gg-h})$	$\delta\sigma \text{ sym}(90\% \text{C.L.})$
CT14NNLO	48.23	1.50
CT18	47.91	1.42

PDF induced errors (at 90% CL) are reduced by about 5% as compared to CT14 predictions.

\rightarrow can we disentangle elements of the global analysis responsible for these improvements?

LHC Run-1 gluon PDF impact in CT14 \rightarrow CT18(Z)

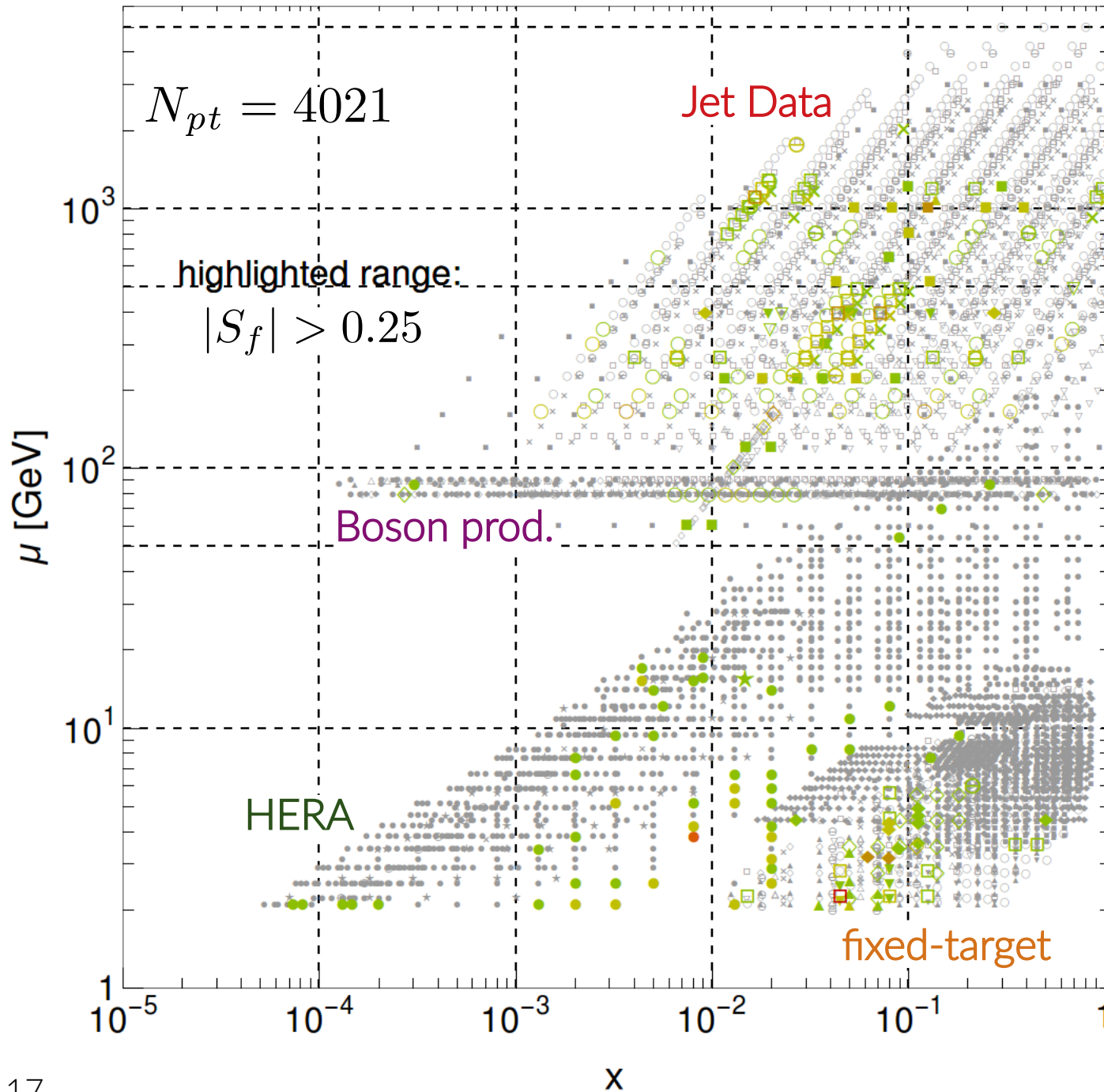


- while LHC Run-1 data drive important PDF improvements, including for the gluon at high-, low- x , the effect is relatively incremental

$|S_f|$ for σ_{H^0} 14 TeV, CT14_{HERA2} NNLO

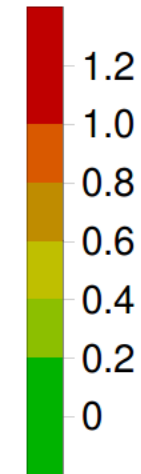
B.-T. Wang, TJH, S. Doyle, J. Gao, T.-J. Hou, P. M. Nadolsky, F. I. Olness

Phys.Rev. D98 (2018) 094030



(magnitude of PDF pull of each datum)

$|S_f|$



• after the aggregated HERA data, inclusive jet production – greatest total sensitivity!

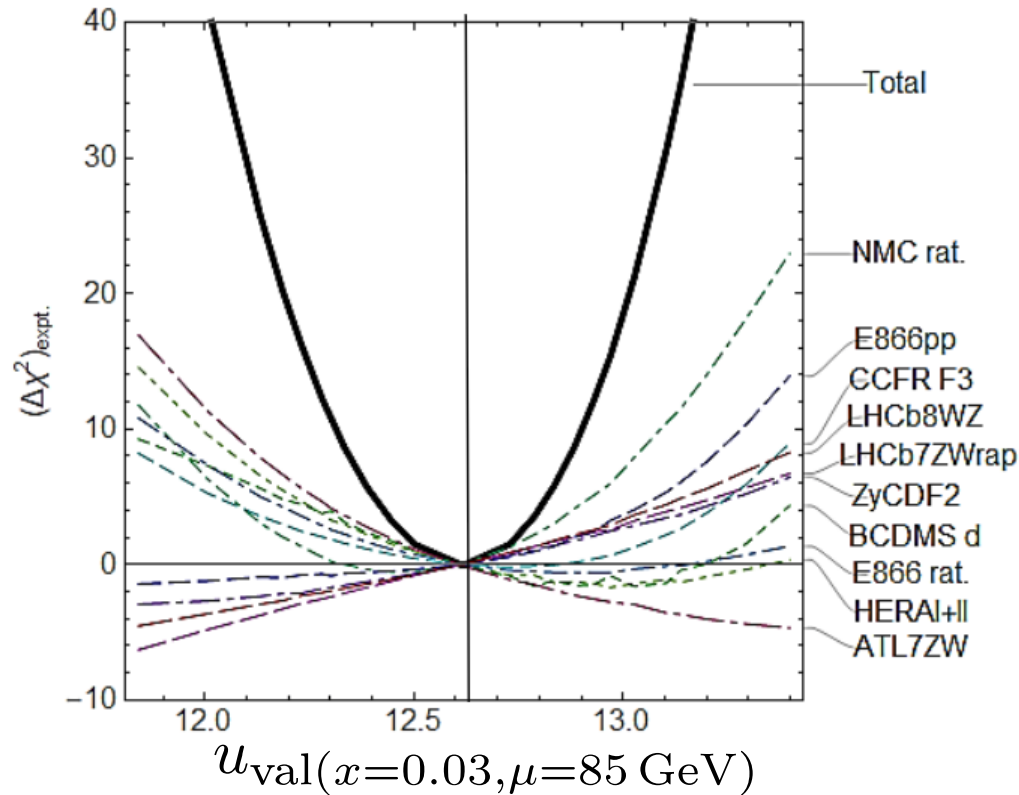
→ large correlations for E866, BCDMS, CCFR, CMS WASY, Z p_T and $t\bar{t}$ production, but smaller numbers of highly-sensitive points

the compatibility of data sets is a crucial issue

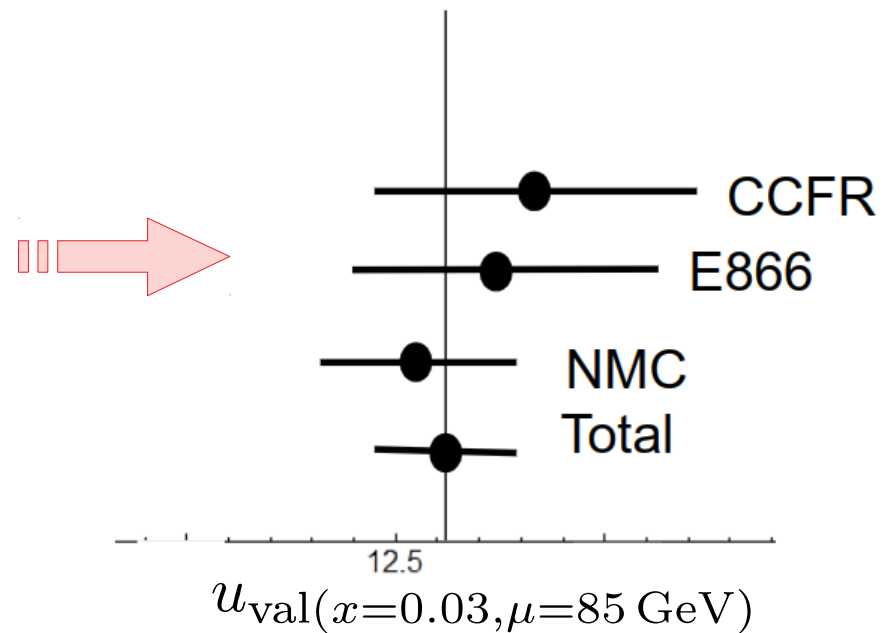
→ within a given QCD fit, data can pull in **competing directions**

'Lagrange Multiplier scan'

CT18Z NNLO



this is a serious impediment to higher precision in PDF/SM predictions



examine the change in χ^2 as a PDF is continuously varied away from its fitted central value

Can repeat for s_2w , M_W , ...

18 → computing these χ^2 growth profiles is VERY computationally costly

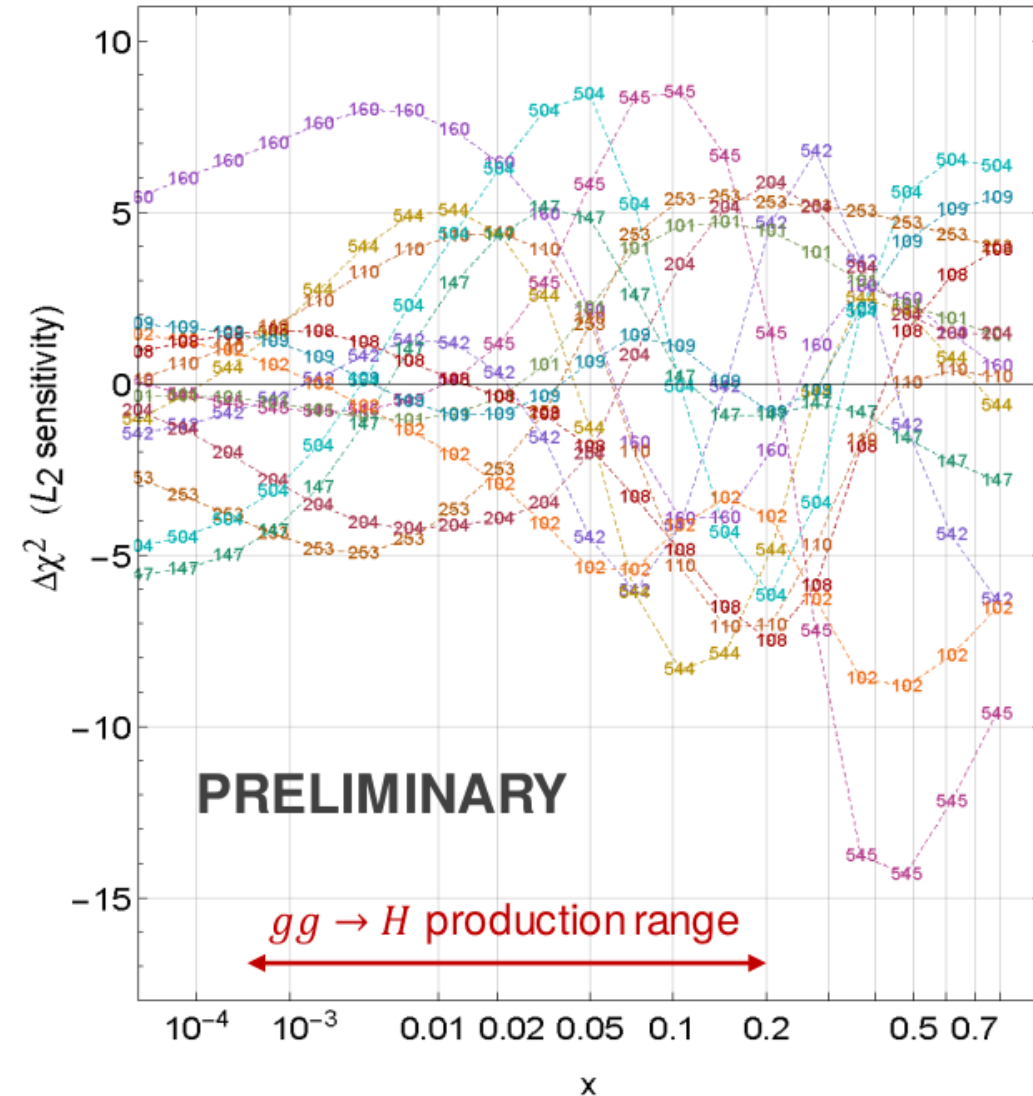
Estimated χ^2 pulls from experiments

(L_2 sensitivity, arXiv:1904.00222, v. 2)

CT18 NNLO, $g(x, 100 \text{ GeV})$

...appearing shortly in Phys. Rev. D

CT18 NNLO, gluon at $Q=100 \text{ GeV}$



Most sensitive experiments

- 253--- ATL8ZpTbT
- 542--- CMS7jtR7y6T
- 544--- ATL7jtR6uT
- 545--- CMS8jtR7T
- 160--- HERAplI
- 101--- BcdF2pCor
- 102--- BcdF2dCor
- 108--- cdhswf2
- 109--- cdhswf3
- 110--- ccfrf2.mi
- 147--- Hn1X0c
- 204--- e866ppxf
- 504--- cdf2jtCor2

stronger
(anti-)
correlation

Experiments with large $\Delta\chi^2 > 0$ [$\Delta\chi^2 < 0$]
pull $g(x, Q)$ in the negative [positive]
direction at the shown x

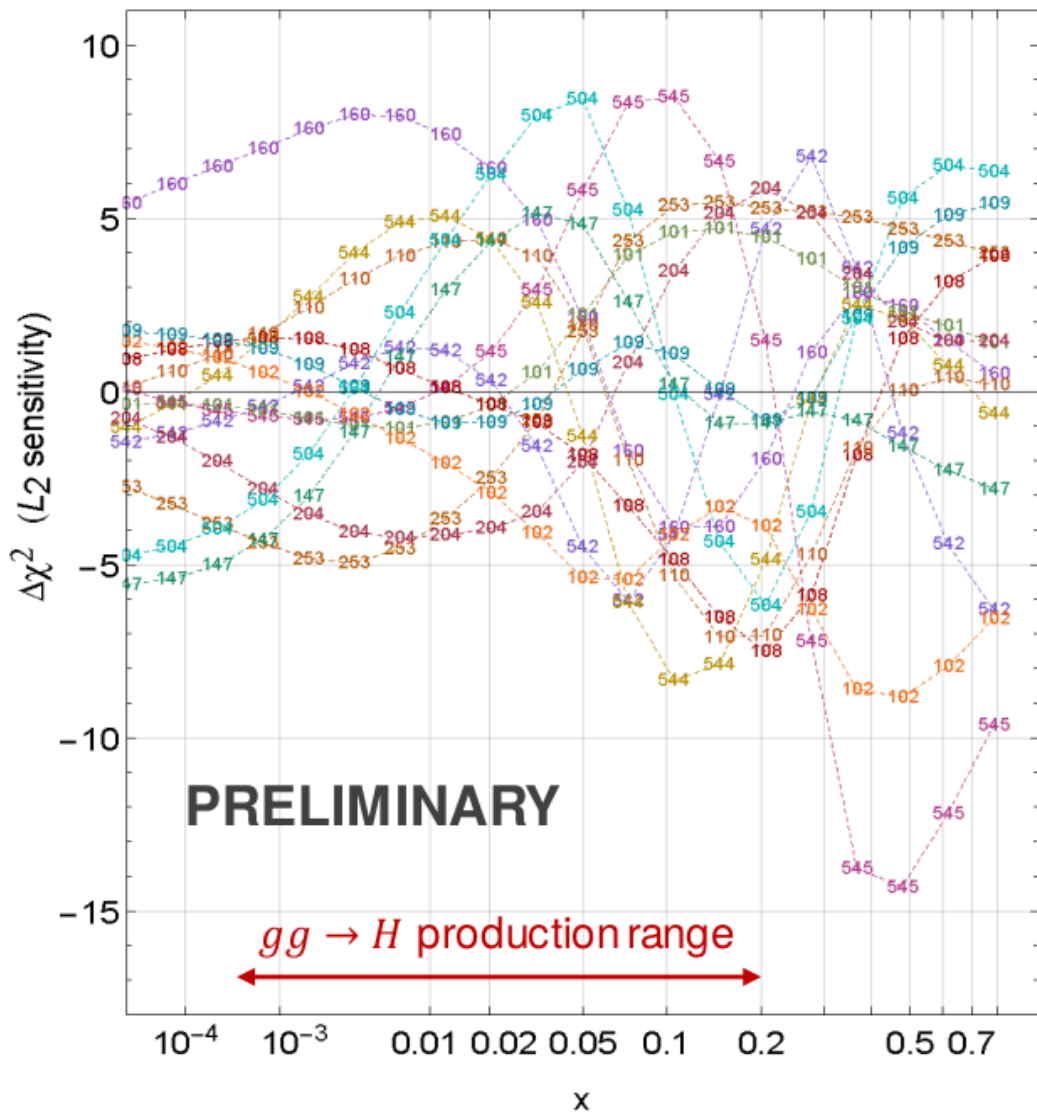
Estimated using CT18 Hessian PDFs

$$S_{f,L_2} \sim \text{Corr}[f_a, \chi_E^2]$$

Estimated χ^2 pulls from experiments

(L_2 sensitivity, arXiv:1904.00222, v. 2)

CT18 NNLO, $g(x, 100 \text{ GeV})$



precise data from EIC sensitive to the gluon PDF Higgs region needed to help unravel the systematic tensions evident here

Most sensitive experiments

- 253--- ATL8ZpTbT
- 542--- CMS7jtR7y6T
- 544--- ATL7jtR6uT
- 545--- CMS8jtR7T
- 160--- HERAplI
- 101--- BcdF2pCor
- 102--- BcdF2dCor
- 108--- cdhswf2
- 109--- cdhswf3
- 110--- ccrf2.mi
- 147--- Hn1X0c
- 204--- e866ppxf
- 504--- cdf2jtCor2

PRELIMINARY

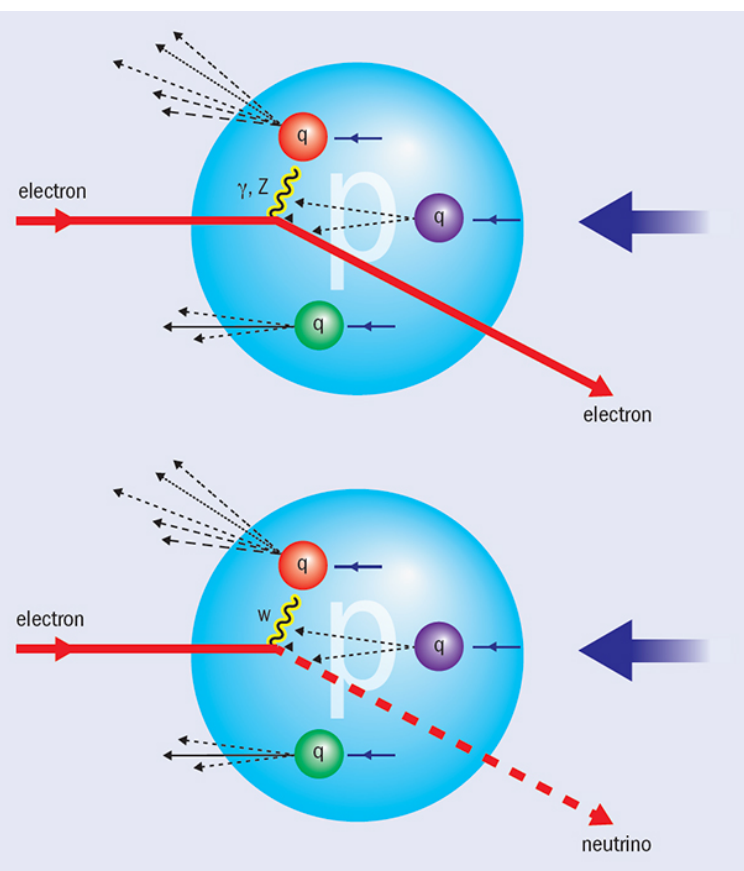
$gg \rightarrow H$ production range

$$S_{f,L_2} \sim \text{Corr}[f_a, \chi_E^2]$$

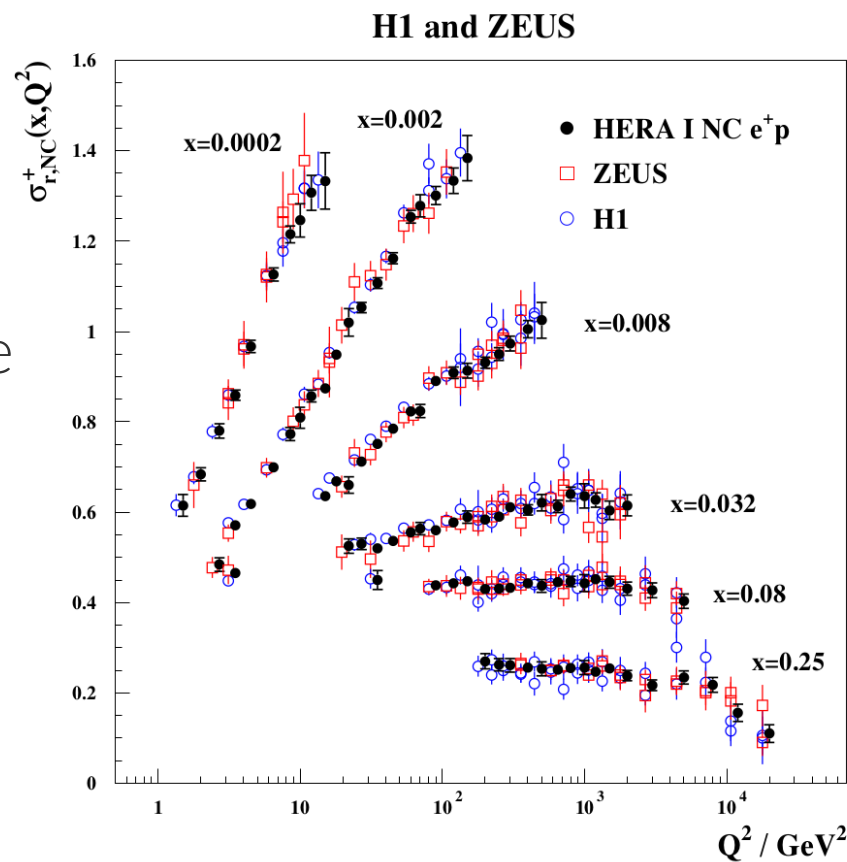


we require a high-precision experimental arbiter

- given the landscape of experiments with variable compatibility: clean, high-statistics DIS collider data from the EIC would serve as an empirical anchor-point to negotiate tensions among data
- a historical antecedent exists for this: **HERA** – the only previous DIS collider



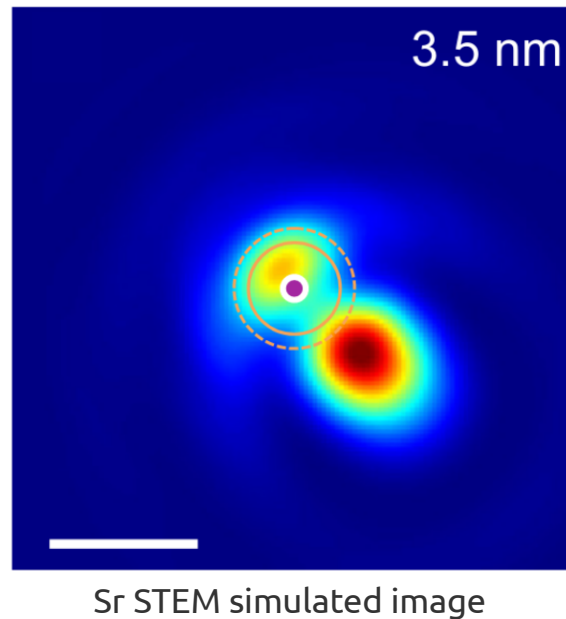
the need to describe a wide reach of DIS data provides a kinematical 'lever arm' on QCD evolution



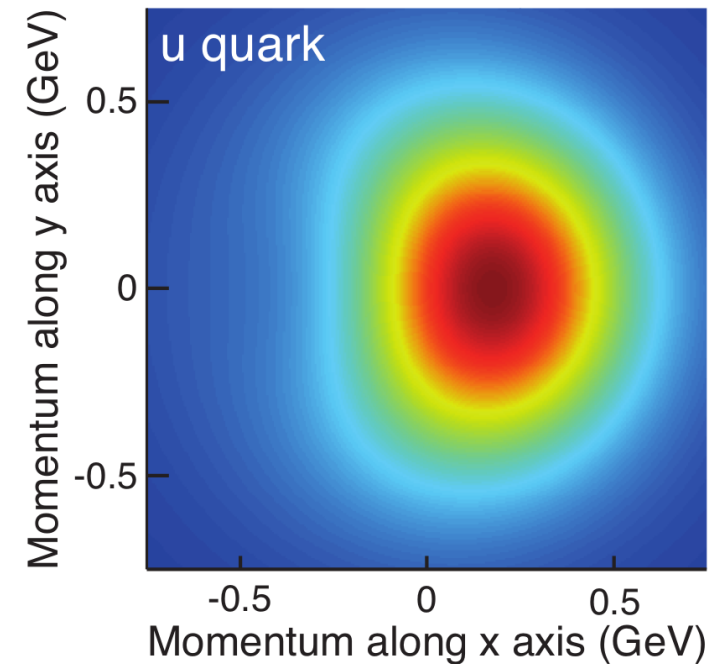
the view from hadronic physics: era of tomography

- the present moment is in many ways reminiscent of the situation in atomic structure theory in the early 20th Century:

Jeong et al., PRB93, 165140 (2016).



Accardi et al., EPJA52 (2016) no.9, 268.



- much as a synthesis of quantum mechanics, electromagnetism, and microscopy deliver modern mapping of atomic structure, a union of high-level theory, QCD, and "femtoscscopy" promises multidimensional imaging of hadron structure

... this is enshrined in the *2015 Nuclear Science Advisory Committee LRP*

→ **AND motivation for JLab12, RHIC program, and EIC**

EIC is the **essential future tool** for hadron tomography and QCD

following an expansive community effort

The National
Academies of
SCIENCES
ENGINEERING
MEDICINE

THE NATIONAL ACADEMIES PRESS

This PDF is available at <http://nap.edu/25171>

SHARE



Summer 2018

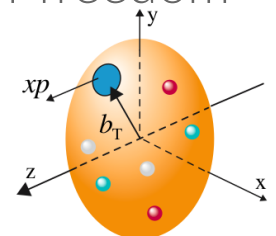


An Assessment of U.S.-Based Electron-Ion Collider Science

“In summary, the committee finds a compelling scientific case for such a facility. The science questions that an EIC will answer are central to completing an understanding of atoms as well as being integral to the agenda of nuclear physics today.”

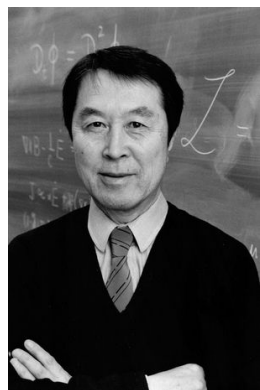
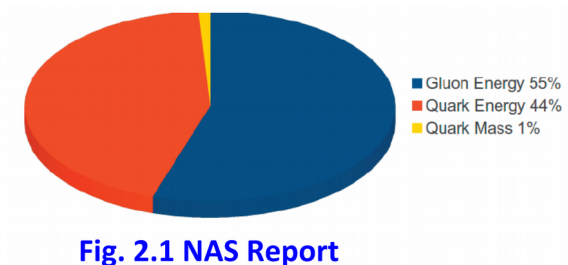
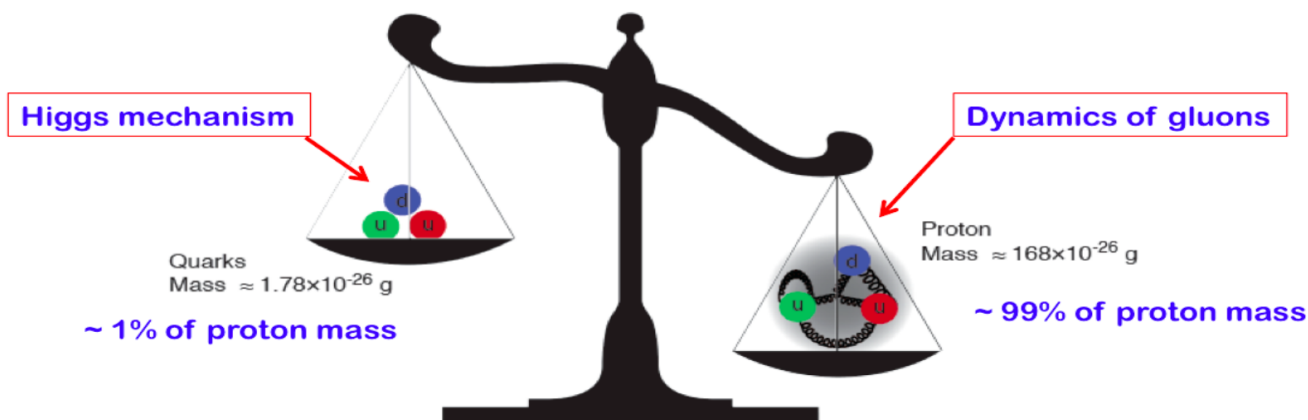
“Top-level” physics objectives – **connecting the bulk properties of hadrons to a parton-level description:**

- the origin of nucleon mass and spin in partonic degrees of freedom
- understanding gluonic systems in the high-density limit
- imaging the nucleon’s **multi-dimensional structure**



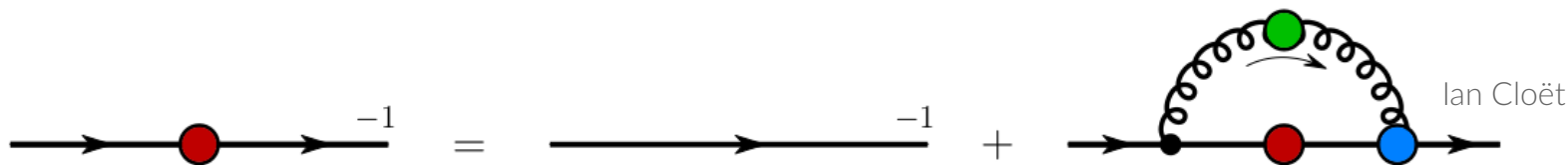
a full understanding of QCD bound states is still forthcoming

→ e.g., the Higgs mechanism accounts for **very little** of the mass of the visible universe



Y. Nambu

QCD has a gap equation through which the dynamics of chiral symmetry breaking generate large masses, e.g., of the bound quark



→ the full mass decomposition involves multiple contributions,

$$M_p = E_q + E_g + \chi_{m_q} + T_g$$

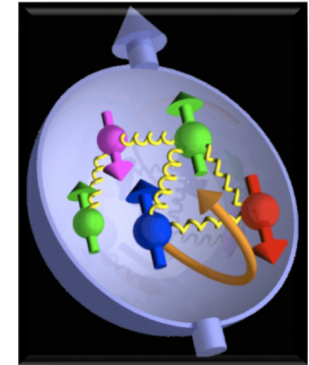
23 ...direct measurement can resolve contribution from quark-gluon motion

an array of other fundamental QCD issues must be tested; e.g.:

→ can we come up with the spin of the proton from quarks/gluons??

$$\frac{1}{2} = \frac{1}{2} \Delta \Sigma + \Delta G + (L_q + L_g)$$

quark spin gluon spin orbital angular momentum

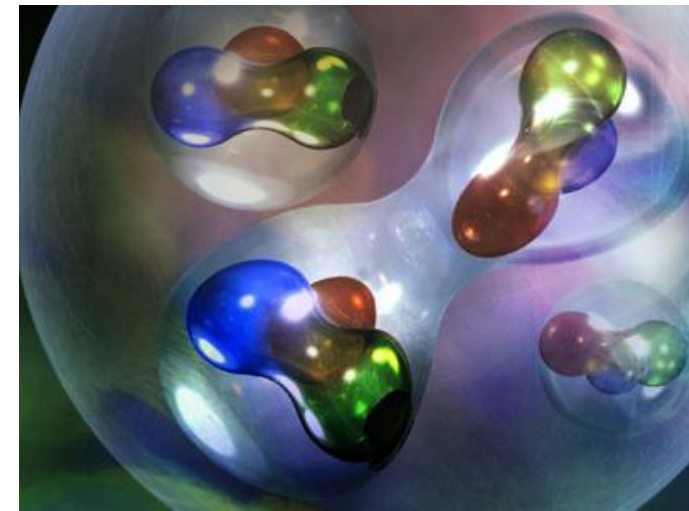


(see talk, Boughezal.)

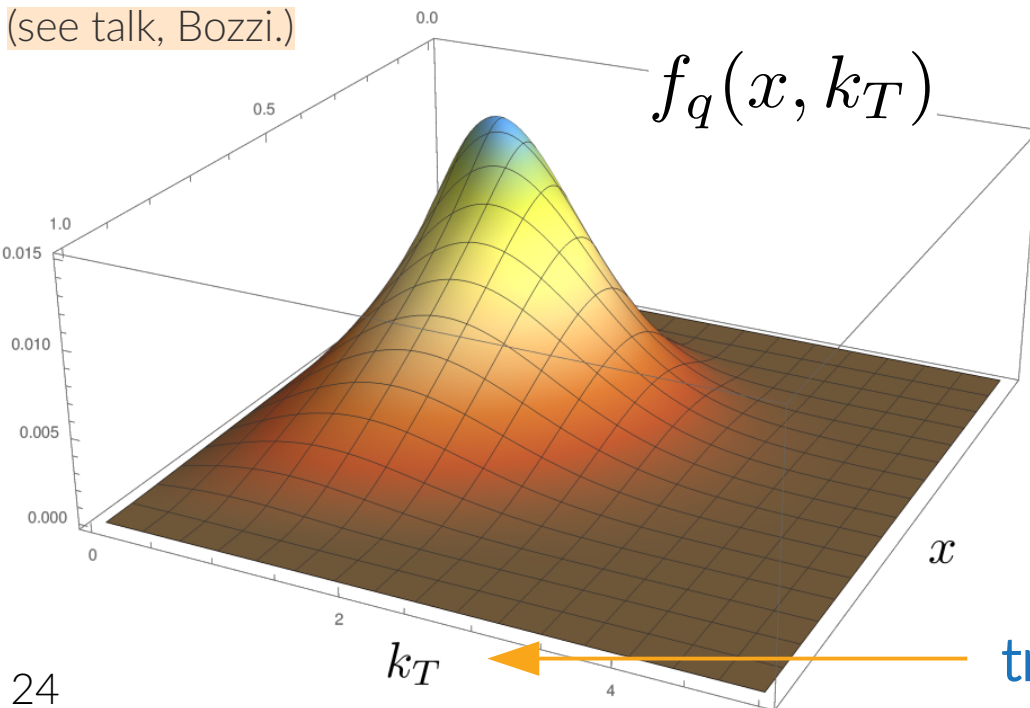
→ how do nucleons deform once embedded inside a nucleus (medium effects)?

(see talks, Zurek, Li, Loizides.)

answering these (and other) questions requires knowing how quarks/gluons are distributed in **more than 1D**



(see talk, Bozzi.)



$$f_q(x) = \int dk_T f_q(x, k_T)$$

i.e., related to the PDFs

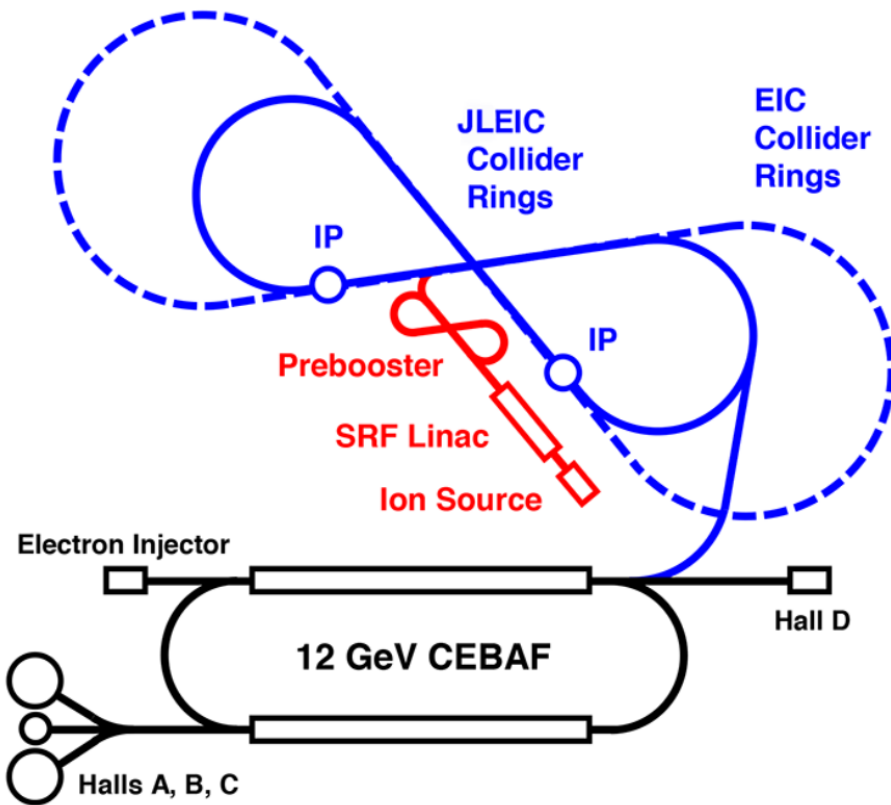
transverse momentum dependence!

the EIC will be a very high-luminosity DIS collider

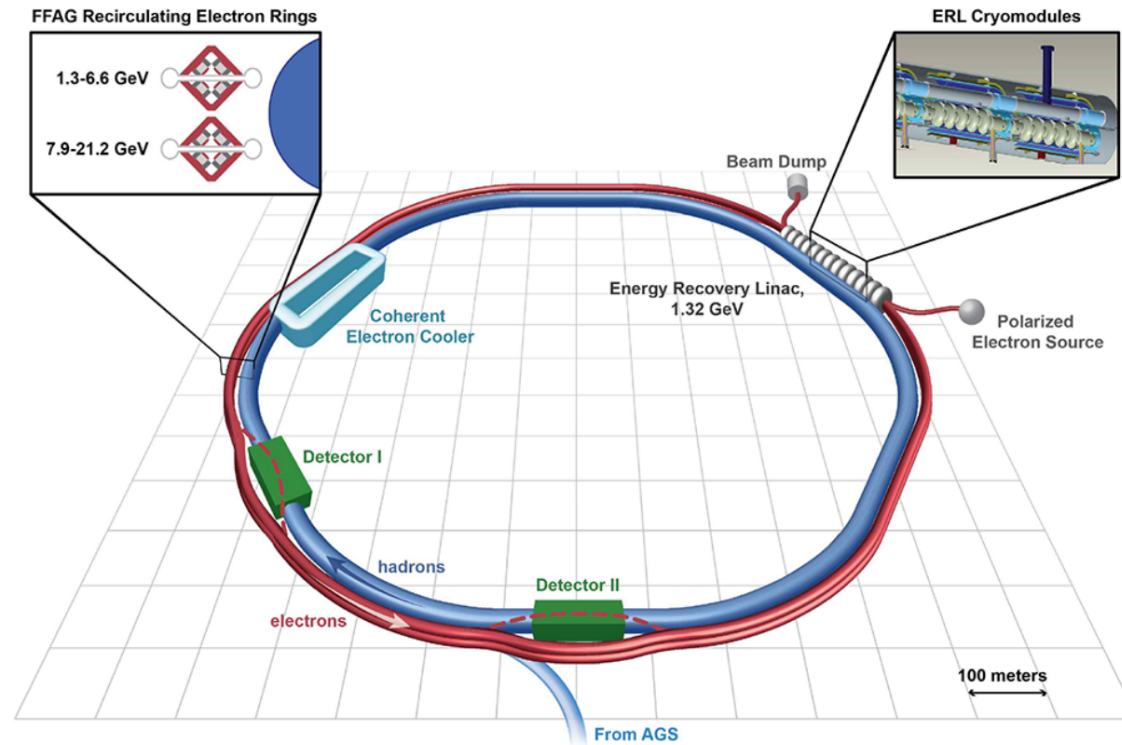
Jefferson Lab concept, JLEIC

Brookhaven concept, eRHIC

(see talks, Deshpande, Aschenauer.)



→ add Ion source, collider rings to existing electron accelerator (CEBAF)



→ add electron source, storage ring to existing heavy-ion collider complex (RHIC)

these designs share many essential features

EIC: the vital design aspects

- EIC is a **very high luminosity** “femtoscope” – larger compared to HERA luminosities by a factor of $10^2 - 10^3$
- reach in center-of-mass energy, $10 \leq \sqrt{s} \leq \underline{100 \text{ GeV}}$ ↘
→ upgradeable to $\sqrt{s} \leq \underline{140 \text{ GeV}}$
- beam polarization of at least $\sim 70\%$ for e^- , p , light A

- as a generic scenario, we consider here the simulated impact of a machine with:
 $10 \text{ GeV } e^\pm$ on $250 \text{ GeV } p$ ($\sqrt{s} = 100 \text{ GeV}$)

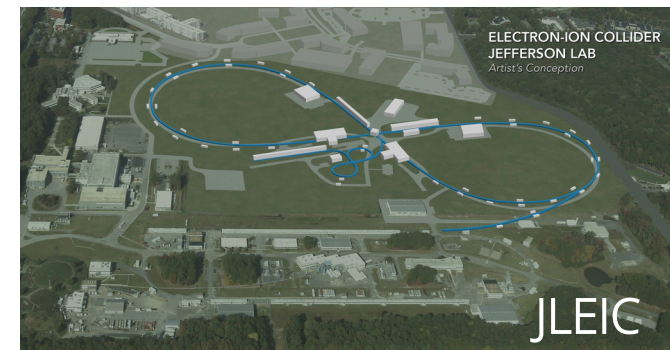
~year of data-taking

{

$\mathcal{L} = 100 \text{ fb}^{-1} e^-$ pseudodata
 $\mathcal{L} = 10 \text{ fb}^{-1} e^+$ pseudodata

→ NC/CC

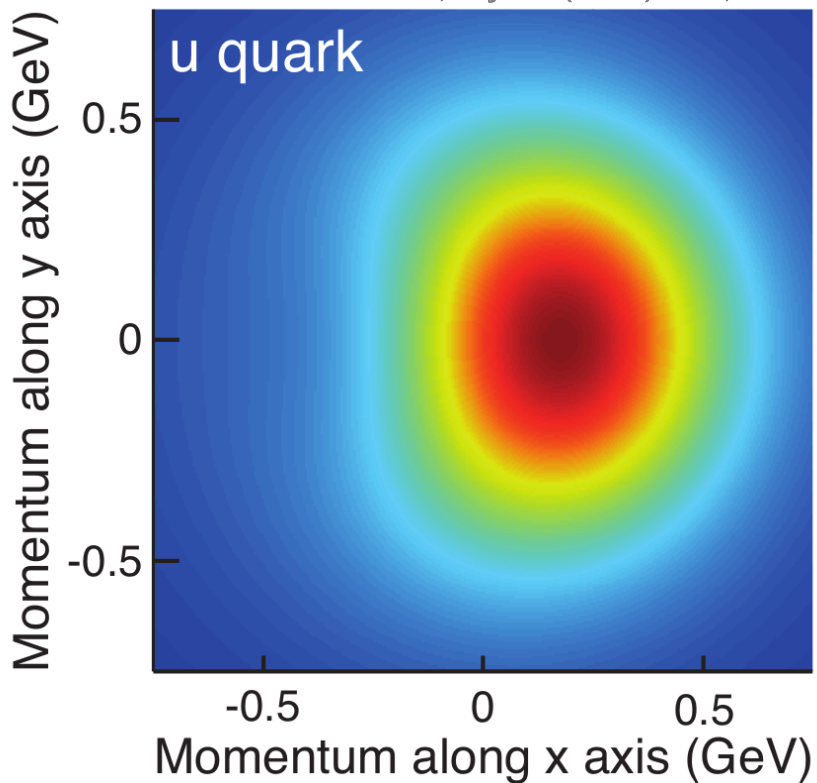
- EIC will map the few GeV **quark-hadron transition** region
- á la HERA, the combination of precision & kinematic coverage provide constraining ‘lever arm’ on QCD evolution
- QCD evolution: (**high x , low Q**) ↔ (**low x , high Q**)



the EIC tomography program will deliver high-precision DIS

- by measuring the nucleon's multi-dimensional wave function with high precision, the EIC will hugely constrain proton collinear structure

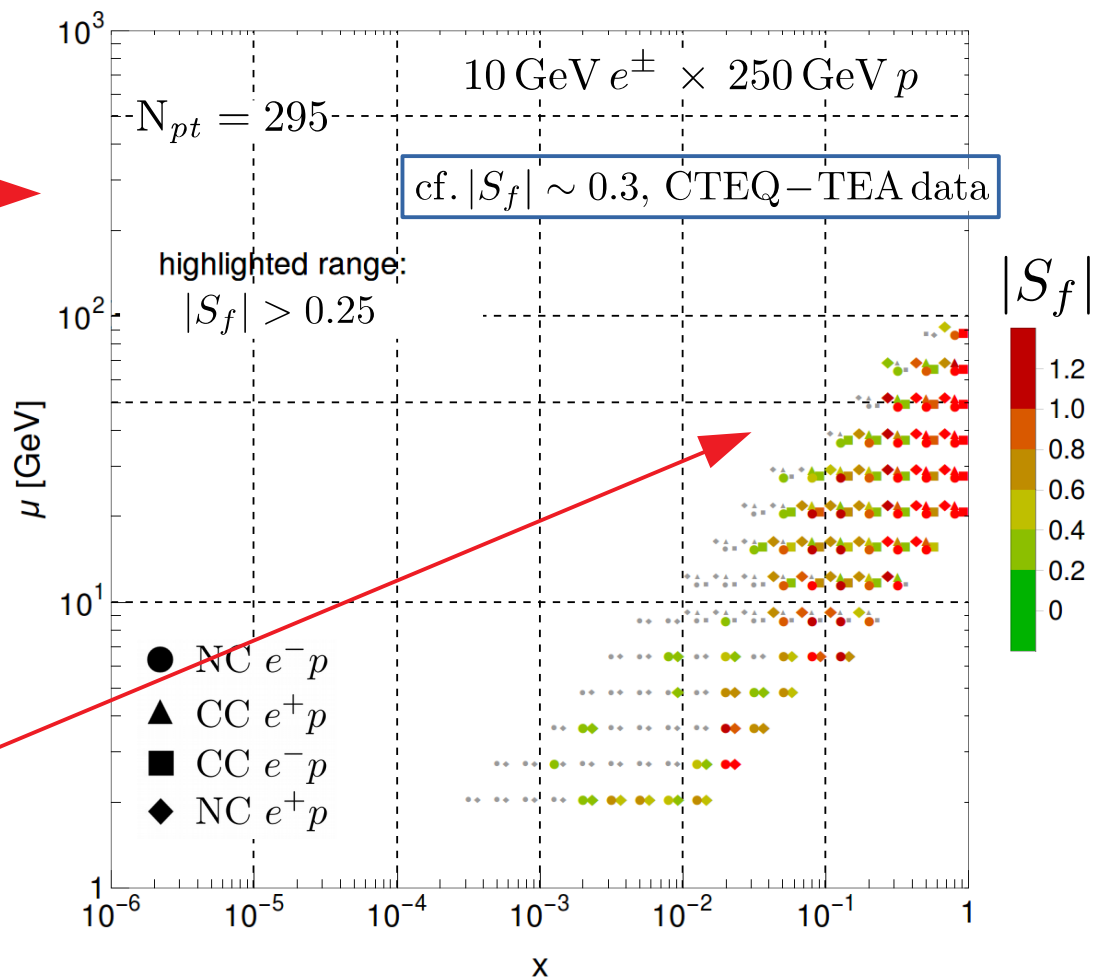
Accardi et al., EPJA52 (2016) no.9, 268.



PROJECTED IMPACT OF EIC PSEUDO-DATA VERY LARGE - RED SIMULATED MEASUREMENTS



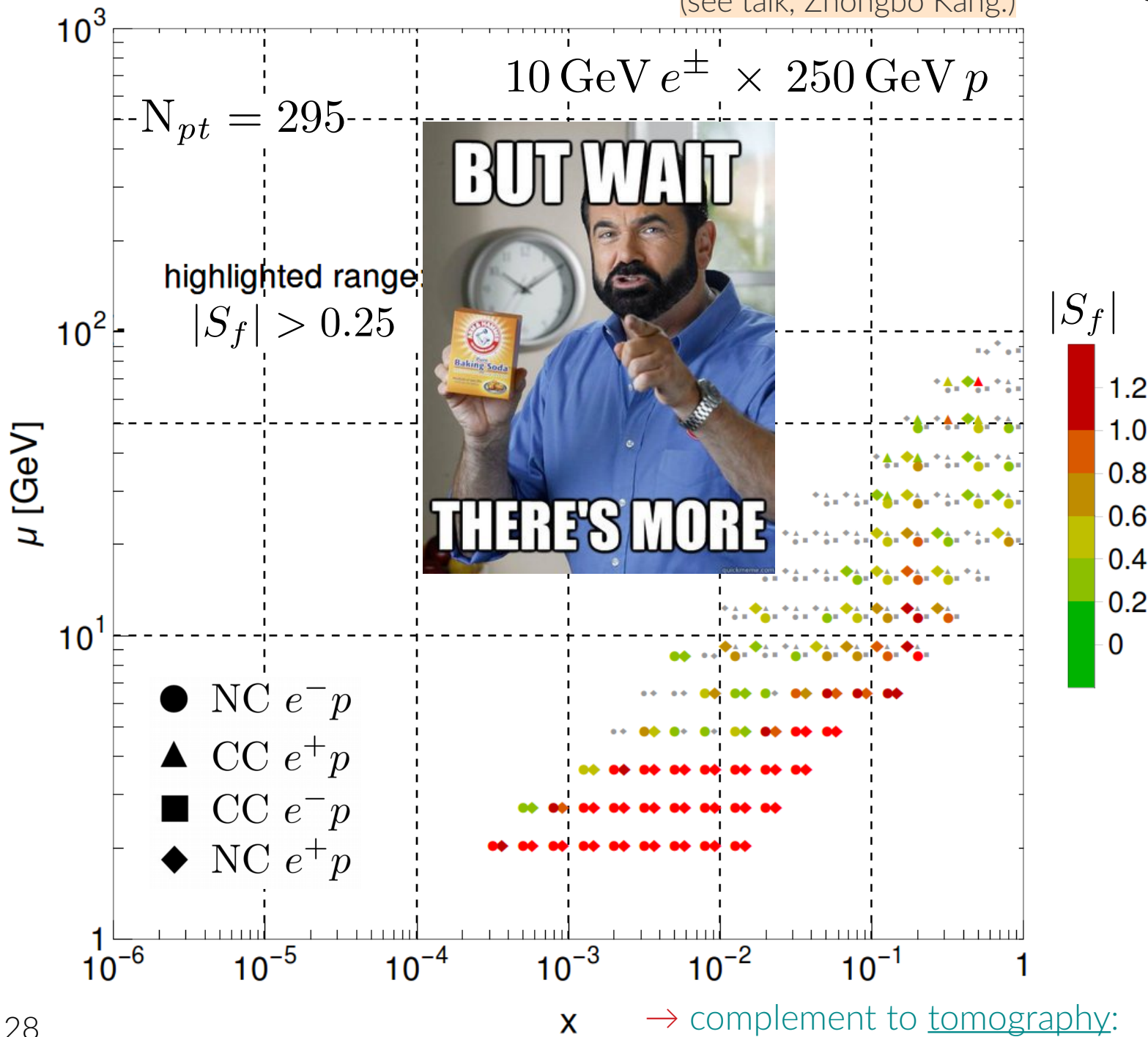
$|S_f|$ for $d/u(x, \mu)$, CT14_{HERA2} NNLO



- DIS cross sections from EIC will supercede the bulk of fixed-target information in contemporary QCD fits; provide an 'anchor-point' to resolve systematic PDF tensions

$|S_f|$ for $g(x, \mu)$ CT14 HERA2 NNLO

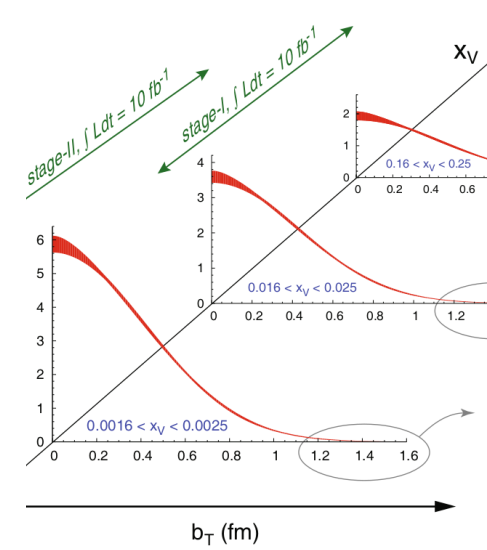
(see talk, Zhongbo Kang.)



- an EIC will provide a sensitive probe to the gluon distribution – especially at low x

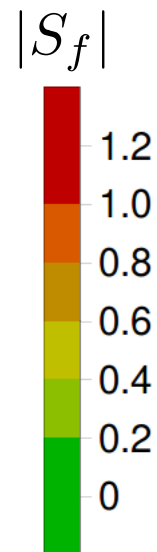
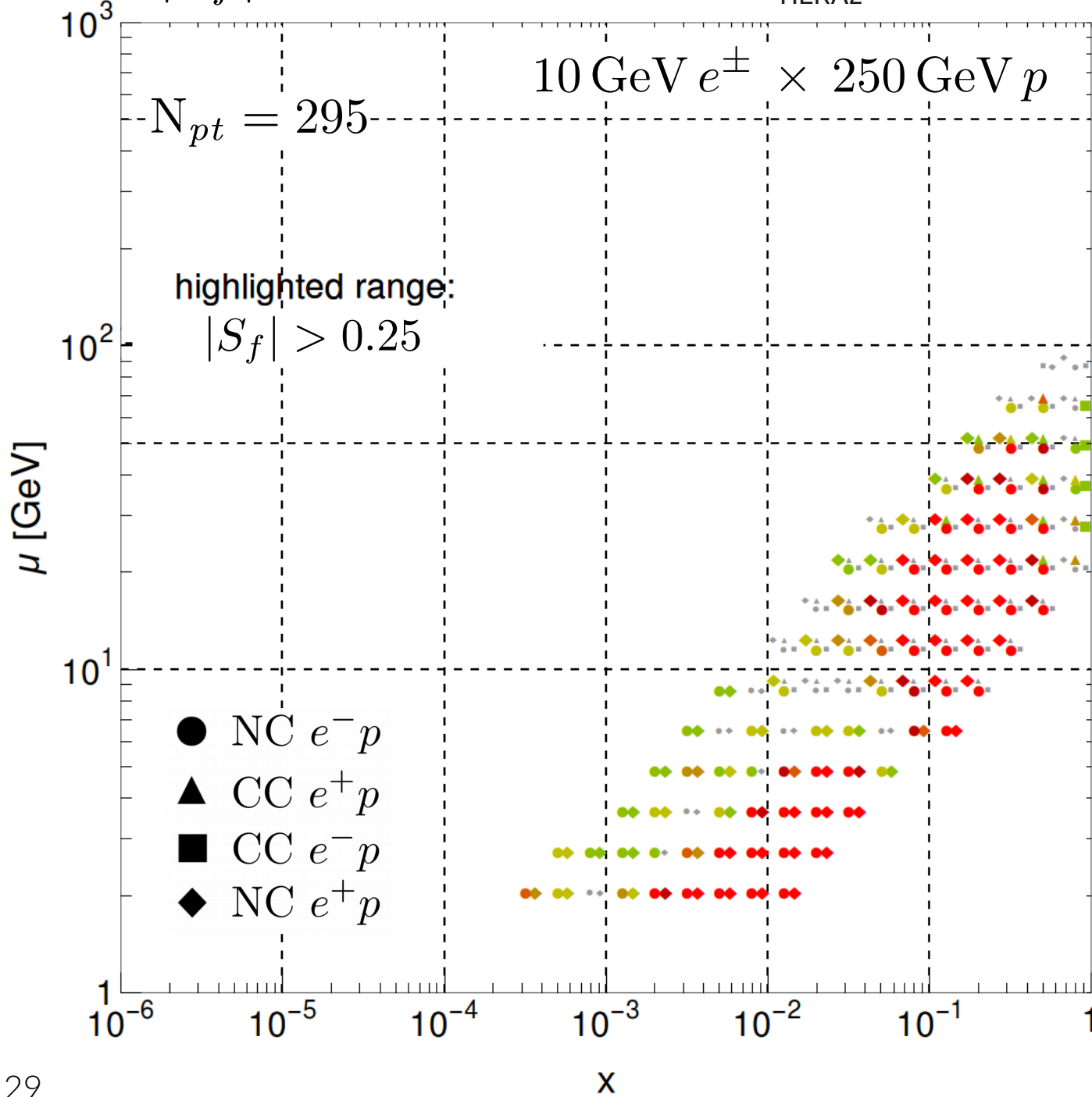
$$x \gtrsim 3 \times 10^{-4}$$

- these constraints arise from high statistics neutral current data on $\sigma_{r,NC}^{e^\pm p}$



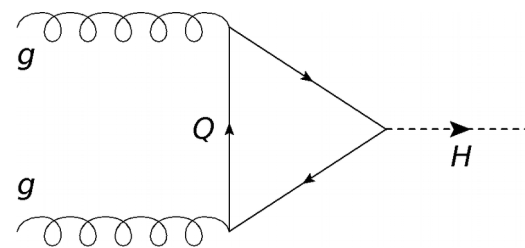
$|S_f|$ for σ_H , 14 TeV CT14_{HERA2} NNLO

strong predicted impact on the Higgs sector



- the impact of an EIC upon the theoretical predictions for inclusive Higgs production arises from a very broad region of the kinematical space it can access

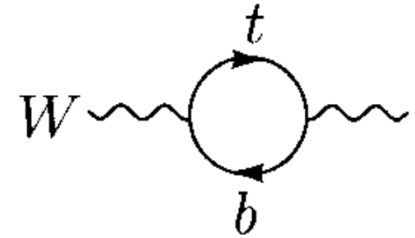
- impact rather closely tied to that of the integrated gluon PDF:



m_W as a sensitive window to BSM physics

- m_W is sensitive to the gauge couplings and masses of heavy SM degrees of freedom, which enter a correction term, Δr

$$m_W^2 \left(1 - \frac{m_W^2}{m_Z^2} \right) = \frac{\pi\alpha}{\sqrt{2}G_\mu} (1 + \Delta r)$$



↑
higher-order corrections

- extended theories **also** generate contributions to Δr through BSM insertions

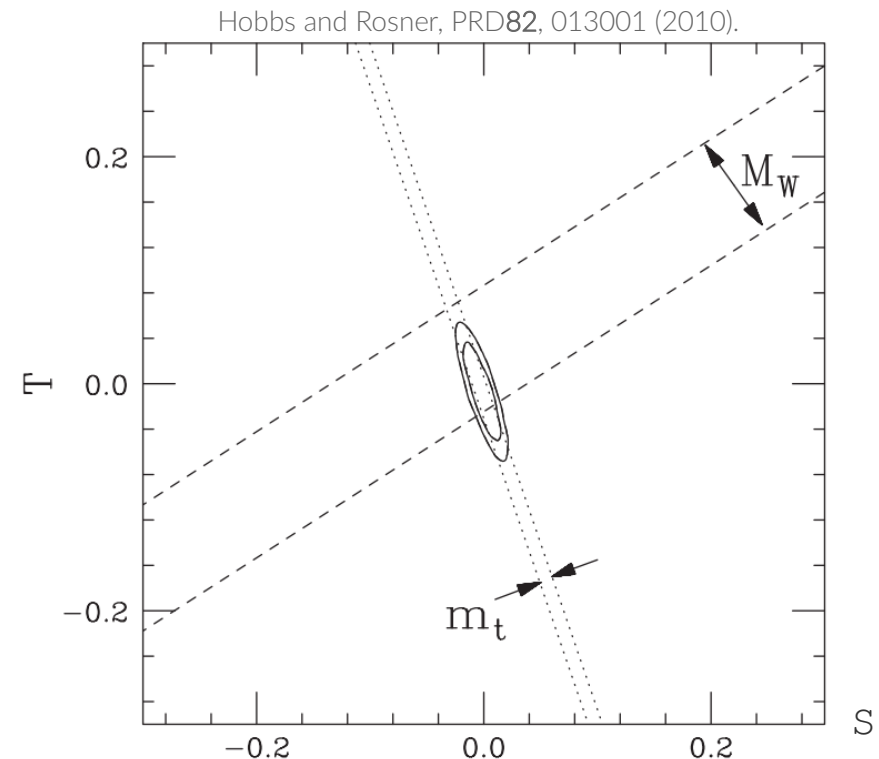
- strategy:** careful comparison of precise measurements with theoretical SM predictions could reveal presence of BSM physics

→ constrain New Physics with a global fit of the electroweak sector:

→ m_W is a crucial limitation

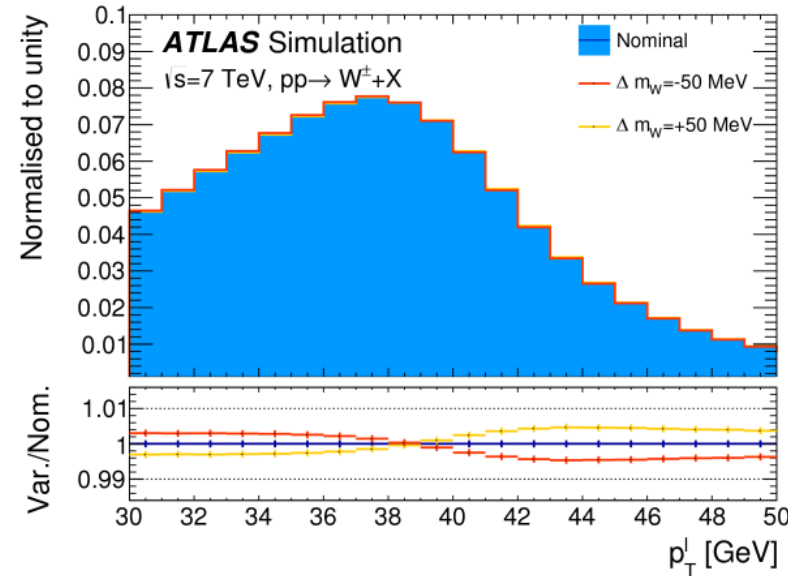
→ important interplay between pp , ν expts

$Q_W(\text{Cs})$
 $M_W(\text{GeV}/c^2)$
 $g_L^2(\nu\text{NC})$
 $g_R^2(\nu\text{NC})$
 $\Gamma_{ll}(Z) (\text{MeV})$
 $\sin^2 \theta^{\text{eff}}$
 m_t
 $\sigma(\nu_\mu)e^-$



strategy for experimentally extracting m_W

- Measurements of distributions sensitive to m_W :
 - Decay lepton $p_T(l)$, W transverse mass m_T , missing transverse energy p_T ("neutrino p_T ") as cross check
- Template-Fit approach:
 - 1) vary m_W in MC and predict the $p_T(l)$, m_T , p_T^{miss} distributions
 - 2) m_W determination by χ^2 minimization to data
- Imperfect QCD modelling distorts templates: significant uncertainty on m_W measurement



- W mass is measured in m_T and $p_T(l)$ distributions in electron and muon channels for W^+ , W^- in different η bins and then these measurements are combined

Decay channel	$W \rightarrow e\nu$
Kinematic distributions	p_T^l, m_T
Charge categories	W^+, W^-
$ \eta_e $ categories	$[0, 0.6], [0.6, 1.2], [1.8, 2.4] \quad [0, 0.8]$

- Transfer of experimental calibration and QCD modeling
 - Large and pure Z sample for detector calib., and well modeled
 - Predictions are fit to Z data to improve modeling and templates



Alessandro Tricoli, ATLAS

EIC and an era of (higher) precision electroweak physics

- theory predictions for the production of gauge bosons are quite sensitive to the nucleon PDFs: e.g., $d(x)$ at $x \sim 1$, which is poorly constrained

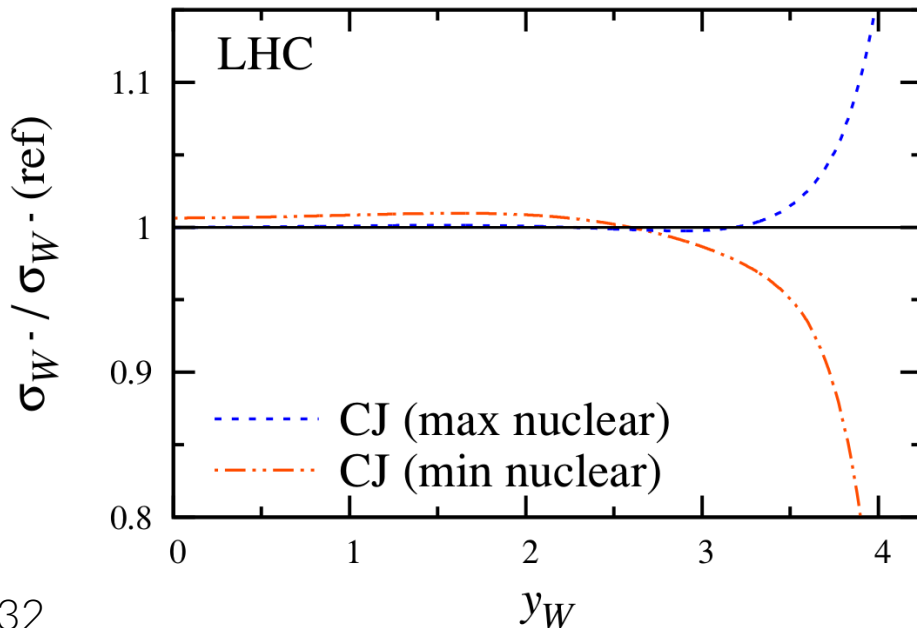
(see talk, Sanghwa Park.)

$$x_{1,2} = \frac{M}{\sqrt{s}} e^{\pm y}$$

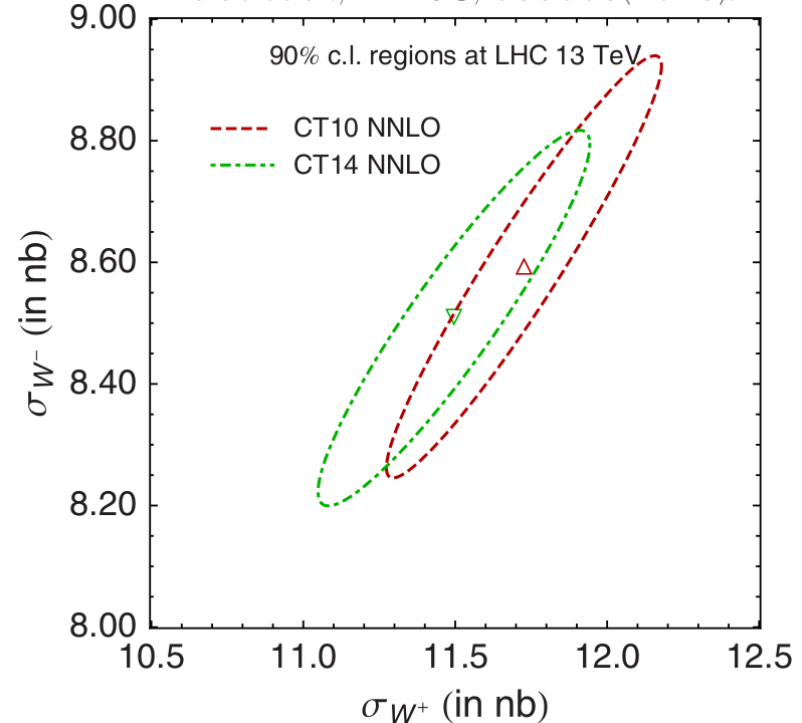
$$\frac{d\sigma}{dy}(pp \rightarrow W^- X) = \frac{2\pi G_F}{3\sqrt{2}} x_1 x_2 \left(\cos^2 \theta_C \{ d(x_1) \bar{u}(x_2) + \bar{u}(x_1) d(x_2) \} + \sin^2 \theta_C \{ s(x_1) \bar{u}(x_2) + \bar{u}(x_1) s(x_2) \} \right)$$

d -type quark distributions are especially problematic

Brady et al., JHEP06 (2012) 019.



Dulat et al., PRD93, 033006(2016).



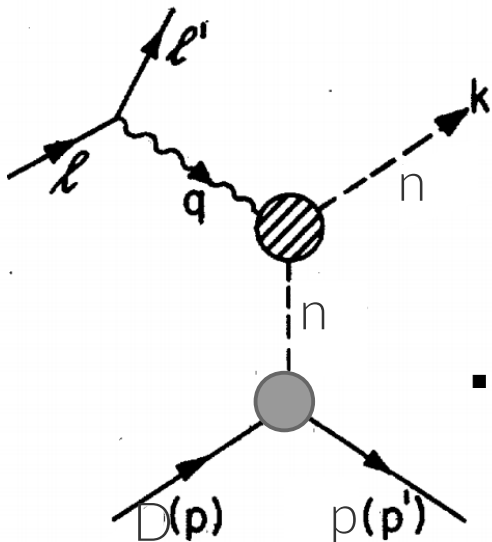
historically, extractions of $d(x)$, $x \rightarrow 1$ have depended on nuclear targets
(and corrections!)

- in principle, a neutron target would allow the flavor separation needed to access $d(x, Q^2)$

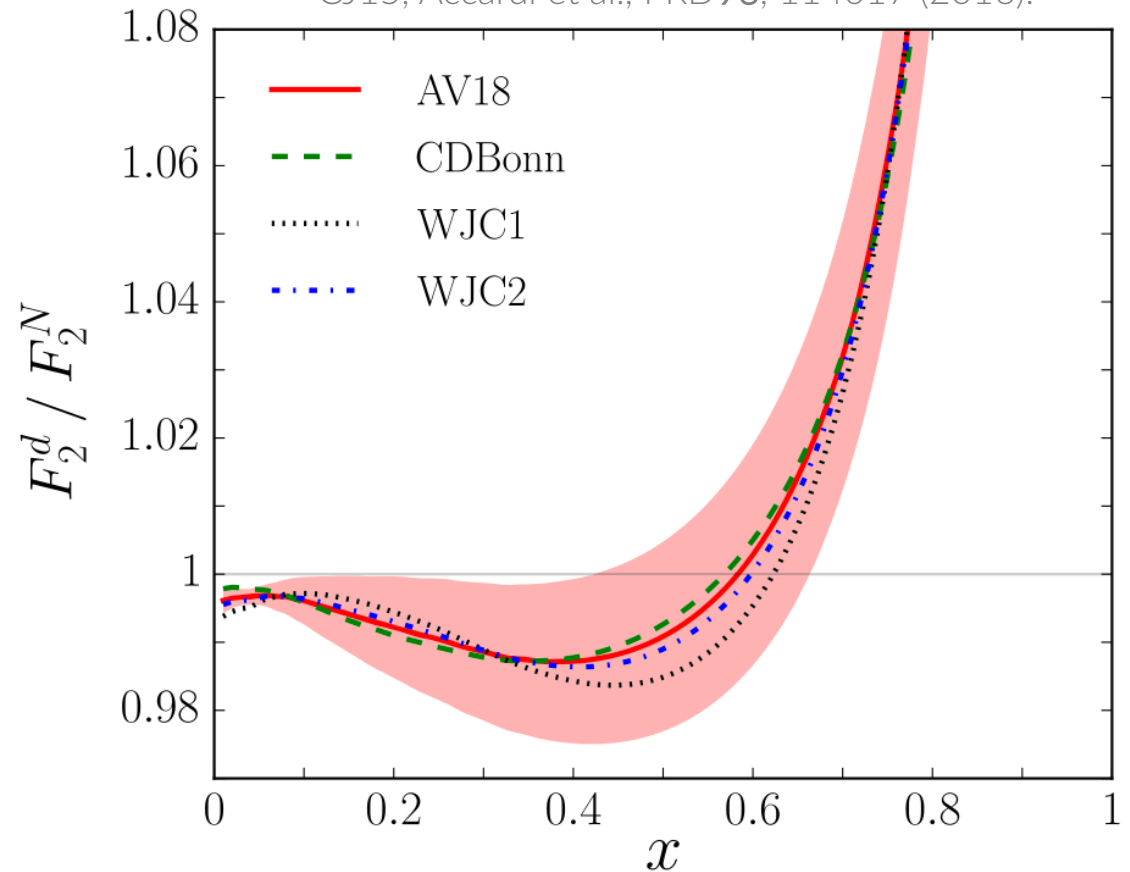
$$F_2^{e^- n} \sim x(4d + u)/9$$

— *vs* —

$$F_2^{e^- p} \sim x(4u + d)/9$$



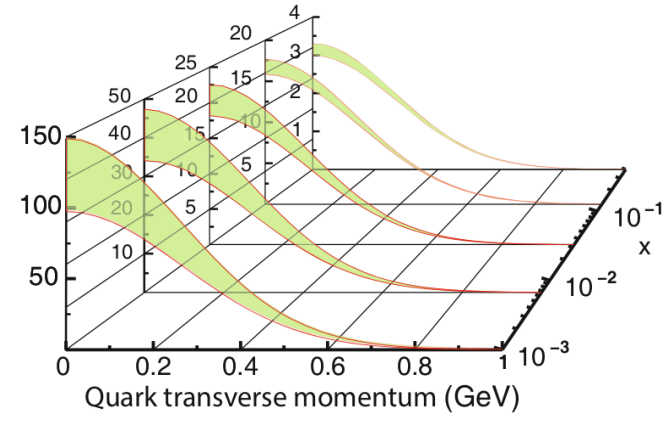
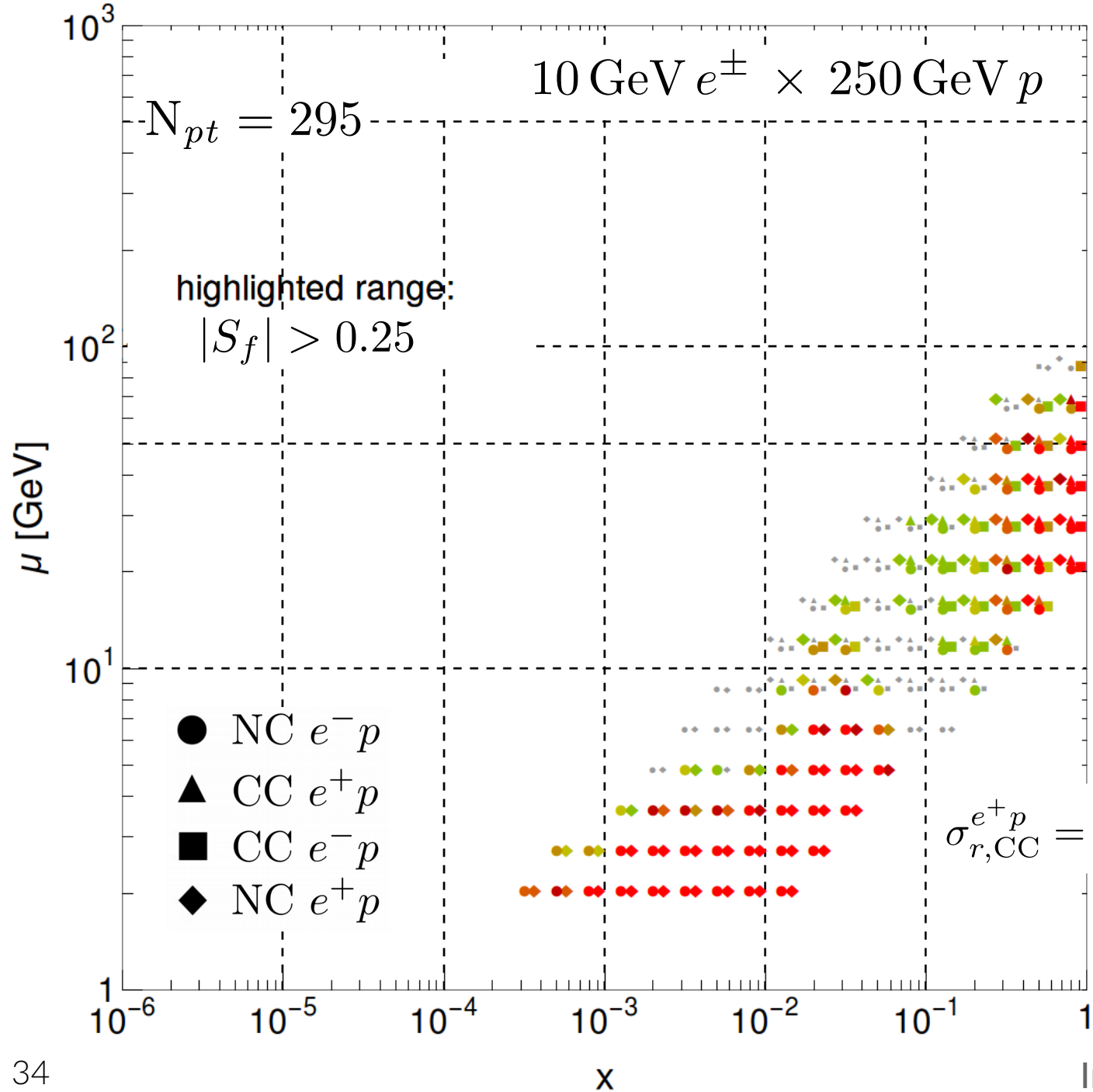
CJ15, Accardi et al., PRD93, 114017 (2016).



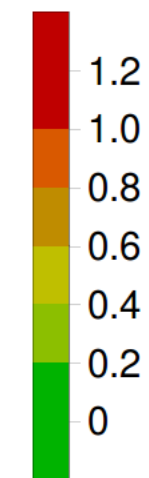
- BUT:** in the absence of a free neutron target, scattering from nuclei (e.g., the deuteron) is necessary

→ **nuclear corrections (Fermi motion) are sizable, especially for large x**

$|S_f|$ for $d(x, \mu)$ CT14 HERA2 NNLO



$|S_f|$



- an EIC affords **strong sensitivities without a nuclear target**; here, at both very high and very low x

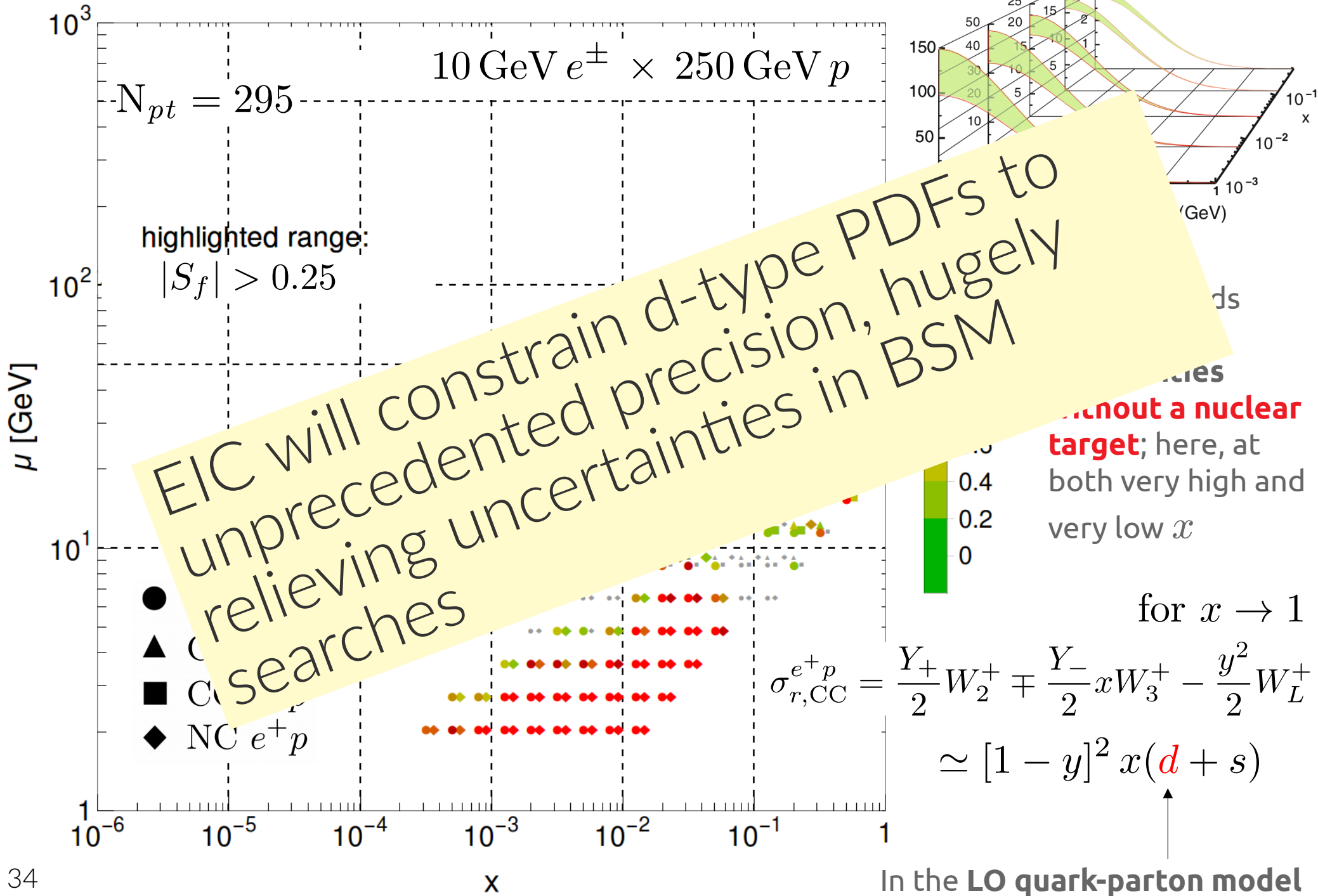
for $x \rightarrow 1$

$$\sigma_{r,CC}^{e^+p} = \frac{Y_+}{2} W_2^+ \mp \frac{Y_-}{2} x W_3^+ - \frac{y^2}{2} W_L^+$$

$$\simeq [1 - y]^2 x (d + s)$$

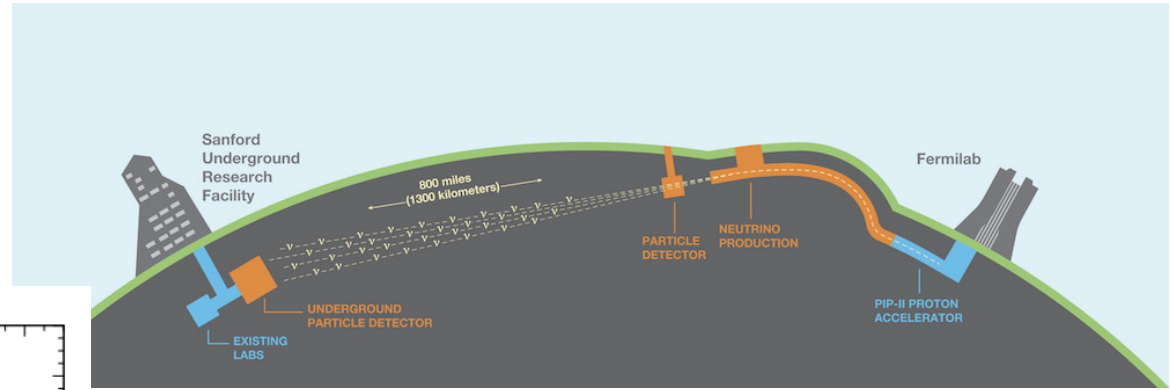
In the LO quark-parton model

$|S_f|$ for $d(x, \mu)$ CT14 HERA2 NNLO



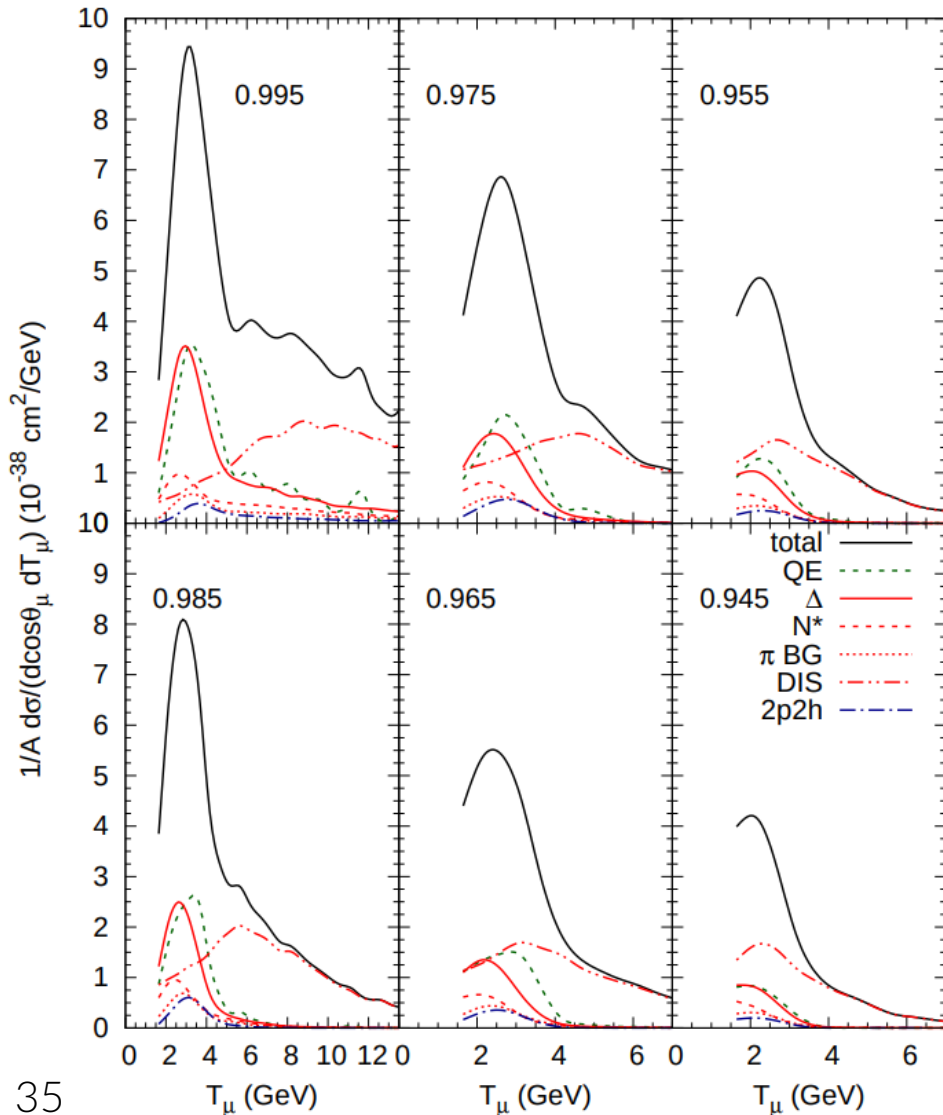
this message transfers directly to neutrino efforts

→ ability to predict neutrino-nucleus cross section limited by many uncertainties



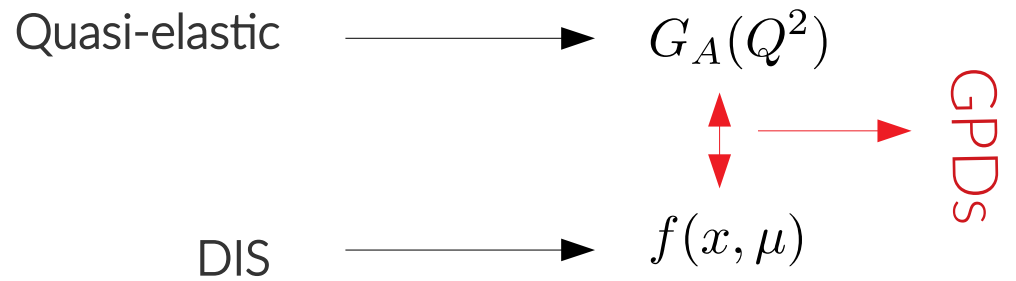
(see talks, Betancourt & Hill.)

→ the νA cross section is determined by an interplay of **quasi-elastic***, DIS*, and resonance contributions (*this talk)



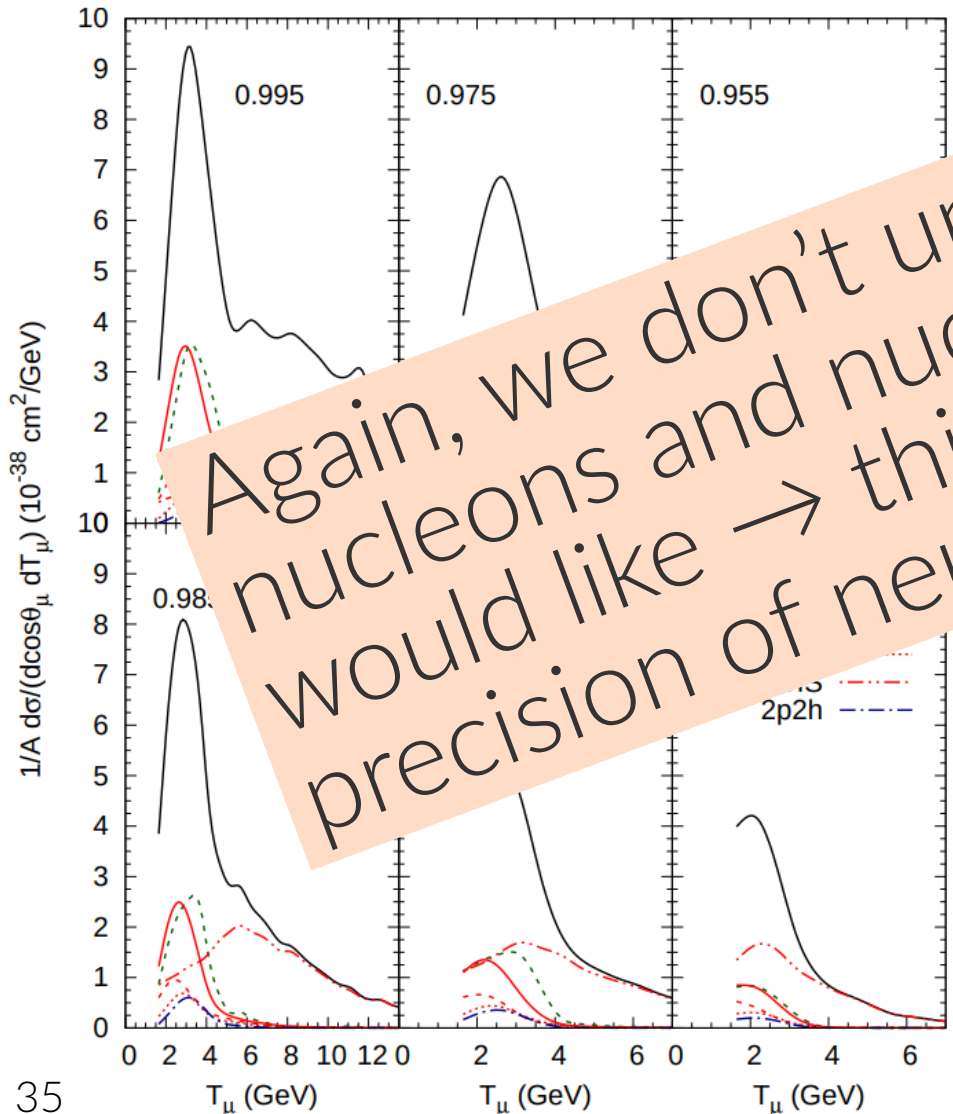
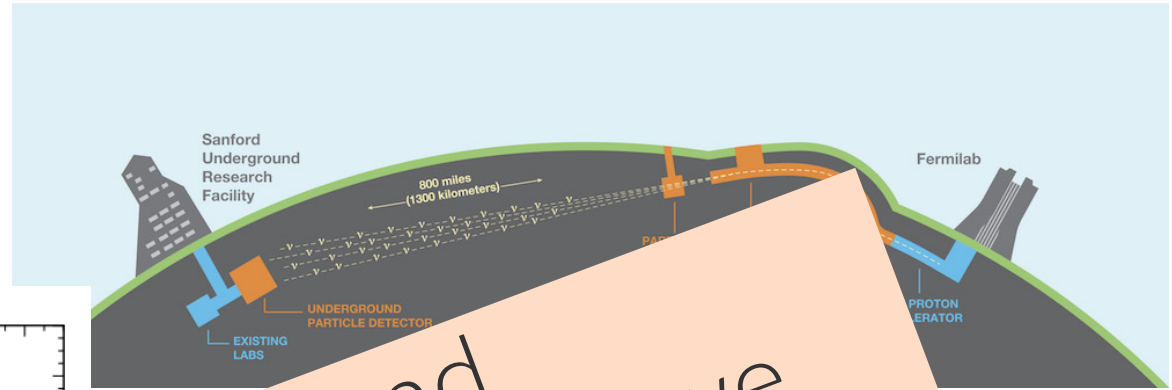
control over single-nucleon inputs essential:

(especially for ~-(sub)percent precision targeted by DUNE)



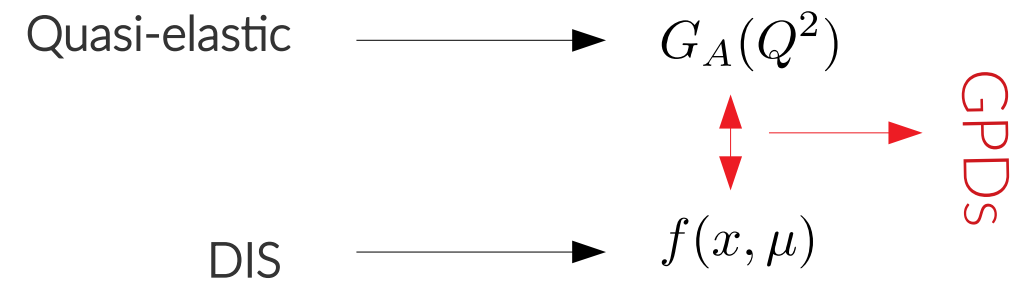
this message transfers directly to neutrino efforts

→ ability to predict neutrino-nucleus cross section limited by many uncertainties



Again, we don't understand nucleons and nuclei as well as we would like → this limits the precision of neutrino experiments

Control over single-nucleon inputs essential:
(especially for ~-(sub)percent precision targeted by DUNE)



example: the neutrino cross section requires control over $G_A(Q^2)$

$$\Delta u - \Delta d = G_A(Q^2 = 0) \equiv g_A$$

Xilin Zhang, TJH, Jerry Miller (in prog.)

- the quasi-elastic contributions to the (anti-)neutrino cross sections depend crucially on **form factors**

$$\frac{d\sigma^{\nu(\bar{\nu})}}{dQ^2} = \frac{G_F^2 \cos^2 \theta_c M^2}{8\pi E_\nu^2} \left[A \mp B \frac{s-u}{M^2} + C \left(\frac{s-u}{M^2} \right)^2 \right]$$

$$A = \frac{(m_\mu^2 + Q^2)}{M^2} \left((1 + \tau) G_A^2 - (1 - \tau) F_{1\nu}^2 + 4\tau F_{1\nu} F_{2\nu} + (1 - \tau)\tau F_{2\nu}^2 + \dots \right)$$

...similar expressions for B, C ...



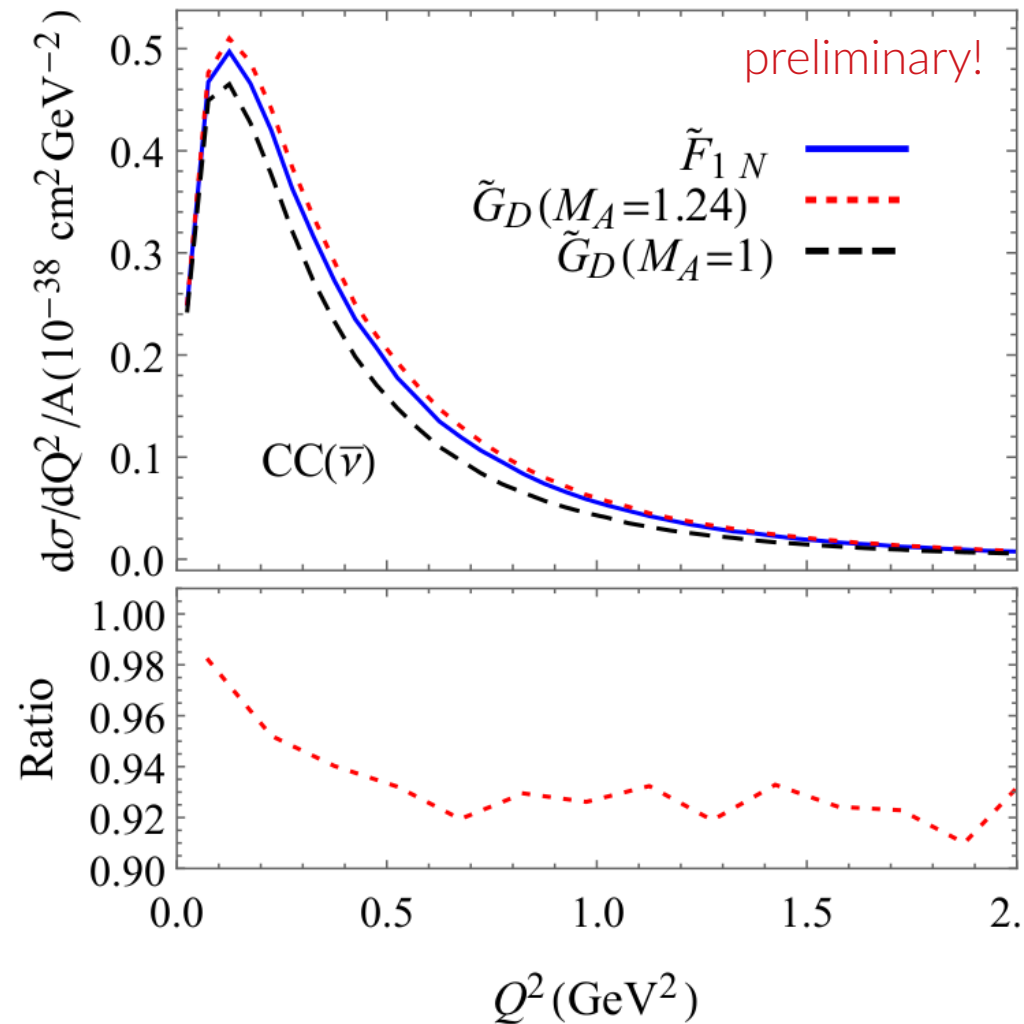
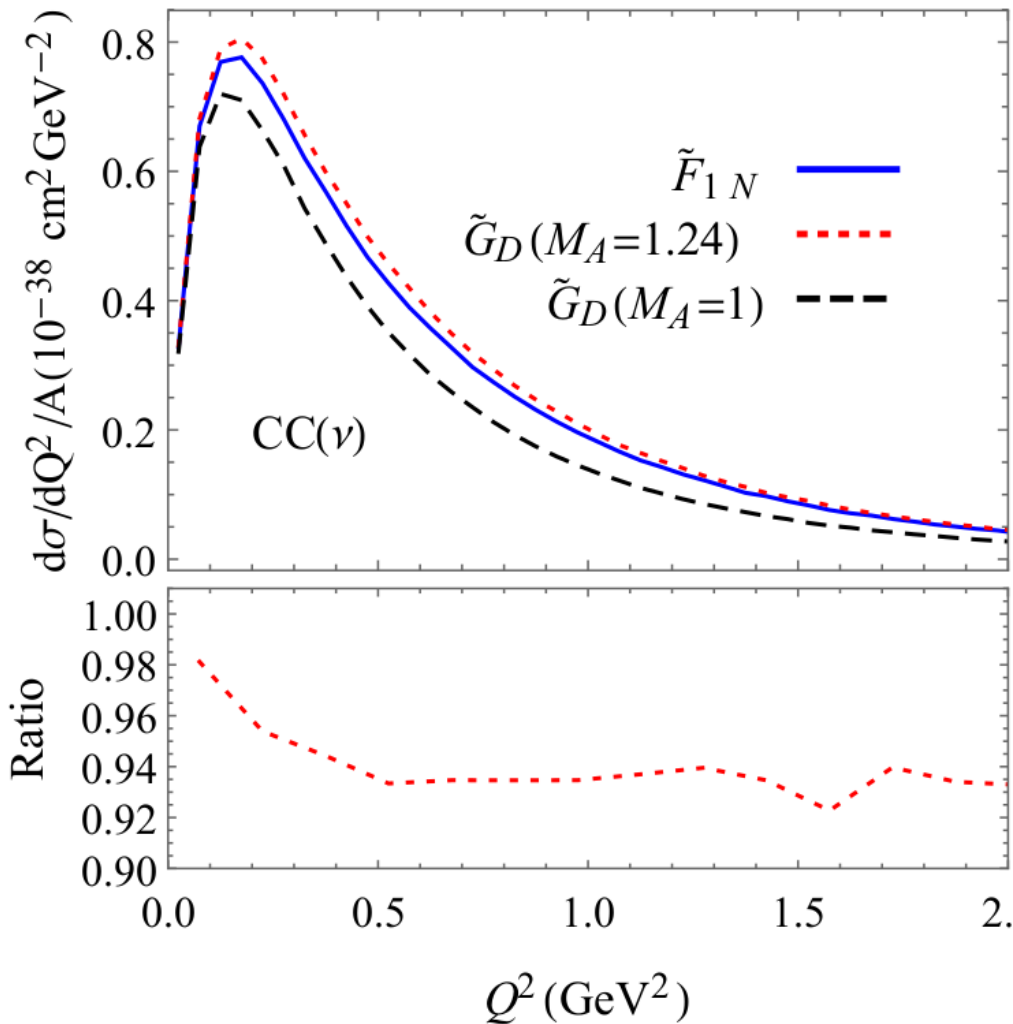
→ historically, dipole ansatz used:

$$G_A(Q^2) = g_A \left(1 + \frac{Q^2}{M_A^2} \right)^{-2} \quad \text{...but is this adequate?}$$

...NO

the behavior of the axial form factor has a large impact in nuclear cross sections!

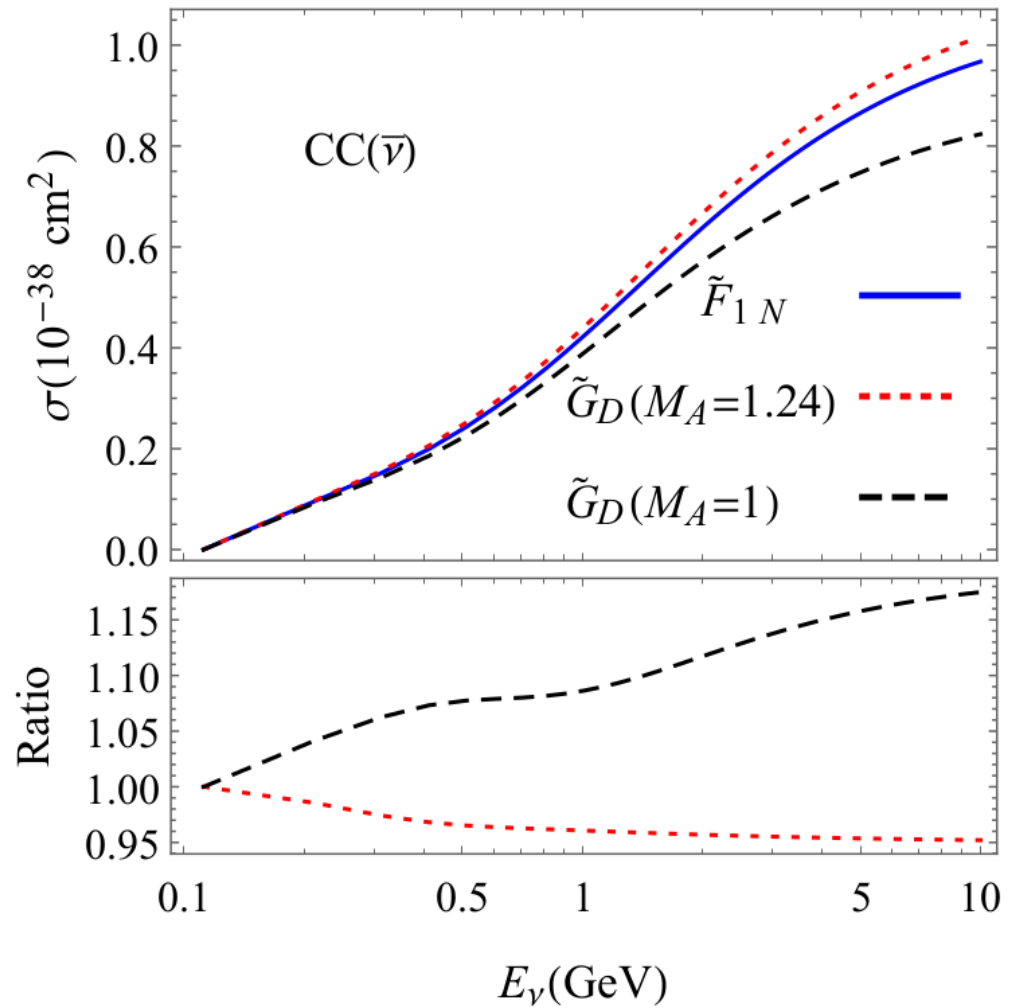
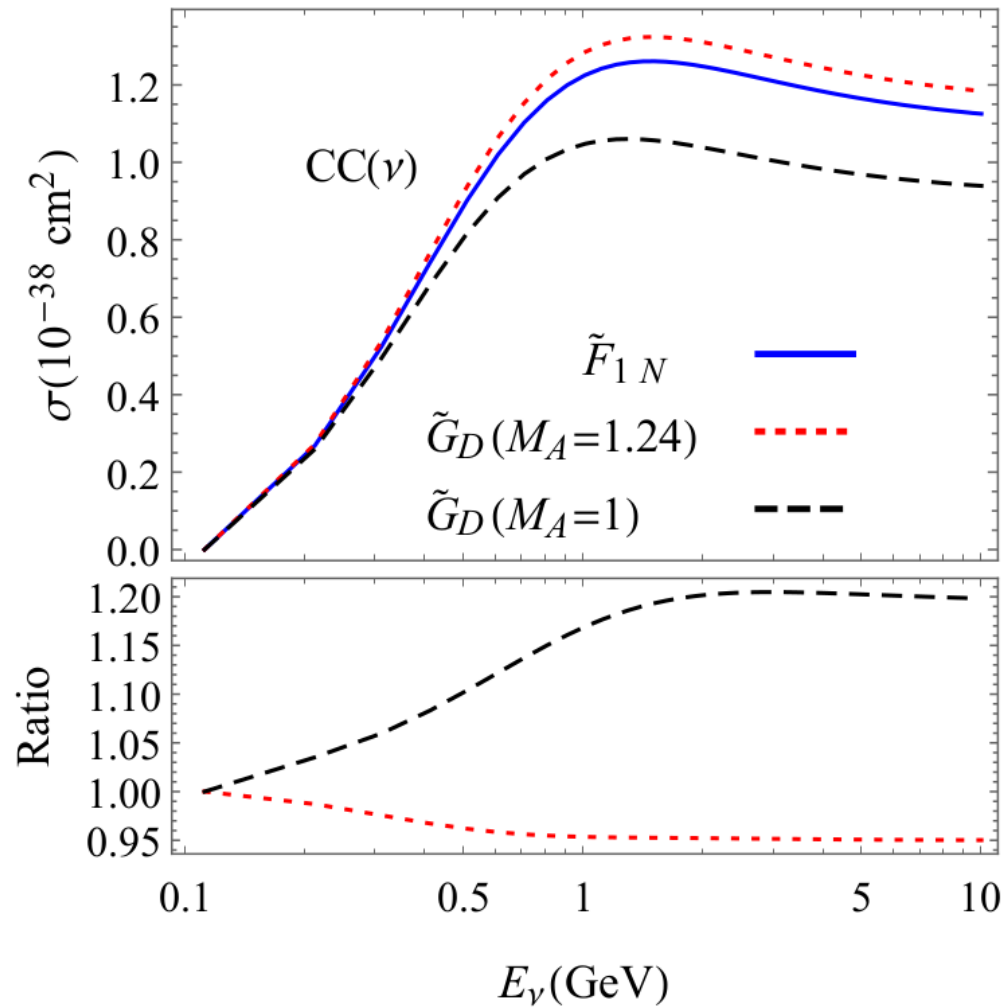
→ input (better) model calculations into GiBUU transport code for $\nu(\bar{\nu}) - {}^{40}\text{Ar}$



~5-10% deviation from naive 1-parameter dipole ansatz!

neutrino-nucleon total cross section

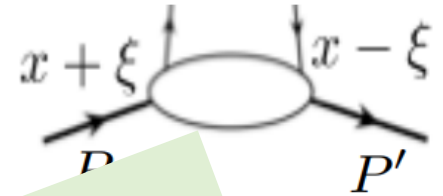
these effects propagate to the total cross section



these are significant effects! the EIC will simultaneously constrain many form factors and distributions...

□ Quark “form factor”:

$$F^q = \frac{1}{2} \int \frac{dz^-}{2\pi} e^{ixP^+z^-} \langle P' | \bar{q}(-\frac{1}{2}z) \gamma^+ q(\frac{1}{2}z) | P \rangle \Big|_{z^+=0, \mathbf{z}=0}$$



$$= \frac{1}{2P^+} \left[H^q(x, \xi, t) \bar{u}(p') \gamma^+ u(p) + E^q(x, \xi, t) \bar{u}(p') \gamma^+ \gamma_5 u(p) \right]$$

with $\xi = (P' - P) \cdot n / 2$

Gauge link:

different nucleon/nuclear matrix elements are interrelated - this can be exploited by the EIC program

quarks: $\tilde{H}_q(x, \xi, t, Q), \tilde{E}_q(x, \xi, t, Q)$
with $\gamma \cdot n \rightarrow \gamma \cdot n \gamma_5$

□ Forward limit connection to collinear PDFs:

$$H^q(x, 0, 0) = q(x), \quad \tilde{H}^q(x, 0, 0) = \Delta q(x) \quad \text{for } x > 0$$

□ Connection to Dirac and Pauli form factors:

axial FF:

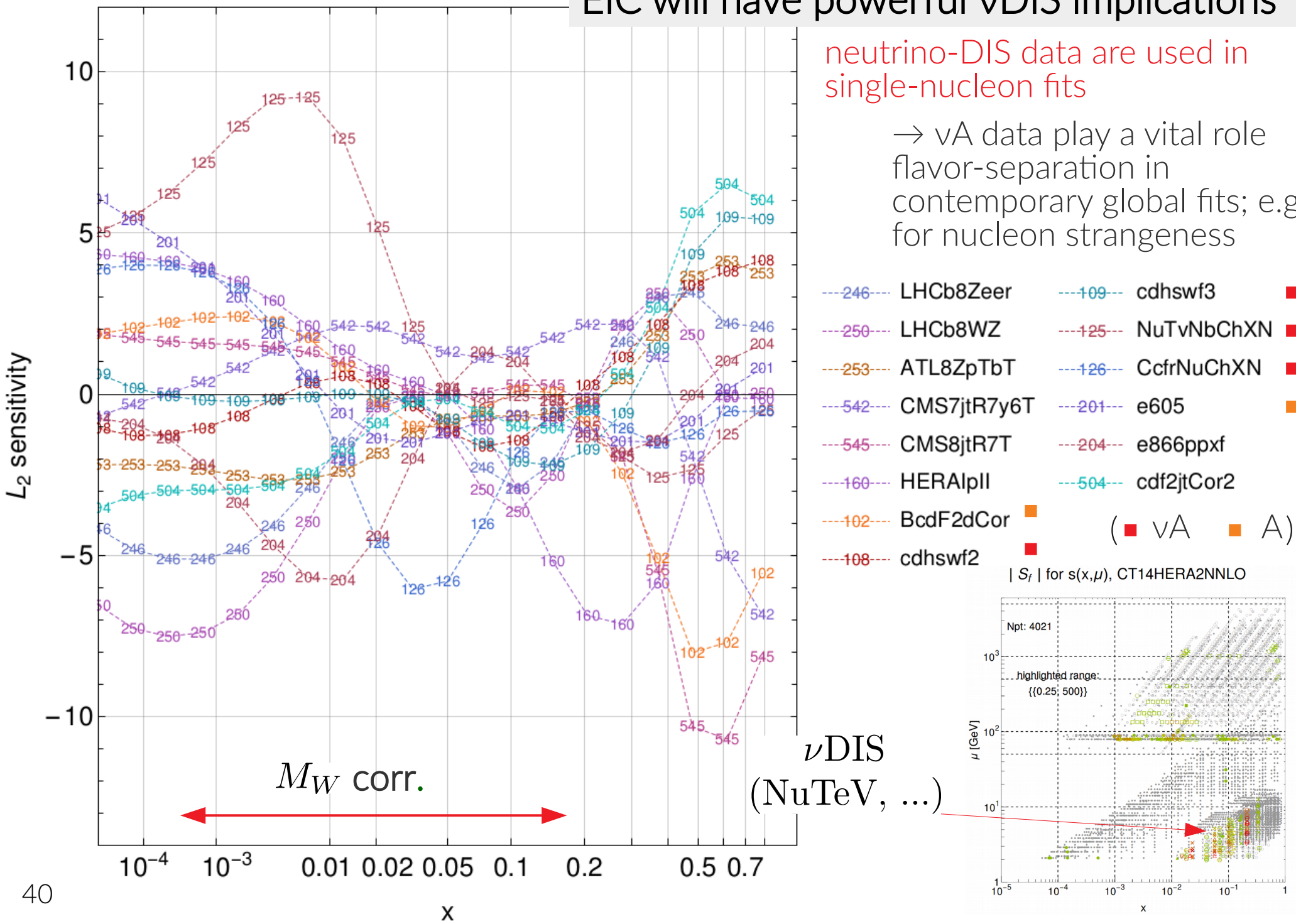
$$\int_{-1}^1 dx H^q(x, \xi, t) = F_1^q(t), \quad \int_{-1}^1 dx E^q(x, \xi, t) = F_2^q(t)$$

$$\int_{-1}^1 dx \tilde{H}^q(x, \xi, t) = g_A^q(t)$$

EIC will have powerful ν DIS implications

neutrino-DIS data are used in single-nucleon fits

→ νA data play a vital role flavor-separation in contemporary global fits; e.g., for nucleon strangeness

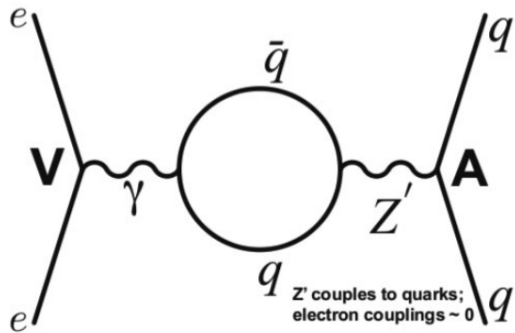


the electroweak sector and **New Physics** searches at EIC

- if measured to sufficient precision, the quark-level electroweak couplings may be sensitive to an extended EW sector, e.g., Z'

$$\mathcal{L}^{\text{PV}} = \frac{G_F}{\sqrt{2}} \left[\bar{e} \gamma^\mu \gamma_5 e \left(C_{1u} \bar{u} \gamma_\mu u + C_{1d} \bar{d} \gamma_\mu d \right) + \bar{e} \gamma^\mu e \left(C_{2u} \bar{u} \gamma_\mu \gamma_5 u + C_{2d} \bar{d} \gamma_\mu \gamma_5 d \right) \right]$$

$$C_{1u} = -\frac{1}{2} + \frac{4}{3} \sin^2 \theta_W$$



- a unique strength of an EIC is its combination of very high precision and **beam polarization**, which allows the observation of **parity-violating helicity asymmetries**:

$$A^{\text{PV}} = \frac{\sigma_R - \sigma_L}{\sigma_R + \sigma_L} \quad (\text{R/L} : e^- \text{ beam helicities})$$

selects γ - Z interference diagrams!

TJH and Melnitchouk, PRD77, 114023 (2008).

$$A^{\text{PV}} = - \left(\frac{G_F Q^2}{4\sqrt{2}\pi\alpha} \right) (Y_1 a_1 + Y_3 a_3)$$

$$a_1 = \frac{2 \sum_q e_q C_{1q} (q + \bar{q})}{\sum_q e_q^2 (q + \bar{q})}$$

$$a_3 = \frac{2 \sum_q e_q C_{2q} (q - \bar{q})}{\sum_q e_q^2 (q + \bar{q})}$$

the electroweak sector and **New Physics** searches at EIC

- if measured to sufficient precision, the quark-level electroweak couplings may be sensitive to an extended EW sector, e.g., Z'

$$\mathcal{L}^{\text{PV}} = \frac{G_F}{\sqrt{2}} \left[\bar{e} \gamma^\mu \gamma_5 e \left(C_{1u} \bar{u} \gamma_\mu u + C_{1d} \bar{d} \gamma_\mu d \right) + \bar{e} \gamma^\mu e \left(C_{2u} \bar{u} \gamma_\mu \gamma_5 u + C_{2d} \bar{d} \gamma_\mu \gamma_5 d \right) \right]$$

$$C_{1u} = -\frac{1}{2} + \frac{4}{3} \sin^2 \theta_W$$

→ with sufficient precision, an EIC (which will be statistics-limited in these measurements) can extract $\sin^2 \theta_W$

- this measurement is potentially sensitive to the TeV-scale in a complementary fashion to energy-frontier searches!

TJH and Melnitchouk, PRD77, 114023 (2008).

$$A^{\text{PV}} = - \left(\frac{G_F Q^2}{4\sqrt{2}\pi\alpha} \right) (Y_1 a_1 + Y_3 a_3)$$

N.B.: extractions are dependent upon knowledge of the PDFs

$$a_1 = \frac{2 \sum_q e_q C_{1q} (q + \bar{q})}{\sum_q e_q^2 (q + \bar{q})}$$

$$a_3 = \frac{2 \sum_q e_q C_{2q} (q - \bar{q})}{\sum_q e_q^2 (q + \bar{q})}$$

the electroweak sector and **New Physics** searches at EIC

- if measured to sufficient precision, the quark-level electroweak couplings may be sensitive to an extended EW sector, e.g., Z'

$$\mathcal{L}^{\text{PV}} = \frac{G_F}{\sqrt{2}} \left[\bar{e} \gamma^\mu \gamma_5 e \left(C_{1u} \bar{u} \gamma_\mu u + C_{1d} \bar{d} \gamma_\mu d \right) + \bar{e} \gamma^\mu e \left(C_{2u} \bar{u} \gamma_\mu \gamma_5 u + C_{2d} \bar{d} \gamma_\mu \gamma_5 d \right) \right]$$

$$C_{1u} = -\frac{1}{2} + \frac{4}{3} \sin^2 \theta_w$$

with sufficient precision
measurements

the takeaway: an EIC will be capable of measurements with immediate potential sensitivity to BSM scenarios (see talks, Mantry & Zhang.)

... to the TeV-scale in a high-energy-frontier searches!

TJH and Melnitch

$$A^{\text{PV}} = -\frac{1}{2\pi\alpha} (Y_1 a_1 + Y_3 a_3)$$

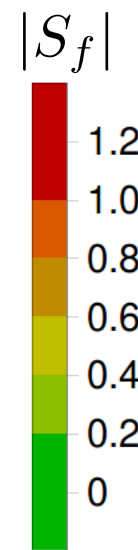
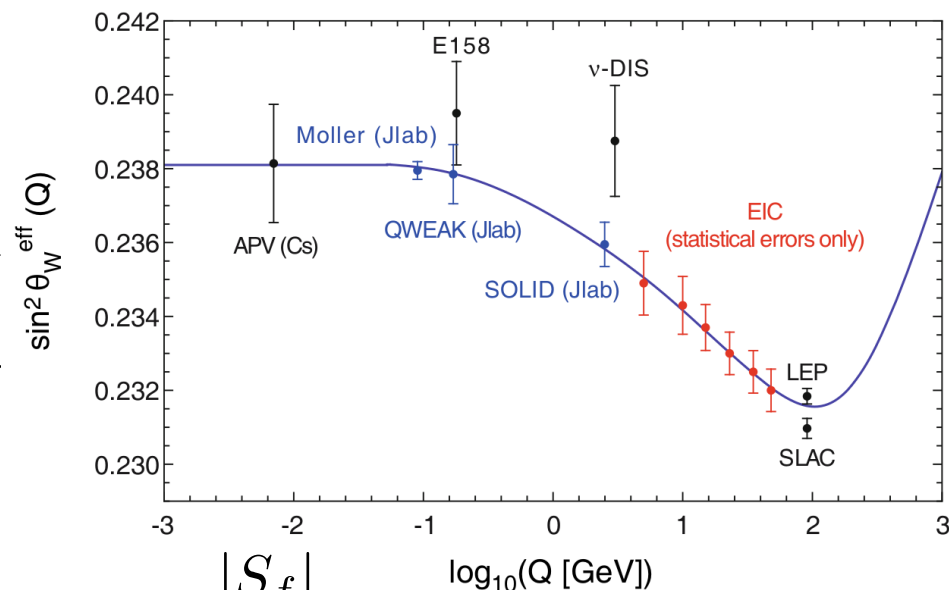
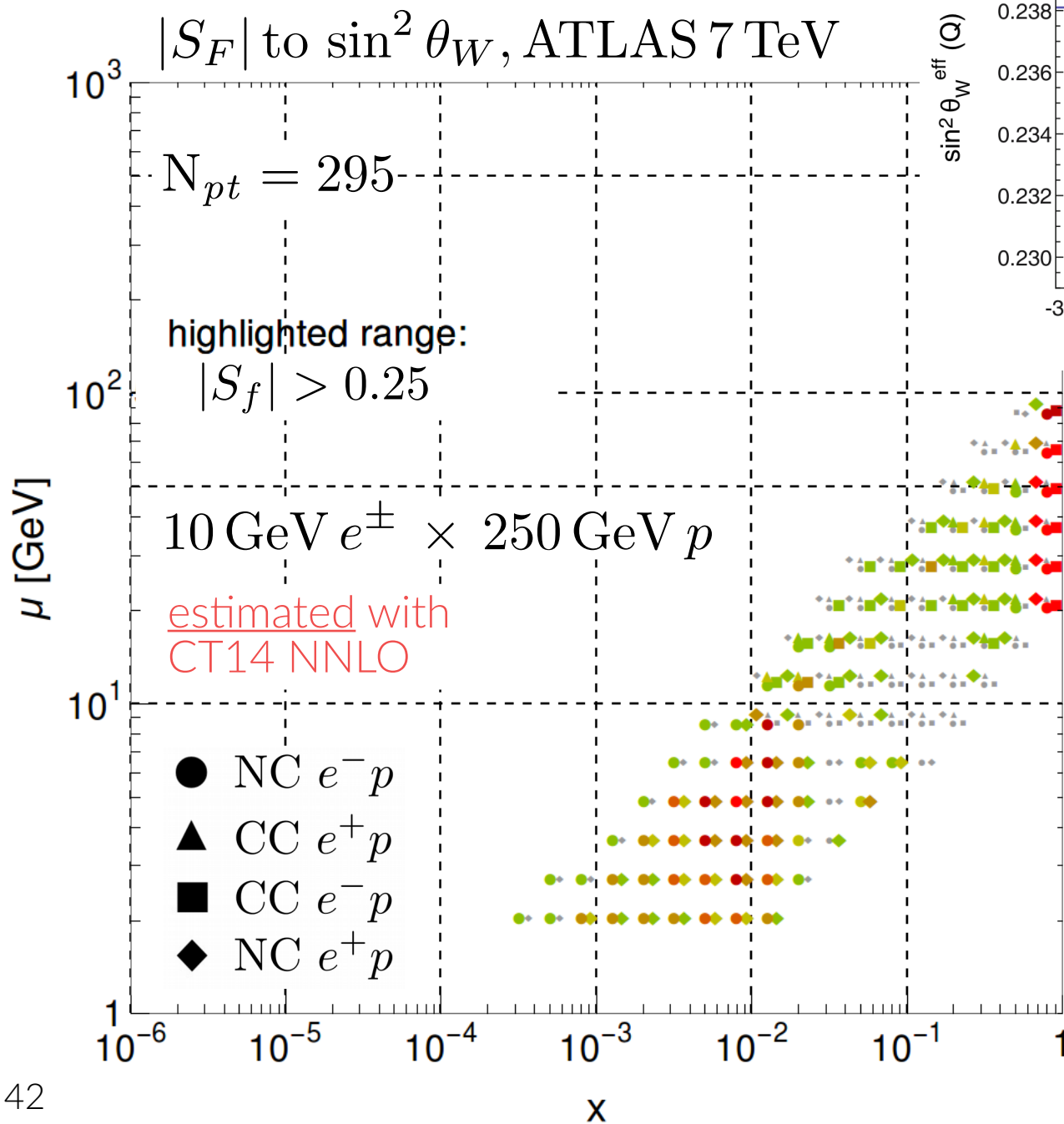
N.B.: extractions are dependent upon knowledge of the PDFs

$$a_1 = \frac{2 \sum_q e_q C_{1q} (q + \bar{q})}{\sum_q e_q^2 (q + \bar{q})}$$

$$a_3 = \frac{2 \sum_q e_q C_{2q} (q - \bar{q})}{\sum_q e_q^2 (q + \bar{q})}$$

an EIC will probe EW parameters and New Physics!

Accardi et al., EPJA52, 268 (2016).



- observe a pronounced sensitivity to the Weinberg angle, especially low and high x , even at

$$\mathcal{L} = 100\text{fb}^{-1}$$

- this corresponds closely to the kinematics at which EIC is likely to measure A^{PV} — relatively large Q^2 and in the x range

$$0.2 \lesssim x \lesssim 0.5$$

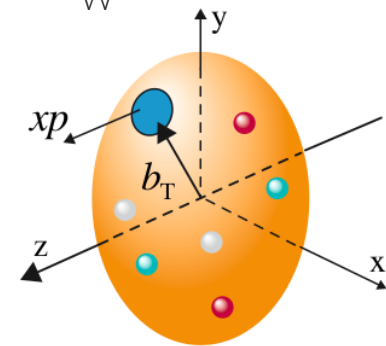
key points...

...and the future.

- numerous observables central to the LHC/LBNF discovery programs are limited by uncertainties associated with nucleon structure

→ for the unpolarized PDFs, systematic tensions among modern world data are an impediment to higher precision for σ_H , M_W , ...

→ an EIC will be ideally suited to perform measurements with the ability to unravel such systematic issues



the EIC impact upon high-energy pheno will be pivotal

→ controlling PDFs/SM backgrounds; **neutrino pheno**; BSM searches; event generators;

(see talks, Hoeche & Diefenthaler.)

- confronting systematic PDF issues and exploring the LHC implications of the EIC require **community efforts**, esp. to optimize the output of the eventual program and its utility to HEP

many areas on both sides of the medium-, high-energy divide in which input is needed.



WE WANT YOU!

again, please join in-person or on Indico

LPC Workshop on Physics Connections between the LHC and EIC

13-15 November 2019

Fermilab, Wilson Hall

America/Chicago timezone



Overview

Call for Abstracts

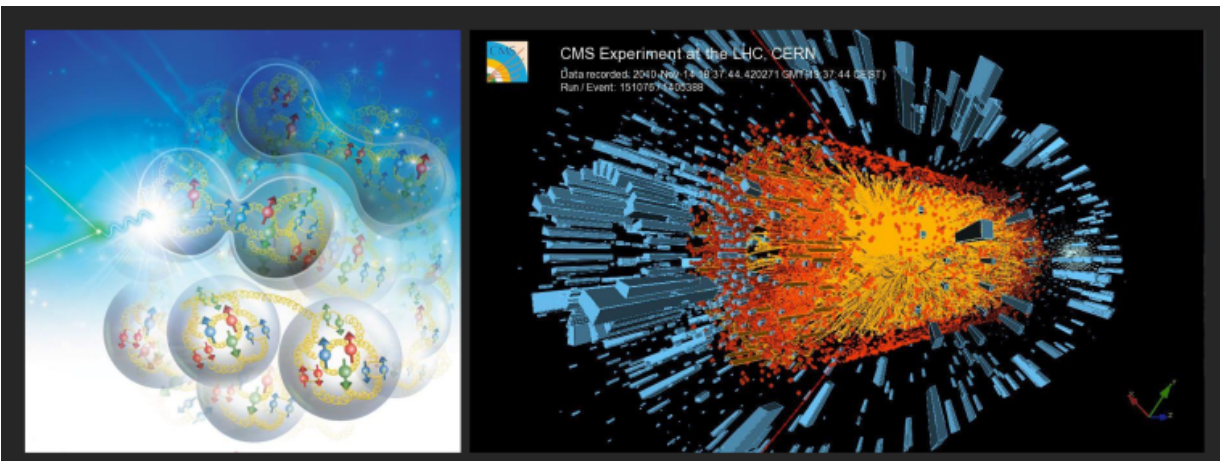
Timetable

Registration

Contribution List

Participant List

This 3-day workshop seeks to bring together members of the LHC and EIC communities under the auspices of the Fermilab LPC to explore possible synergies between the EIC program and LHC phenomenology. The areas of overlap to be discussed fall broadly along the lines of precision QCD, Monte Carlo event generators, lattice QCD and advanced computation, and opportunities in the electroweak sector, including potential improvements to neutrino phenomenology and BSM searches. The goal of this workshop is to identify and develop common working areas for which EIC science objectives can both inform and benefit from energy-frontier efforts at the LHC.



Sunrise,
WH11NE

—— supplementary material ——

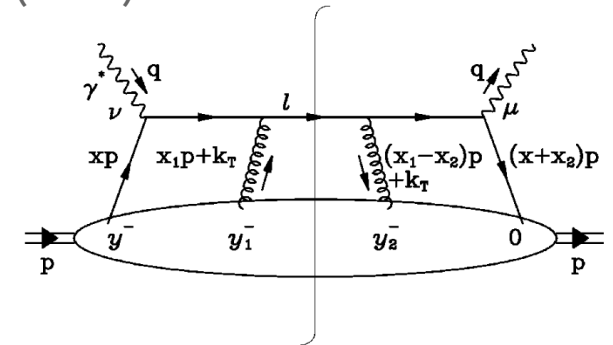
interactions with multiple partons at EIC: nuclear case

- consider jet production in electron-nucleus vs. electron-nucleon DIS

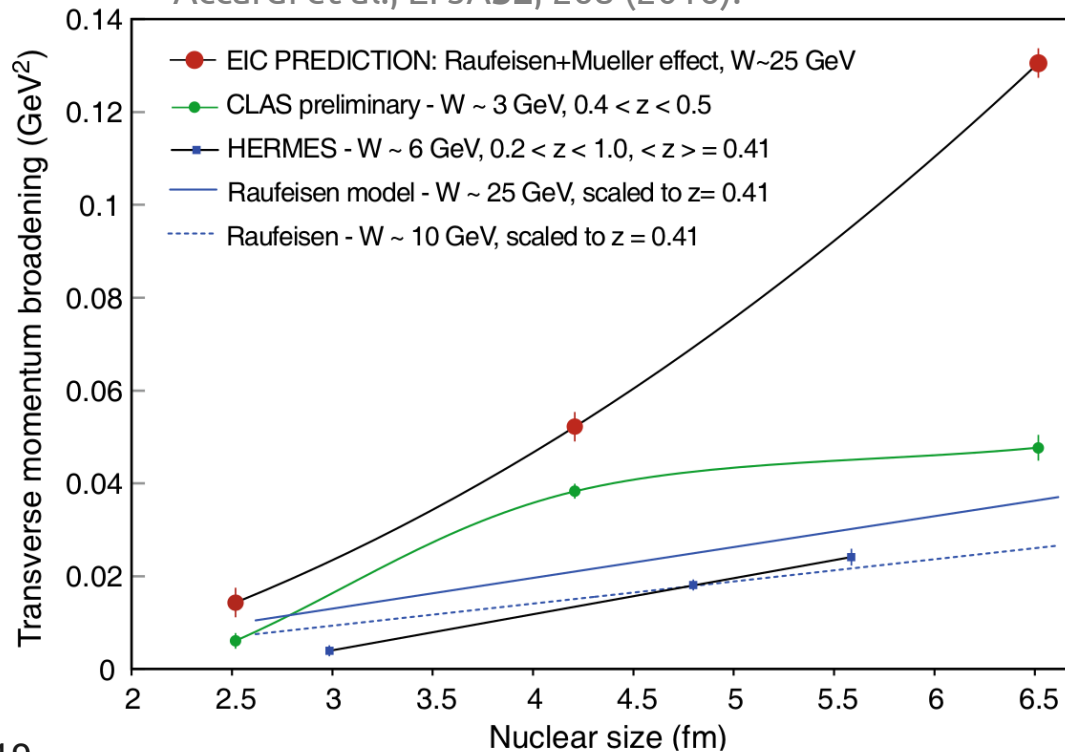
X. Guo, PRD58, 114033 (1998).

$$\Delta \langle p_T^2 \rangle \equiv \langle p_T^2 \rangle_{eA} - \langle p_T^2 \rangle_{ep}$$

$$\langle p_T^2 \rangle = \int dp_T^2 p_T^2 \frac{d\sigma}{dx_B dQ^2 dp_T^2} / \frac{d\sigma}{dx_B dQ^2}$$



Accardi et al., EPJA52, 268 (2016).



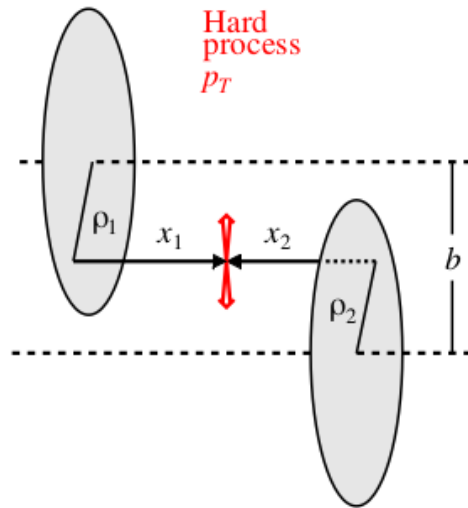
- multi-parton interactions in nuclear scattering:

→ multiple scatterings of produced quark with nuclear medium

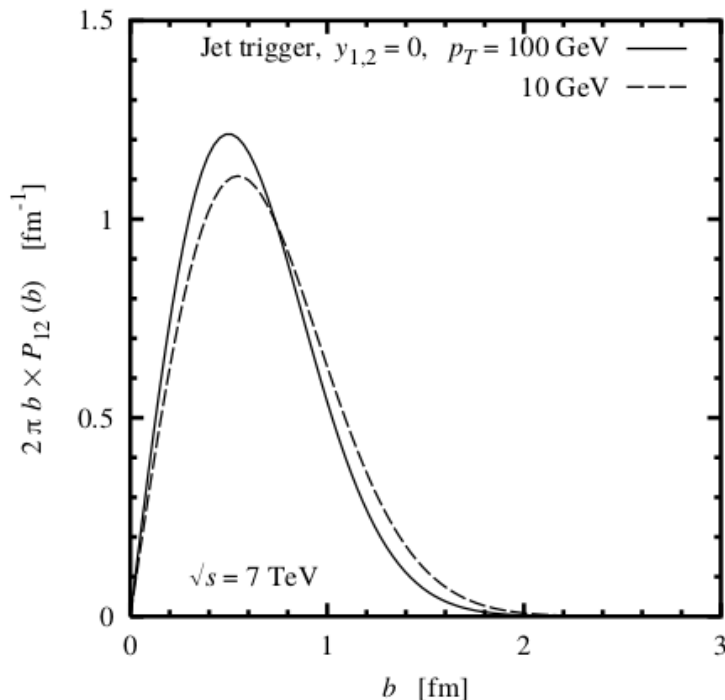
→ qualitatively different dependence on nuclear size predicted at EIC energies

→ more phase space for radiation, larger $\Delta \langle p_T^2 \rangle$

Transverse geometry in pp: Hard processes



Thanks to Christian Weiss!



- Hard process from parton-parton collision

Local in transverse space $p_T^2 \gg (\text{transv. size})^{-2}$

- Cross section as function of pp impact par

$$\sigma_{12}(b) = \int d^2\rho_1 d^2\rho_2 \delta(\mathbf{b} - \boldsymbol{\rho}_1 + \boldsymbol{\rho}_2) \times G(x_1, \rho_1) G(x_2, \rho_2) \sigma_{\text{parton}}$$

→ precise GPDs furnished by EIC will be crucial!

Calculable from known transverse distributions
Integral $\int d^2b$ reproduces inclusive formula

Normalized distribn $P_{12}(b) = \sigma_{12}(b) / [\int \sigma_{12}]$

- New information available

Model spectator interactions depending on b
Underlying event

Predict probability of multiple hard processes
Dynamical correlations? FSW04

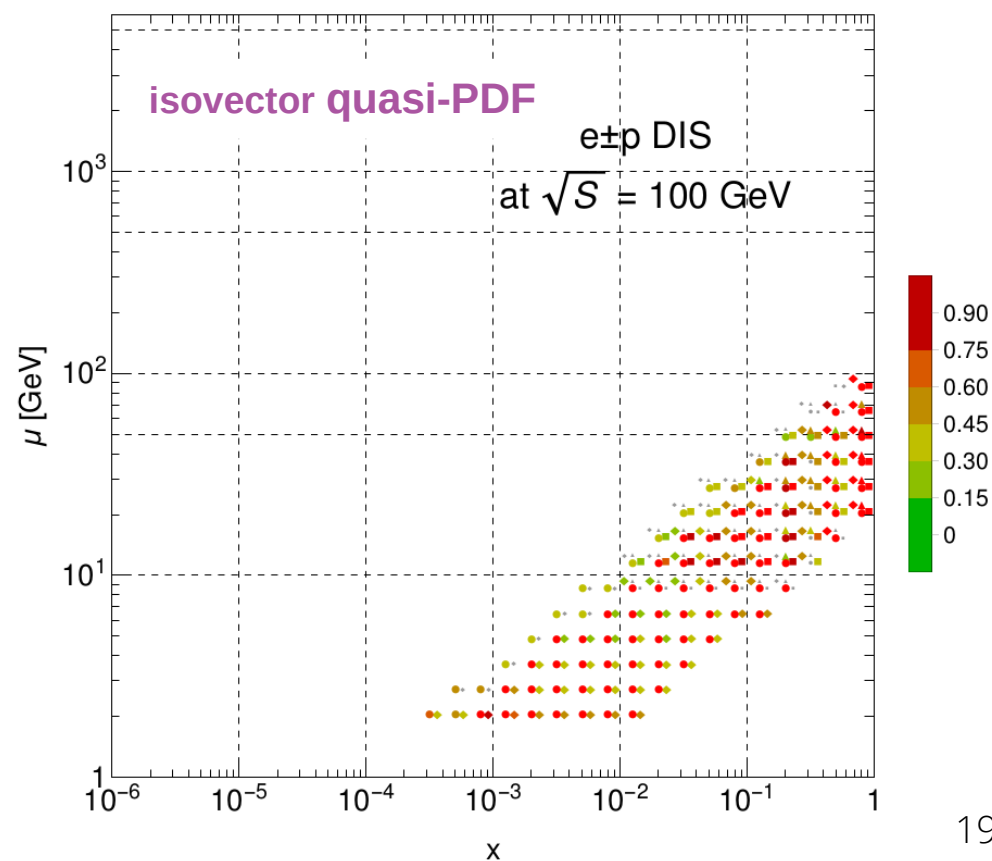
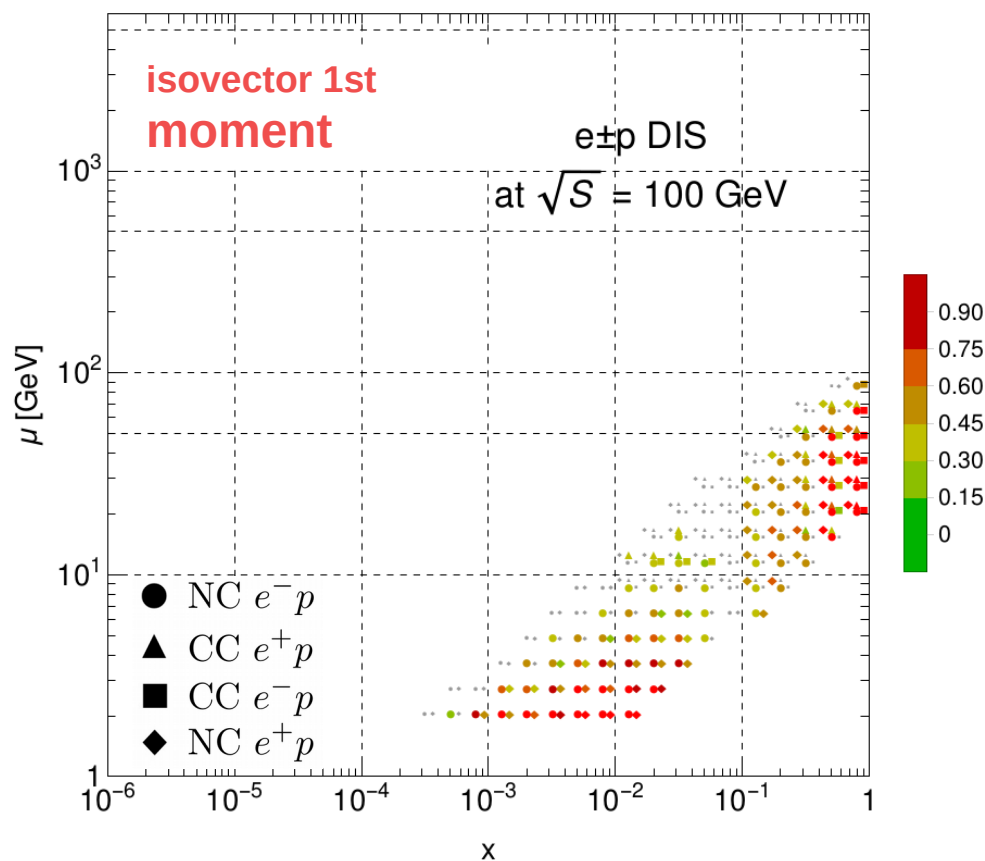
Diffraction: Gap survival probability
Determined largely by transverse geometry FHSW 07

- A high-luminosity lepton-hadron collider will impose very tight constraints on many lattice observables; below, the isovector first moment and qPDF; **this is crucial for benchmarking!**
- Many of the experiments most sensitive to PDF Mellin moments and qPDFs involve nuclear targets → eA data from EIC would sharpen knowledge of nuclear corrections

$$\langle x^n \rangle_{q,g} = \int dx x^n f_{q,g}(x, \mu = 2 \text{ GeV}) \quad \tilde{q}(x, P_z, \tilde{\mu}) = \int dy Z \left(\frac{x}{y}, \frac{\Lambda}{P_z}, \frac{\mu}{P_z} \right) q(y, \mu) + \mathcal{O} \left(\frac{\Lambda_{\text{QCD}}^2}{P_z^2}, \frac{M^2}{P_z^2} \right)$$

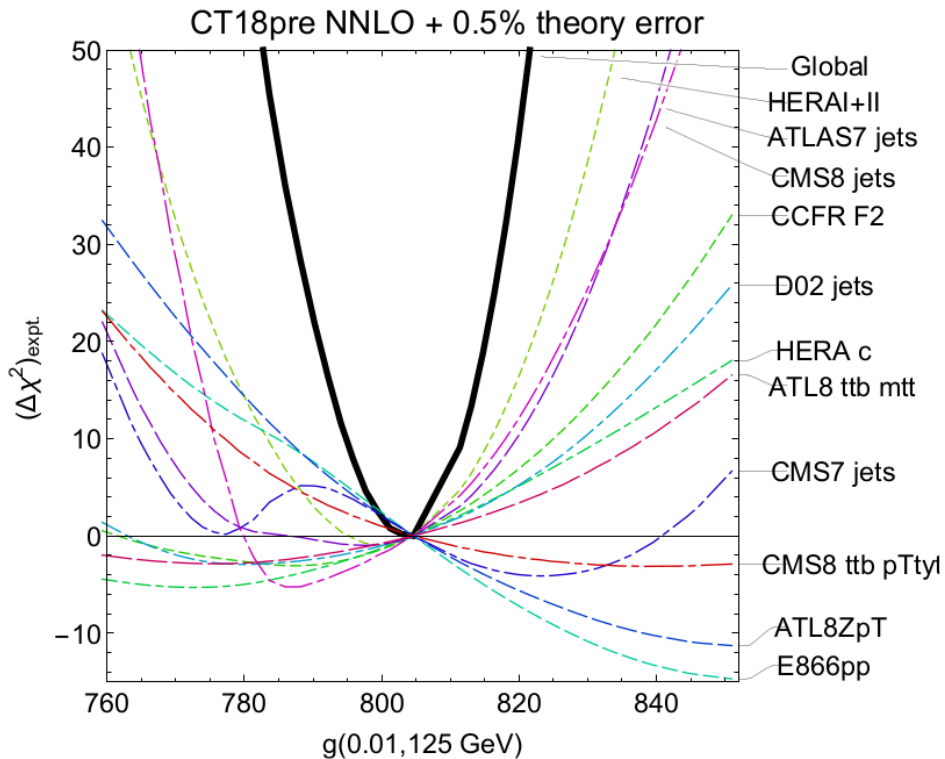
| S_f | for $\langle x^1 \rangle_{u^+ - d^+}$, CT14HERA2

| S_f | for $[\tilde{u} - \tilde{d}](x=0.85, P_z=1.5\text{GeV})$, CT14HERA2



we use the Higgs region $g(x)$ to validate PDFSense

...for the gluon PDF in the Higgs region, $g(0.01, m_H)$



$g(x=0.01, \mu=125 \text{ GeV})$		
PDFSENSE		LM scan
CT14HERA2	CT18pre	CT18pre
HERAI+II'15	HERAI+II'15	HERAI+II'15
CMS8jets'17	CMS8jets'17	CMS8jets'17
CMS7jets'14	CMS7jets'14	ATLAS7jets'15
ATLAS7jets'15	E866pp'03	E866pp'03
E866pp'03	ATLAS7jets'15	ATLAS7jets'15
BCDMSd'90	BCDMSd'90	CCFR-F2'01
CCFR-F3'97	BCDMSp'89	D02jets'08
D02jets'08	D02jets'08	HERAc'13
NMCrat'97	NMCrat'97	NuTeV-nub'06
BCDMSp'89	CDHSW-F2'91	CCFR-F3'97

- PDFSense identifies the most sensitive experiments with high confidence and in accord with other methods such as the LM scans. It works the best when the uncertainties are nearly Gaussian, and experimental constraints agree among themselves [arXiv:1803.02777]

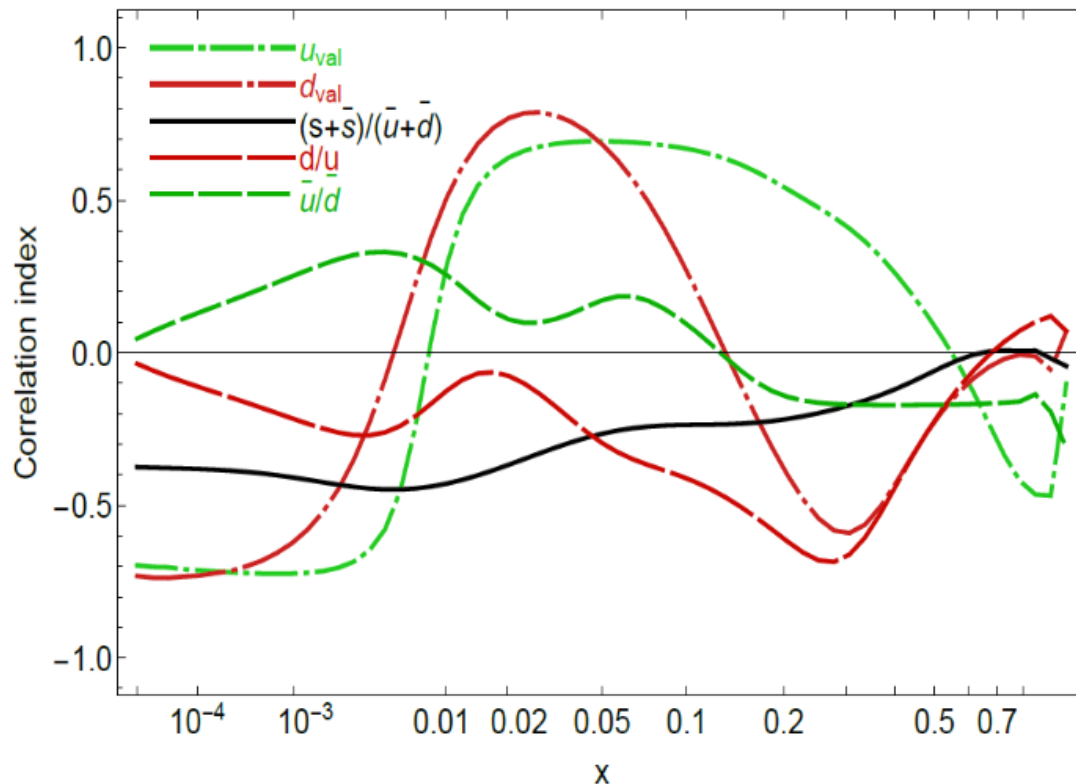
$\sin^2 \theta_W$ (and, eventually, M_W)

...as a follow-on to Alessandro's EW-focused overview:

important PDF correlations for the ATLAS extraction of $\sin^2 \theta_W$

Example: $\sin^2 \theta_{weak} \equiv s2w$ measured by ATLAS 8 TeV

Correlation, $\sin^2 \theta_W$ (ATLAS 8 TeV CB) and $f(x,Q)$ at $Q=81.45$ GeV
2018/11/11, PRELIMINARY, CT14 NNLO



Strongest correlations of $s2w$ with u_{val}, d_{val} at $0.005 \lesssim x \lesssim 0.2$

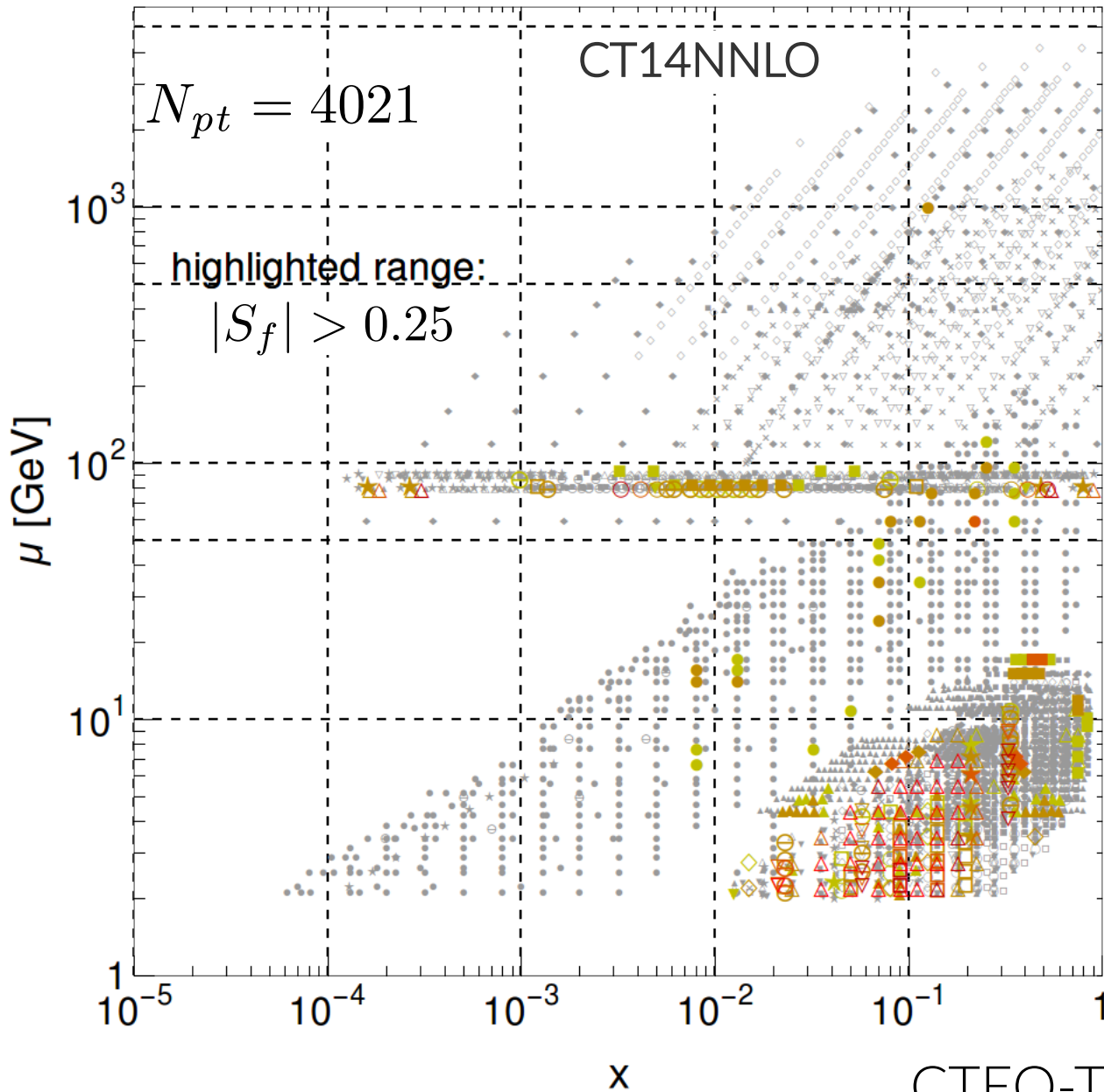
weak correlations with $\bar{u}, \bar{d}, \bar{s}, g$

u_{val}, d_{val} changed between CT10 and CT14 [1506.07433, Sec. 2B]

It is instructive to explore the data pulls on u_{val}, d_{val}

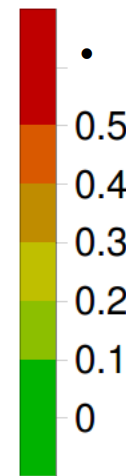
$$\sin^2 \theta_W$$

PDF sensitivity of $\sin^2 \theta_W$ from 7 TeV ATLAS data



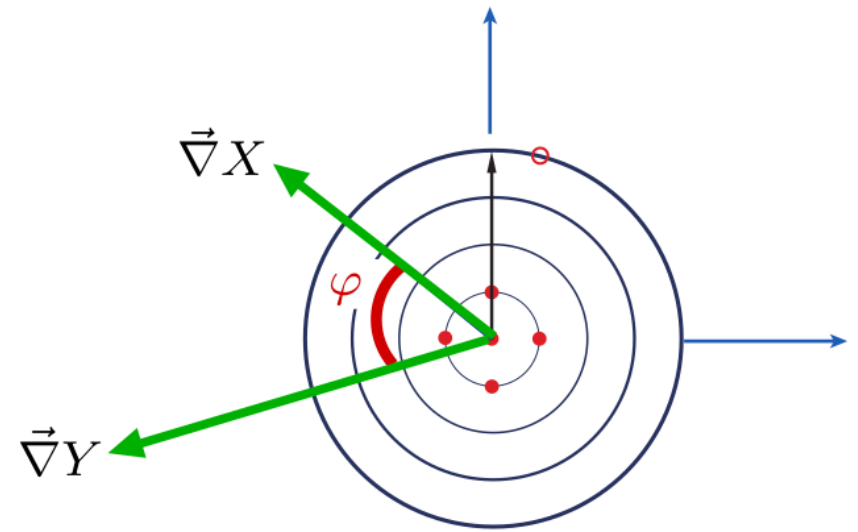
CTEQ-TEA sensitivities to $\sin^2 \theta_W$

- **combined HERA1 DIS [most sensitive]**
- CCFR νp DIS $F_{3,2}$
- BCDMS $F_2^{p,d}$
- NMC ep, ed DIS
- CDHSW νA DIS
- NuTeV $\nu A \rightarrow \mu\mu X$
- CCFR $\nu A \rightarrow \mu\mu X$
- E866 $pp \rightarrow \ell^+ \ell^- X$
- ATLAS 7 TeV W/Z (35 pb^{-1})



rather than the costly LM scans, we can examine a “cheaper” measure which yields comparable information

the L_2 sensitivity



L_2 sensitivity. Take $X = f_a(x_i, Q_i)$ or $\sigma(f)$; $Y = \chi_E^2$ for experiment E . Find $\Delta Y(\vec{z}_{m,X})$ for the displacement $|\vec{z}_{m,X}| = 1$ along the direction $\vec{\nabla} X / |\vec{\nabla} X|$ (corresponding to $\Delta \chi_{tot}^2 = T^2$ and $X(\vec{z}) = X(0) + \Delta X$):

$$S_{f,L_2} \equiv \Delta Y(\vec{z}_{m,X}) = \vec{\nabla} Y \cdot \vec{z}_{m,X} = \vec{\nabla} Y \cdot \frac{\vec{\nabla} X}{|\vec{\nabla} X|}$$

$$= \Delta Y \cos \varphi$$

$$\text{or, } \sim \text{Corr}[f_a, \chi_E^2]$$

...extent to which total χ_E^2 of specific expts. correlates with x -dep. of PDFs

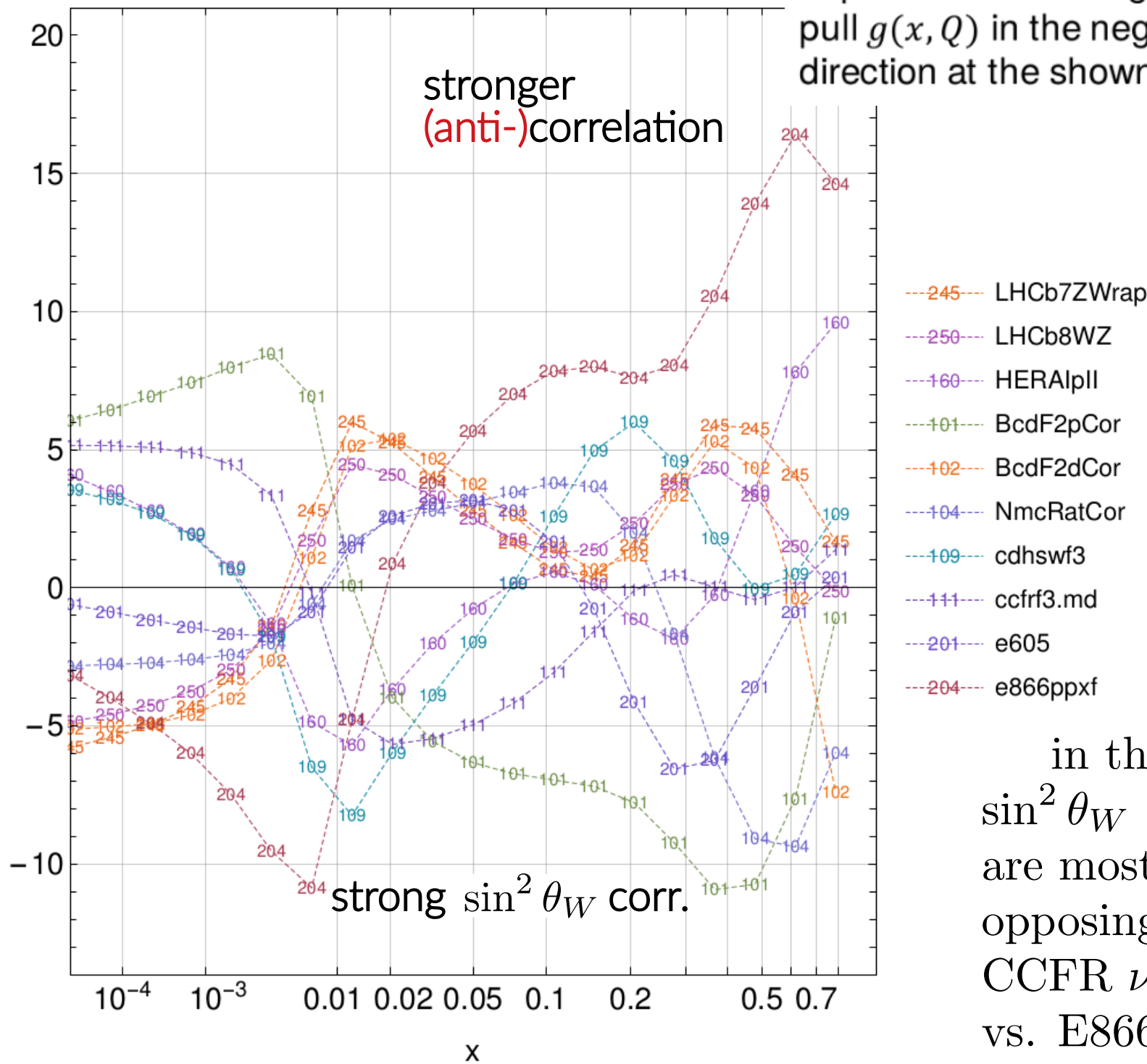
CT18 NNLO, $u_V(x, Q)(x, 100 \text{ GeV})$

Experiments with large $\Delta\chi^2 > 0$ [$\Delta\chi^2 < 0$]
pull $g(x, Q)$ in the negative [positive]
direction at the shown x

stronger
(anti-)correlation

tension between
LHCb W/Z
data (245, 250);
fixed-target DIS,
Drell-Yan
(CDHSW F_3
[109], E866pp
[204])

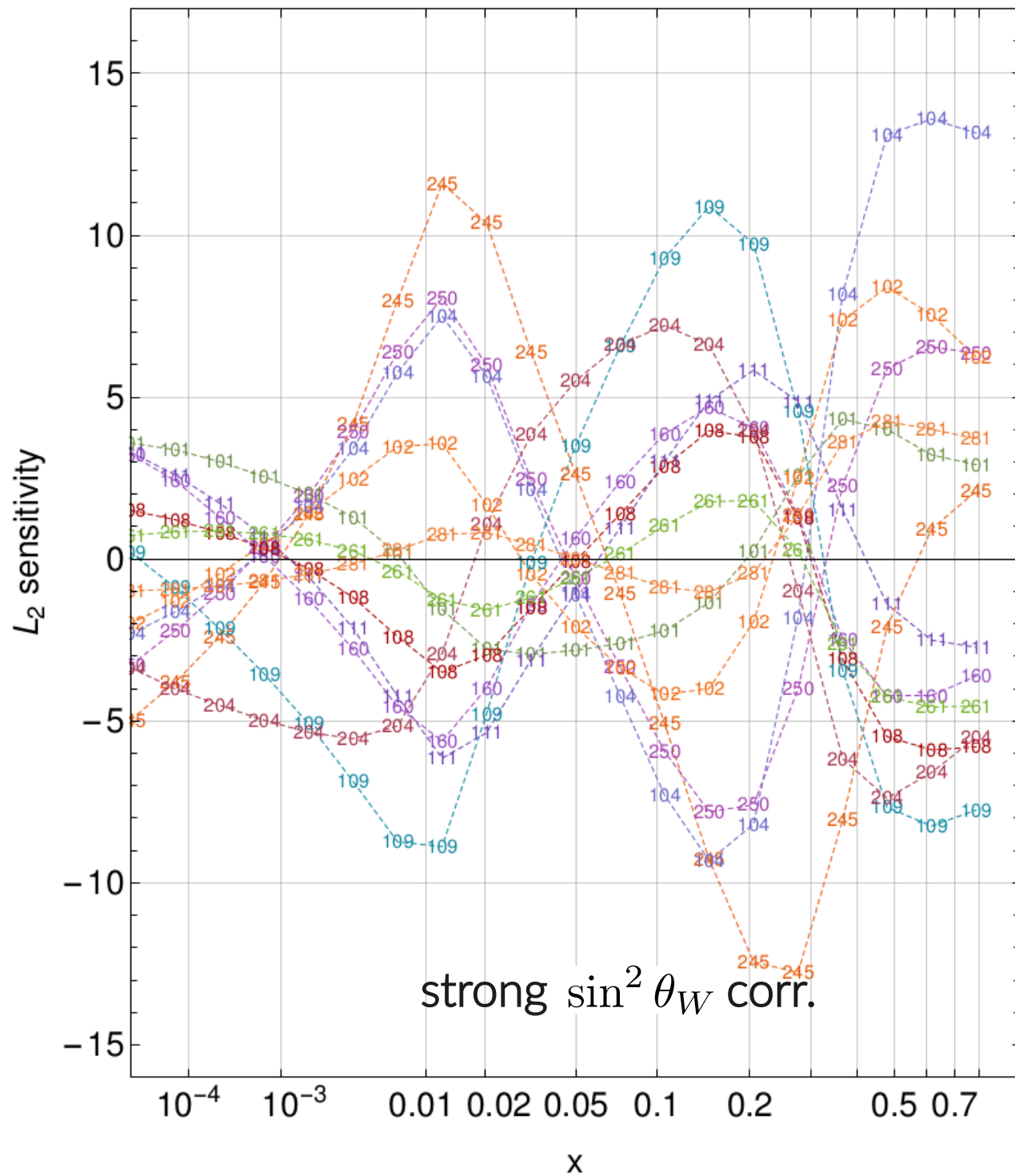
L_2 sensitivity



strong $\sin^2 \theta_W$ corr.

in the region where
 $\sin^2 \theta_W$ and u_v
are most correlated,
opposing pulls from
CCFR ν DIS, BCDMS
vs. E866 pp , NMC rat.

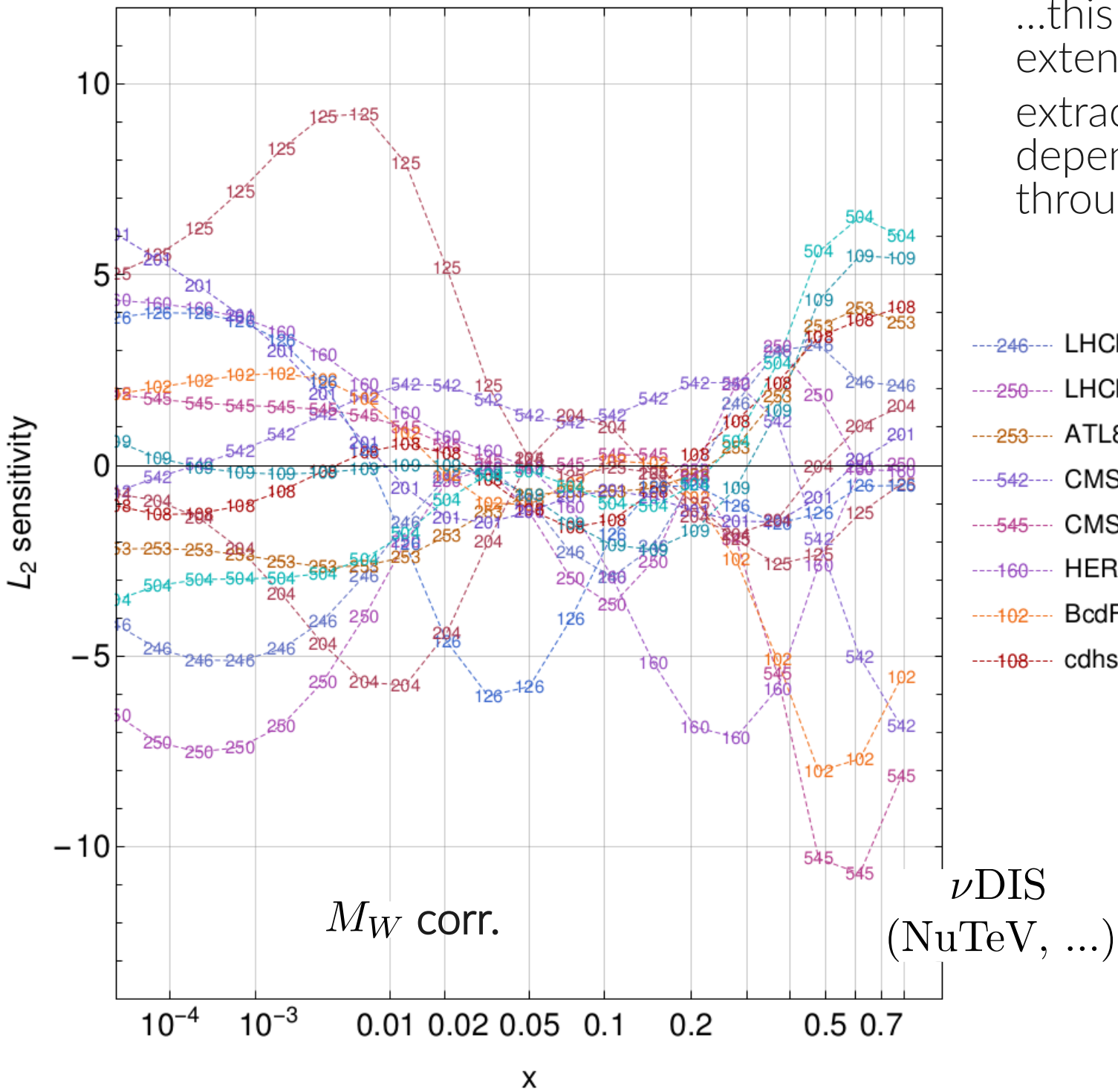
CT18 NNLO, $d_V(x, Q)(x, 100 \text{ GeV})$



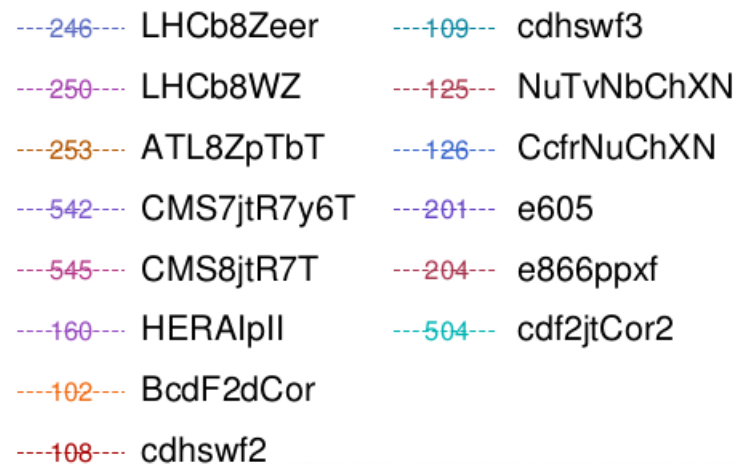
tension between LHCb W/Z data (245, 250); fixed-target DIS, Drell-Yan (CDHSW F_3 [109], E866pp [204])

- 245--- LHCb7ZWrap
- 250--- LHCb8WZ
- 160--- HERA1pII
- 101--- BcdF2pCor
- 102--- BcdF2dCor
- 104--- NmcRatCor
- 108--- cdhswf2
- 109--- cdhswf3
- 111--- ccfrf3.md
- 204--- e866ppxf
- 261--- ZyCDF2
- 281--- d02Easy5

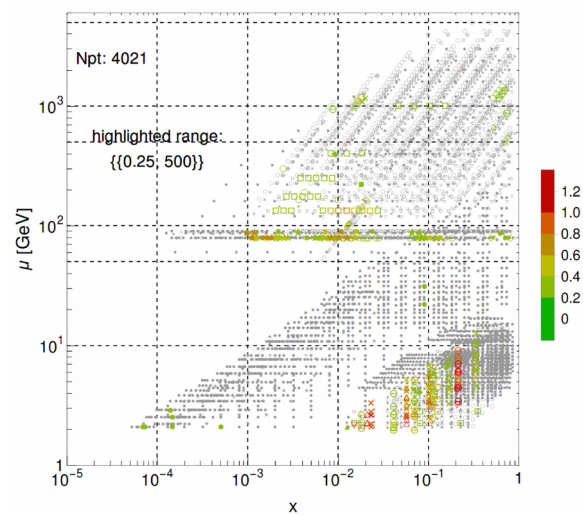
again, tensions observed between, e.g., NMC ratio data and CDHSW, E866pp

M_W CT18 NNLO, $s(x, 100 \text{ GeV})$ 

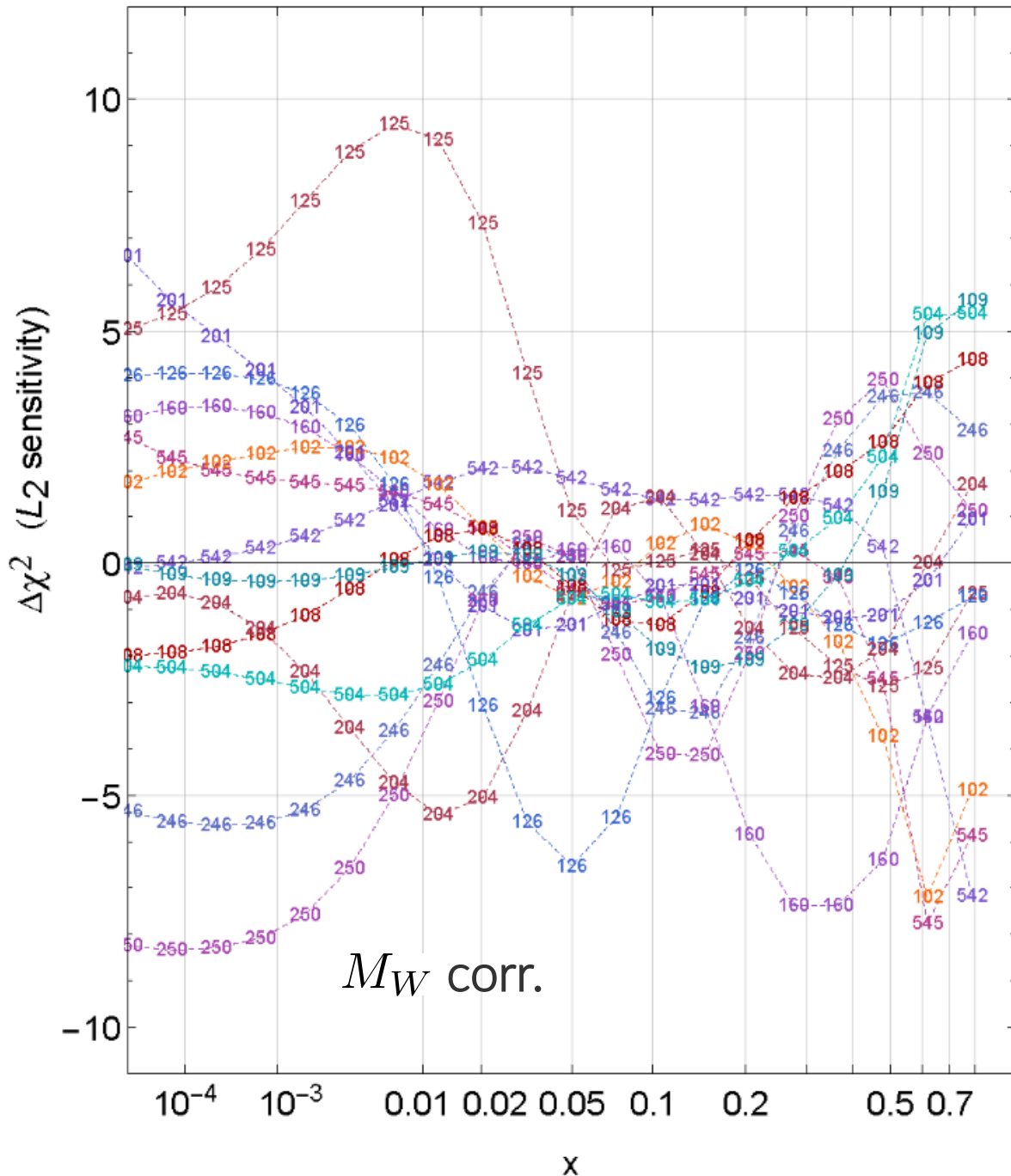
...this analysis can be extended to M_W ,
 extractions of which are dependent upon $s(x)$,
 through Z-calibration



$|S_i|$ for $s(x, \mu)$, CT14HERA2NNLO



CT18 NNLO, $s(x, 2 \text{ GeV})$



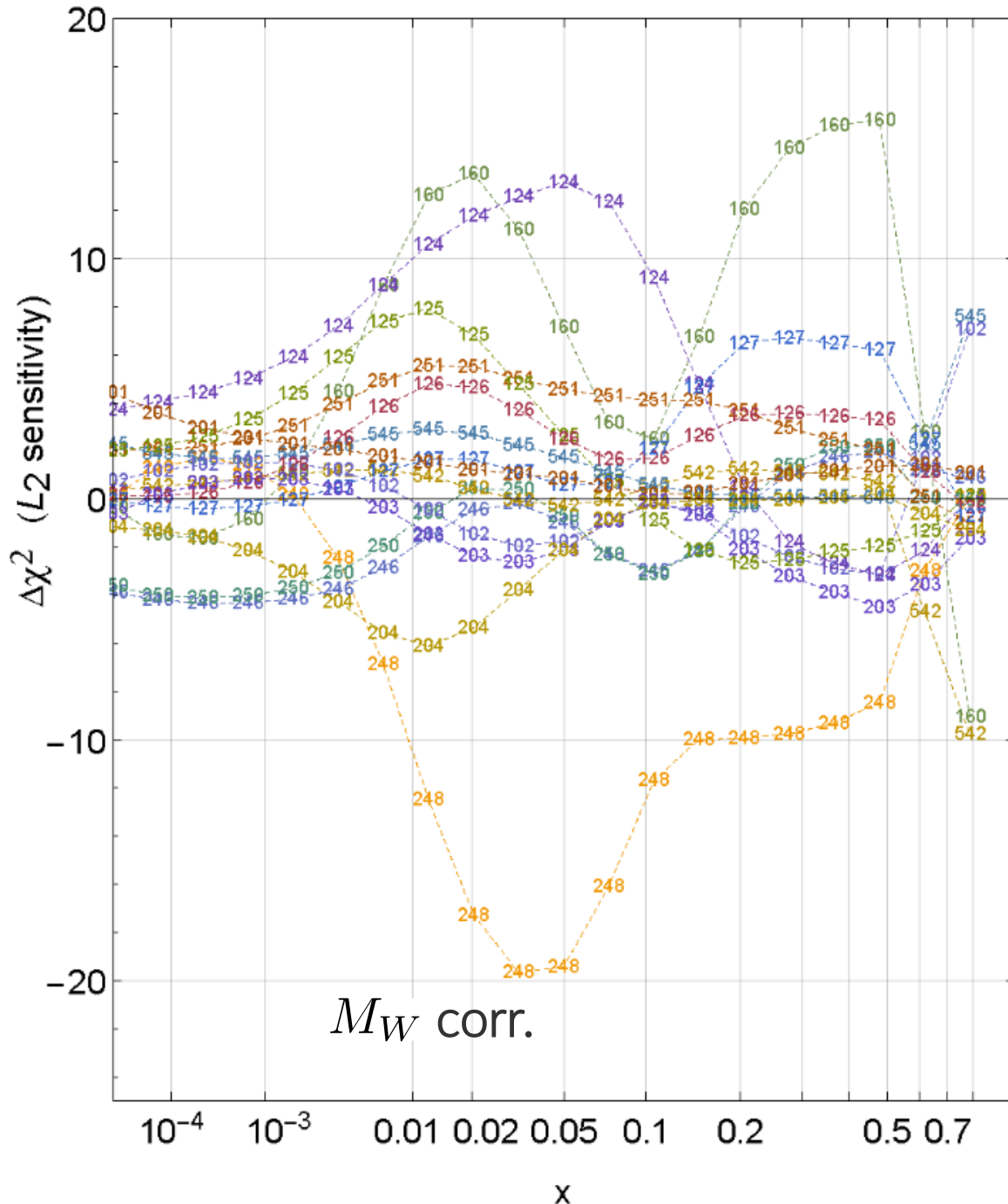
L_2 sensitivity, strangeness: CT18

Most sensitive experiments

- 246--- LHCb8Zeer
- 250--- LHCb8WZ
- 542--- CMS7jtR7y6T
- 545--- CMS8jtR7T
- 160--- HERA I+II
- 102--- BcdF2dCor
- 108--- cdhswf2
- 109--- cdhswf3
- 125--- NuTeVNbChXN
- 126--- CcfrNuChXN
- 201--- e605
- 204--- e866ppxf
- 504--- cdf2jtCor2

A tension trend between DIS (HERA I+II, CCFR, NuTeV) and Drell-Yan (ATLAS 7 Z/W, LHCb W/Z, E866 pp, ...) experiments

CT18Z NNLO, $s(x, 2 \text{ GeV})$



L_2 sensitivity, strangeness: CT18Z

Most sensitive experiments

- 246--- LHCb8Zeer
- 248--- ATLAS7ZW.xF
- 250--- LHCb8WZ
- 251--- ATLAS8DY
- 542--- CMS7jtR7y6T
- 545--- CMS8jtR7T
- 160--- HERAIIplI
- 102--- BcdF2dCor
- 124--- NuTeVNuChXN
- 125--- NuTeVNbChXN
- 126--- CcfrNuChXN
- 127--- CcfrNbChXN
- 201--- e605
- 203--- e866f
- 204--- e866ppxf

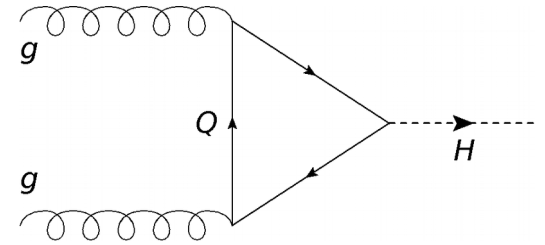
A tension trend between DIS (HERA I+II, CCFR, NuTeV) and Drell-Yan (ATLAS 7 Z/W, LHCb W/Z, E866 pp, ...) experiments

pronounced effect of ATLAS 7 TeV Z/W data!

QCD at high energies: an EIC and control over the gluon

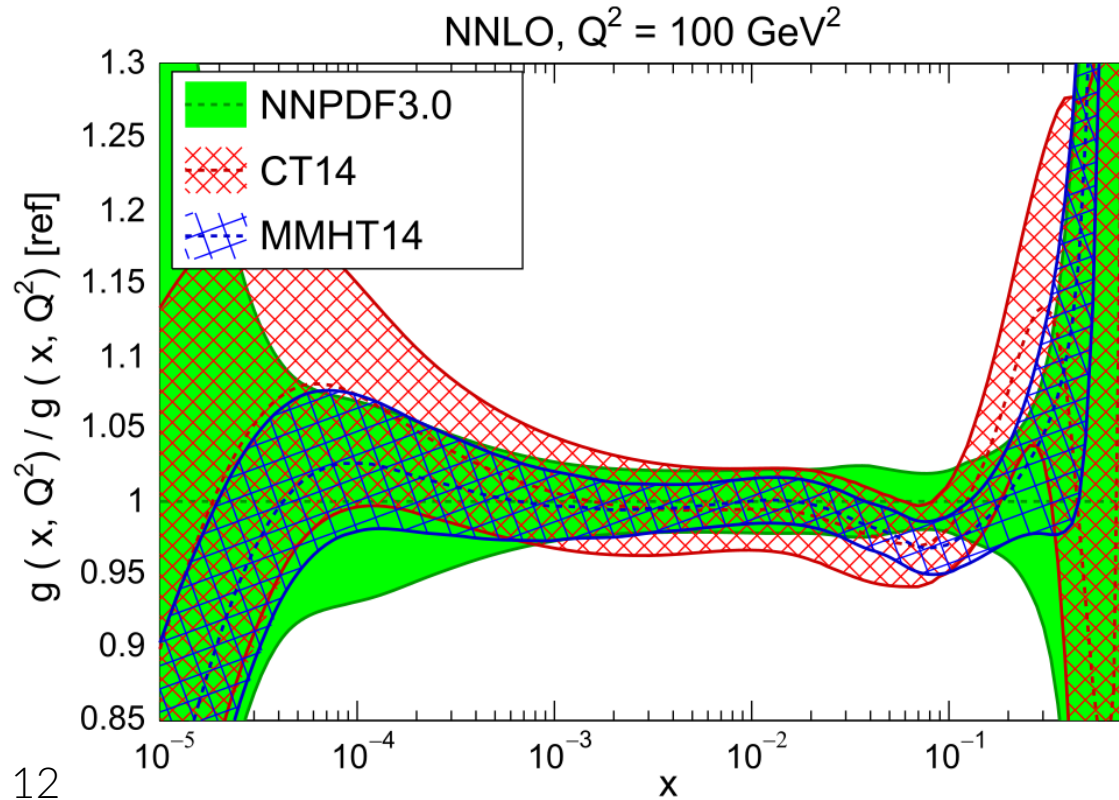
- the gluon is crucial to the mass of hadronic bound states, and $gg \rightarrow H$ is the dominant channel in Higgs production

_____ BUT _____

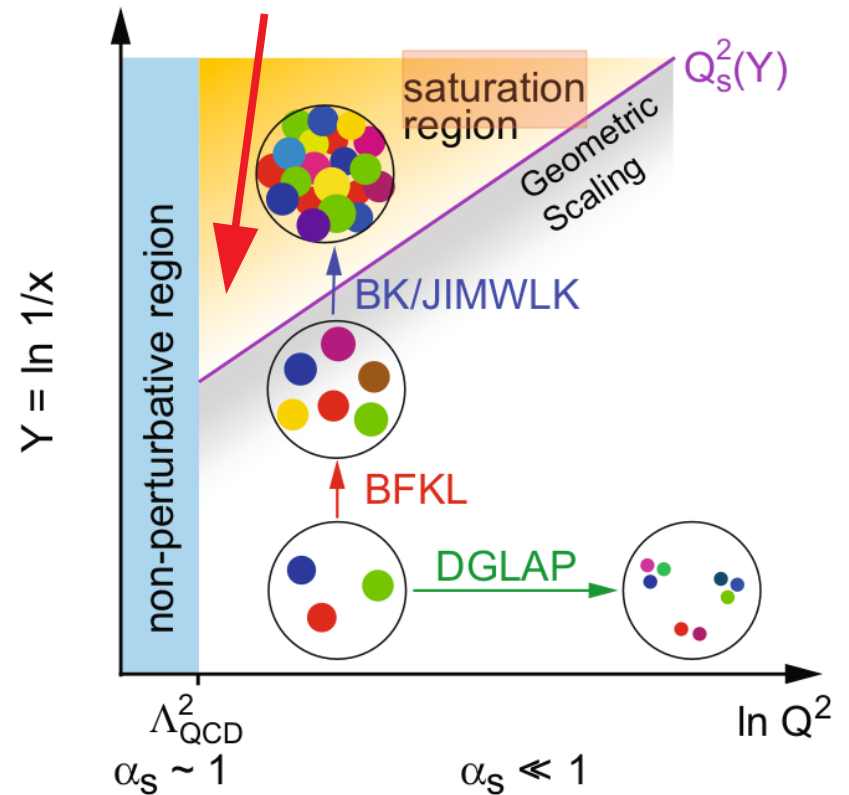


- while under better control at intermediate x , the collinear gluon PDF is poorly known toward the distribution endpoints, *i.e.*, $g(x, \mu)$ for $x \rightarrow 0, 1$

Rojo et al., J. Phys. G42, 103103 (2015).



can we begin to observe this transition?



the goal is to quantify the strength of the constraints placed on a particular set of PDFs by both individual and aggregated measurements *without direct fitting*

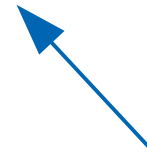
- for single-particle hadroproduction of gauge bosons at, e.g., LHC, factorization gives

$$\sigma(AB \rightarrow W/Z+X) = \sum_n \alpha_s^n(\mu_R^2) \sum_{a,b} \int dx_a dx_b$$

$$\times f_{a/A}(x_a, \mu^2) \hat{\sigma}_{ab \rightarrow W/Z+X}^{(n)}(\hat{s}, \mu^2, \mu_R^2) f_{b/B}(x_b, \mu^2)$$



PDFs determined by fits to data; e.g., "CT14H2"



pQCD matrix elements – specified by theoretical formalism in a given fit

- idea*: study the statistical correlation between PDFs and the quality of the fit at a measured data point(s); fit quality encoded in a (Theory) – (shifted Data) *residual*:

$$r_i(\vec{a}) = \frac{1}{s_i} (T_i(\vec{a}) - D_{i,sh}(\vec{a}))$$

s_i : uncorrelated uncert.

\vec{a} : PDF parameters

a brief statistical aside, i

- the CTEQ-TEA global analysis relies on the Hessian formalism for its error treatment

$$\chi_E^2(\vec{a}) = \sum_{i=1}^{N_{pt}} r_i^2(\vec{a}) + \sum_{\alpha=1}^{N_\lambda} \bar{\lambda}_\alpha^2(\vec{a})$$

← nuisance parameters to handle correlated errors

$$r_i(\vec{a}) = \frac{1}{s_i} (T_i(\vec{a}) - D_{i,sh}(\vec{a}))$$

these result in systematic shifts to data central values:

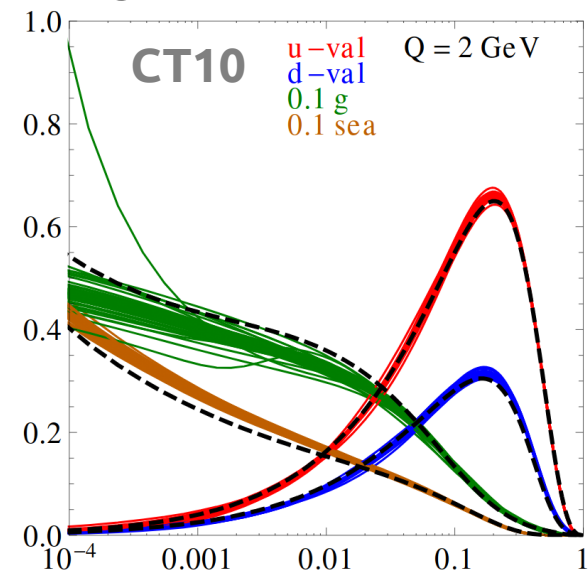
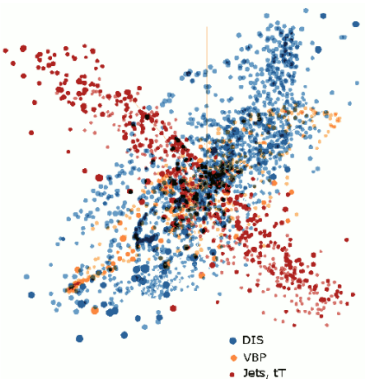
$$D_i \rightarrow D_{i,sh}(\vec{a}) = D_i - \sum_{\alpha=1}^{N_\lambda} \beta_{i\alpha} \bar{\lambda}_\alpha(\vec{a})$$

- a 56-dimensional parametric basis \vec{a} is obtained by diagonalizing the Hessian matrix H determined from χ^2 (following a 28-parameter fit)

use this basis to compute 56-component "normalized" residuals:

$$\delta_{i,l}^\pm \equiv (r_i(\vec{a}_l^\pm) - r_i(\vec{a}_0)) / \langle r_0 \rangle_E$$

where $\langle r_0 \rangle_E \equiv \sqrt{\frac{1}{N_{pt}} \sum_{i=1}^{N_{pt}} r_i^2(\vec{a}_0)}$

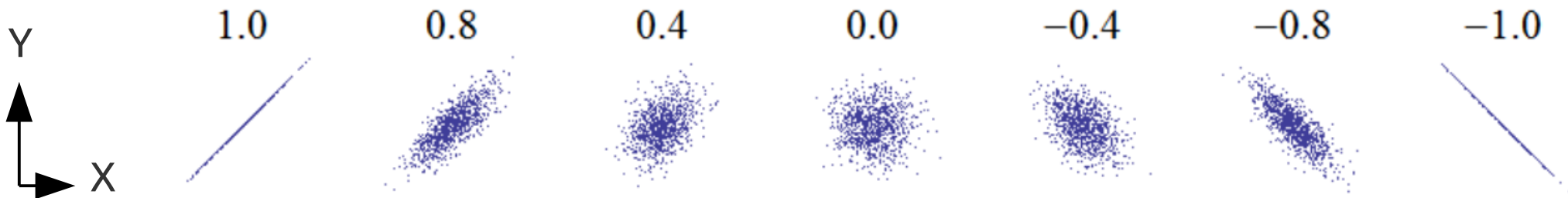


a brief statistical aside, ii

- ... but how does the behavior of these residuals relate to the fitted PDFs and their uncertainties?

for example, how does the PDF uncertainty (at specific x, μ) correlate with the residual associated with a theoretical prediction at the same x, μ ?

examine the Pearson correlation over the 56-member PDF error set between a PDF of given flavor and the residual



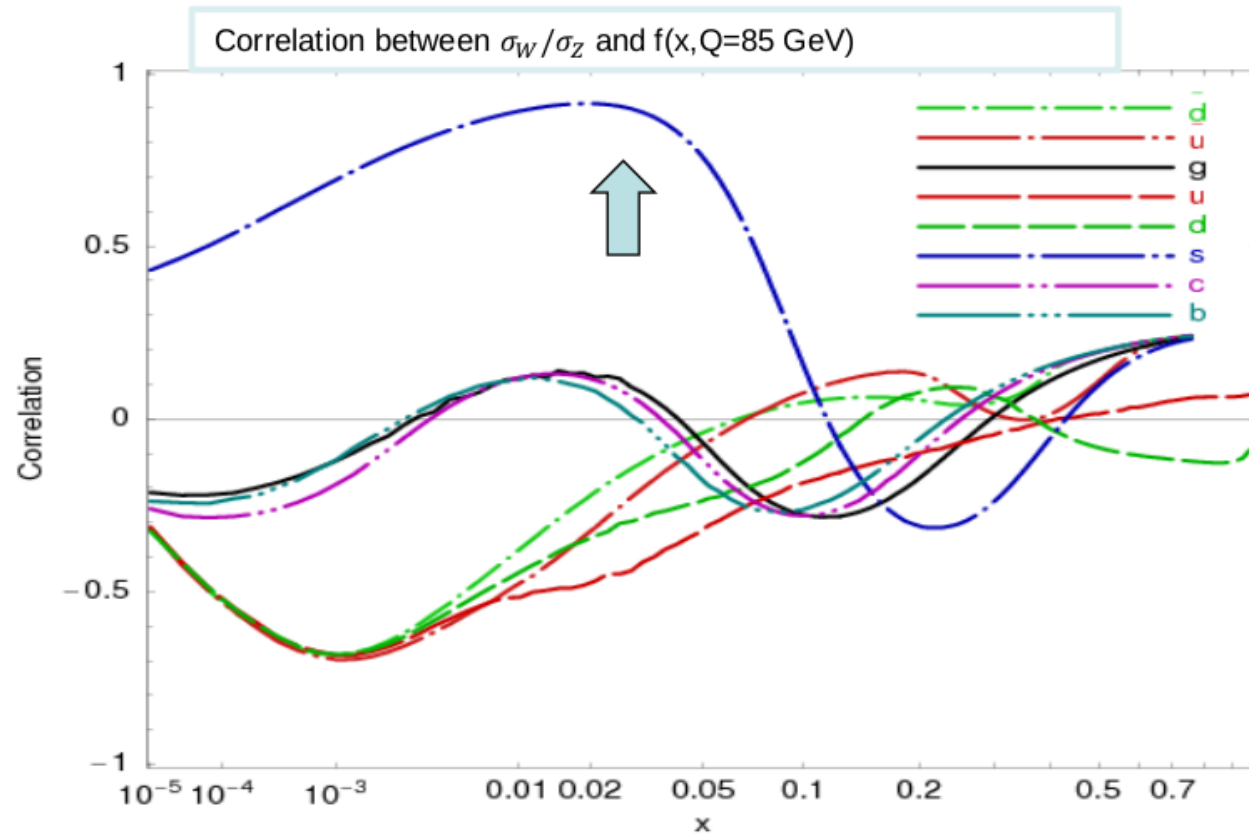
[X,Y] are exactly (anti-)correlated at the far (right) left above.

- we may then evaluate correlations between arbitrary PDF-derived quantities over the ensemble of error sets ([X,Y] may be PDFs, cross sections, residuals,...):

$$\text{Corr}[X, Y] = \frac{1}{4\Delta X \Delta Y} \sum_{j=1}^N (X_j^+ - X_j^-)(Y_j^+ - Y_j^-) \quad \Delta X = \frac{1}{2} \sqrt{\sum_{j=1}^N (X_j^+ - X_j^-)^2}$$

...we may turn to the Pearson correlations between PDFs and δ_i , but we first note

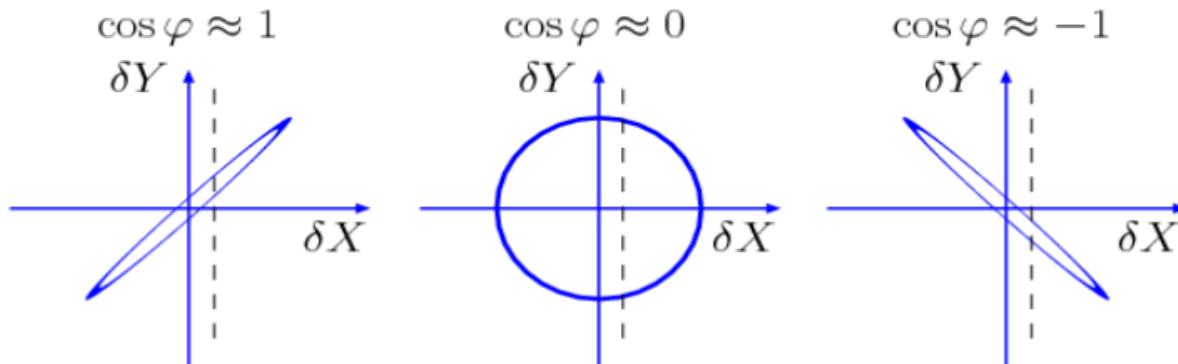
Correlations carry useful, but limited information



CTEQ6.6 [arXiv:0802.0007]:

$\cos \varphi > 0.7$ shows that the ratio σ_W/σ_Z at the LHC must be sensitive to the strange PDF $s(x, Q)$

$\cos \varphi \approx \pm 1$ suggests that a measurement of X **may** impose tight constraints on Y



But, $\text{Corr}[X, Y]$ between **theory** cross sections X and Y does not tell us about **experimental** uncertainties

Correlation C_f and sensitivity S_f

The relation of data point i on the PDF dependence of f can be estimated by:

- $C_f \equiv \text{Corr}[\rho_i(\vec{a}), f(\vec{a})] = \cos\varphi$

$\vec{\rho}_i \equiv \vec{\nabla}r_i / \langle r_0 \rangle_E$ -- gradient of r_i normalized to the r.m.s. average residual in expt E;

$$(\vec{\nabla}r_i)_k = (r_i(\vec{a}_k^+) - r_i(\vec{a}_k^-))/2$$

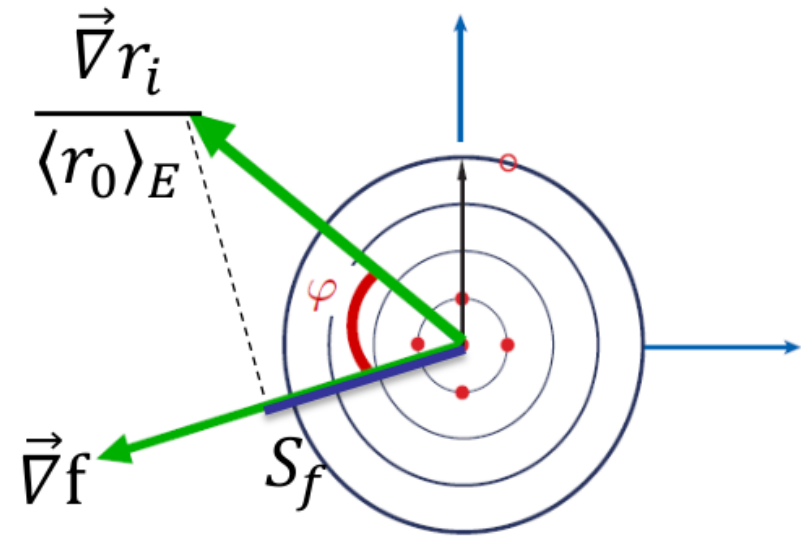
$$\text{Corr}[X, Y] = \frac{1}{4\Delta X \Delta Y} \sum_{j=1}^N (X_j^+ - X_j^-)(Y_j^+ - Y_j^-)$$

C_f is **independent** of the experimental and PDF uncertainties. In the figures, take $|C_f| \gtrsim 0.7$ to indicate a large correlation.

- $S_f \equiv |\vec{\rho}_i| \cos\varphi = C_f \frac{\Delta r_i}{\langle r_0 \rangle_E}$ -- projection of $\vec{\rho}_i(\vec{a})$ on $\vec{\nabla}f$

S_f is proportional to $\cos\varphi$ and the ratio of the PDF uncertainty to the experimental uncertainty. We can sum $|S_f|$.

In the figures, take $|S_f| > 0.25$ to be significant.



2nd aside: kinematical matchings

- residual-PDF correlations and sensitivities are evaluated at parton-level kinematics determined according to leading-order matchings with physical scales in measurements

deeply-inelastic scattering:

$$\mu_i \approx Q|_i, \quad x_i \approx x_B|_i$$

x_i : parton mom. fraction

μ_i : factorization scale

hadron-hadron collisions:

$AB \rightarrow CX$

$$\mu_i \approx Q|_i, \quad x_i^\pm \approx \frac{Q}{\sqrt{s}} \exp(\pm y_C)|_i$$

single-inclusive jet production:

$$Q = 2p_{Tj}, \quad y_C = y_j$$

$t\bar{t}$ pair production:

$$Q = m_{t\bar{t}}, \quad y_C = y_{t\bar{t}}$$

etc...

$d\sigma/dp_T^Z$ measurements:

$$Q = \sqrt{(p_T^Z)^2 + (M_Z)^2}, \quad y_C = y_Z$$

Sensitivity ranking tables

... to assess the impact of separate experiments

No.	Expt.	N_{pt}	Rankings, CT14 HERA2 NNLO PDFs												
			$\sum_f S_f^E $	$\langle \sum_f S_f^E \rangle$	$ S_{\bar{d}}^E $	$\langle S_{\bar{d}}^E \rangle$	$ S_{\bar{u}}^E $	$\langle S_{\bar{u}}^E \rangle$	$ S_g^E $	$\langle S_g^E \rangle$	$ S_u^E $	$\langle S_u^E \rangle$	$ S_d^E $	$\langle S_d^E \rangle$	$ S_s^E $
1	HERAI+II'15	1120.	620.	0.0922	B		A	3	A	3	A	3	B		C
2	CCFR-F3'97	86	218.	0.423	C	1	C	1		3	B	1	C	2	
3	BCDMSp'89	337	184.	0.0908			C		C		B	3	C		
4	NMCrat'97	123	169.	0.229	C	2					C	2	B	2	
5	BCDMSd'90	250	141.	0.0939	C				C	3	C	3	C	3	
6	CDHSW-F3'91	96	115.	0.199	C	2	C	2		3	C	2	C	3	
7	E605'91	119	113.	0.158	C	2	C	2				3			
8	E866pp'03	184	103.	0.0935		3	C	3			C	3			
9	CCFR-F2'01	69	89.1	0.215		3		3	C	2		3		2	3
10	CMS8jets'17	185	87.6	0.0789					C	3					
11	CDHSW-F2'91	85	82.4	0.162		3		3		3		3	C	3	
12	CMS7jets'13	133	63.8	0.0799					C	3					
13	NuTeV-nu'06	38	58.9	0.259		3		3				3		3	C 1
14	CMS7jets'14	158	57.5	0.0606					C	3					
15	CCFR SI nub'01	38	49.4	0.217		3		3				3		3	C 1
16	ATLAS7jets'15	140	48.2	0.0574						3					
17	CCFR SI nu'01	40	48.	0.2		3		3				3		3	C 1

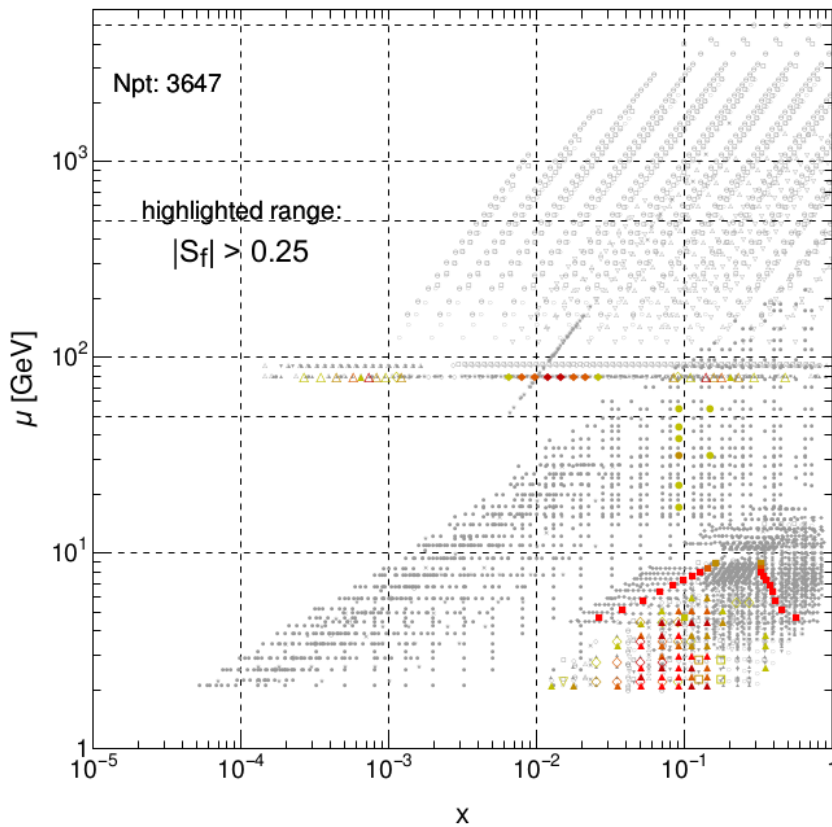
Experiments are listed in the descending order of the summed sensitivities to $\bar{d}, \bar{u}, g, u, d, s$

For each flavor, A and 1 indicate the strongest total sensitivity and strongest sensitivity per point

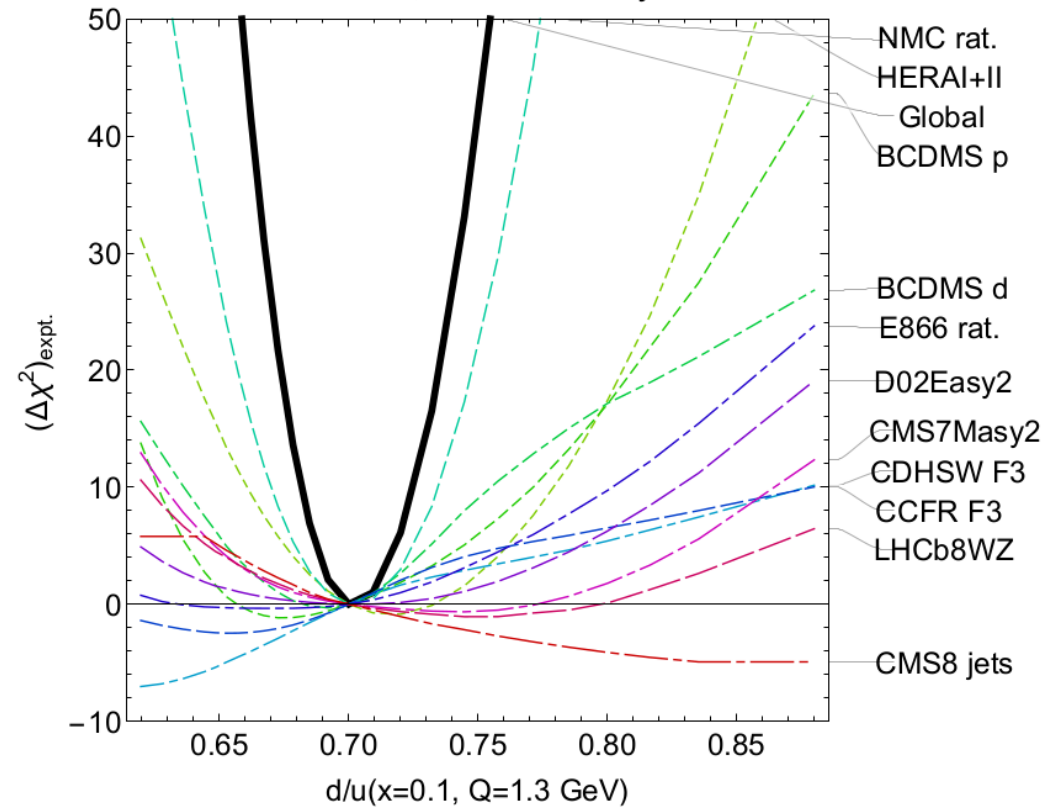
C and 3 indicate marginal sensitivities; low sensitivities are not shown

PDFSense predictions can be validated against actual fits

$|S_f|$ for $d/u(0.1,1.3)$, CT18pre NNLO



CT18 NNLO, + 0.5% theory error



- PDFSense successfully predicts the highest impact data sets *before* fitting, as shown in this illustration for the large x PDF ratio d/u
- Lagrange Multiplier scans provide an independent test of which datasets most drive the global fit in connection with specific PDFs

HERA and fixed-target (BCDMS, NMC) data are dominant!